



UNIVERSITÀ POLITECNICA DELLE MARCHE  
FACOLTÀ DI INGEGNERIA

---

Corso di Laurea Magistrale in Biomedical Engineering

**Mechanoelectric phenomena contributing to  
sport-related sudden cardiac death**

**Advisor**

**Prof. Laura Burattini**

**Co-Advisor**

**Dott. Agnese Sbrollini**

**Dott. Gianluca Zitti**

**Master Thesis by**

**Sofia Romagnoli**

**Academic Year 2019/2020**

## Abstract

Sport-related sudden cardiac death (SrSCD) is the leading medical cause of death across all sports. Physical exercise is a potential trigger for sudden cardiac death (SCD). Thus, the aim of this Master Thesis is to investigate the mechanoelectric phenomena contributing to SrSCD. Increased cardiovascular load during exertion in people with an underlying cardiovascular abnormality (both of electrical and structural origin) can trigger SCD. SrSCD could occur not only during sport activity but also after exercise at rest or during sleep. Given the growing sport participation among general population, SrSCD is recognized as a public health concern. Prevention is the main weapon to contrast sudden cardiac arrest (SCA) which leads to SCD. Prevention is based on pre-participation screening of athletic population during which cardiac status is evaluated by electrocardiography (ECG) and auscultation. Several protocol and ECG interpretation guidelines have been developed for athletic screening in order to recognise pathologies and avoid the erroneous disqualification of healthy athletes. This is the case of “grey zone” athletes, whose sport-related cardiovascular adaptation may overlap with pathologic signs. For this reason, after an introductory section on anatomy and physiology of cardiovascular system, the I Section is a literature review about sport-related cardiovascular adaptations, aetiology of SrSCD and first level screening. Particular attention is paid to all factors (age, gender, ethnicity, type of sport, intensity and amount of training) affecting the physiological cardiovascular remodelling and the incidence/manifestation of pathology most related with SrSCD. These factors are fundamental to develop targeted and personalized pre-participation screening, increasing its accuracy. Given the wide debate on cost-effectiveness of pre-participation screening, the two experimental sections address the improvement in accuracy of athletic population screening in both Bioengineering and Biofluid dynamic fields. The ‘II Section’ aims to develop normal reference values for interpretation of pre-exercise ECG acquired by wearable sensors, namely BioHarness 3.0 by Zephyr ([www.zephyranywhere.com](http://www.zephyranywhere.com)). The scope is to make pre-participation screening wider by continuous monitoring of athlete’s status and screening amateur athletic population through wearable technology. The parameters extracted from healthy ECG (by chest strap BioHarness 3.0 by Zephyr) coincided with the normal values from 12 lead ECG. Further, we found a significant difference between male and female median QRS duration (95 ms vs 85 ms,  $p=0.005$ ) and the QTc measurement confirmed to be longer in female. These results suggested that gender stratification is central to produce more accurate and personalized pre-participation screening. The

'III Section' aims to provide a reliable geometry of coronary anatomy for preliminary qualitative models of right and left coronary arteries. Qualitative models and computational fluid dynamic software permits to study the vascular remodelling as well as the biofluid dynamic contribution to SCD, specifically the anomalous wave dynamics and impaired perfusion potentially behind SrSCD. A reliable geometry was modelled from angiographic measurements of healthy coronary vessels and future studies are needed to implement a more accurate model of materials and boundary conditions. The spectrum of mechanoelectric phenomena contributing to SrSCD is extremely wide, but targeted pre-participation screening of athletic population can contrast it. Pre-participation screening accuracy can be further improved by exploiting the precious developments provided by wearable technologies and computational fluid dynamic.

# Index

<b>Introduction</b> .....	1
<b>Introductory Section: Anatomy and physiology of the cardiovascular system</b> .....	1
<b>1.1 The heart</b> .....	1
<b>1.1.1 Anatomy</b> .....	1
<b>1.1.2 Electrical physiology</b> .....	7
<b>1.1.2.1 Electrocardiography</b> .....	11
<b>1.1.3 Mechanical physiology</b> .....	13
<b>1.2 Circulation</b> .....	20
<b>1.2.1 Coronary arteries anatomy</b> .....	20
<b>1.2.2 Vessel structure</b> .....	25
<b>1.2.3 Mechanical properties of normal coronary arteries</b> .....	26
<b>1.3 Regulation of cardiovascular system</b> .....	27
<b>1.3.1 Regulation of heart rate</b> .....	30
<b>1.3.2 Regulation of myocardium contraction and relaxation</b> .....	31
<b>1.3.3 Regulation of cardiovascular function during exercise</b> .....	32
<b>I Section: Review on athlete’s heart and mechanoelectric contribution to sport-related sudden cardiac death</b> .....	34
<b>2.1 Introduction</b> .....	34
<b>2.2 Methods for literature review</b> .....	36
<b>2.3 The determinants of athlete’s heart</b> .....	37
<b>2.4 Incidence of sport related sudden cardiac death</b> .....	42
<b>2.5 The athlete’s heart: physiological changes with athletic training</b> .....	44
<b>2.5.1 Structural adaptations</b> .....	44
<b>2.5.1.1 Left ventricle</b> .....	46
<b>2.5.1.2 Right ventricle</b> .....	47
<b>2.5.1.3 Left atrium</b> .....	49
<b>2.5.1.4 Right atrium</b> .....	51
<b>2.5.2 Vascular adaptation</b> .....	51
<b>2.5.3 Functional adaptations</b> .....	53
<b>2.5.4 Electrical adaptations</b> .....	55
<b>2.6 Aetiology of sport related sudden cardiac death</b> .....	60
<b>2.6.1 Physical activity as a promoter of cardiac damage and arrhythmic substrate</b> .....	60
<b>2.6.2 Physical activity as a trigger for arrhythmias in presence of underlying pathology</b> .....	61

2.6.2.1 Inherited structural cardiac abnormalities.....	63
2.6.2.2 Inherited Electrical disorders .....	72
2.6.2.3 Acquired Structural cardiac abnormalities .....	75
2.6.2.4 Other acquired causes .....	76
2.6.2.5 Sudden cardiac death of unknown causes.....	77
2.7 Screening.....	78
2.7.1 Electrocardiography.....	79
2.7.2 Imaging.....	85
2.7.2.1 Echocardiography .....	85
2.7.2.2 Cardiac Magnetic Resonance.....	85
2.7.2.3 Stress Imaging.....	86
<b>II Section: Cardiac monitoring through wearable sensors: normative electrocardiographic reference standards for athletes .....</b>	<b>88</b>
3.1 Background.....	88
3.2 Materials and Methods .....	90
3.2.1 Study population.....	90
3.2.2 Experimental methods .....	90
3.2.3 Statistics .....	91
3.3 Results .....	92
3.4 Discussion and Conclusion.....	95
<b>III Section: Preliminary biofluid dynamic numerical models of coronary artery in athletes.....</b>	<b>98</b>
4.1 Background.....	98
4.1.1 Normal geometry of coronary arteries.....	99
4.1.1.1 Normal geometry of coronary arteries in athletic population .....	102
4.1.1.2 Aorta and physiological remodeling with exercise .....	104
4.1.2 Pulsatile coronary blood flow and Wave Dynamics .....	105
4.1.2.1 Pulsatile coronary blood flow and wave dynamics during exercise .....	111
4.1.3 Computational fluid dynamics and three-dimensional model of pulsatile coronary blood flow .....	113
4.1.3.1 Numerical model of the coronary arteries .....	114
4.1.3.2 Boundary conditions for the pulsatile flux.....	116
4.2 Materials and methods.....	118
4.2.1 Reconstruction of coronary artery geometry .....	118
4.2.2 Numerical simulation .....	120
4.2.2.1 Mesh creation .....	120
4.2.2.2 Setup .....	121

<b>4.3 Results</b> .....	124
<b>4.3.1 Reconstruction of coronary artery geometry</b> .....	124
<b>4.3.2 Meshing</b> .....	128
<b>4.3.3 Numerical simulation results</b> .....	129
<b>4.4 Discussion and Conclusion</b> .....	133
<b>Discussion and Conclusion</b> .....	II
<b>Reference</b> .....	IV
<b>Acknowledgement</b> .....	XVIII

## Introduction

Sport-related sudden cardiac death (SrSCD) is the leading medical cause of death across all sports. Physical exercise is a potential trigger for sudden cardiac death (SCD). Increased cardiovascular load during exertion in people with an underlying cardiovascular abnormality (both of electrical and structural origin) can trigger SCD [1][2][3]. SrSCD could occur not only during sport activity but also after exercise at rest or during sleep [1]. Given the growing sport participation among general population, SrSCD is recognized as a public health concern [4]. Prevention is the main weapon to contrast sudden cardiac arrest (SCA) which leads to SCD. Prevention is based on pre-participation screening of athletic population during which cardiac status is mainly evaluated by electrocardiography (ECG). ECG monitoring can be further performed continuously before, during and after training in both competitive and amateur athletes through wearable sensors. Given the manifestation with abnormal signs of sport-related physiological adaptation, European and American cardiology associations have proposed several interpretation guidelines for standard 12 lead ECG acquired at rest from athletes but not for ECG signal acquired by wearable technologies. ECG showed to have low sensitivity and specificity in detecting mechanical causes of SrSCD as coronary arteries anomalies and diseases, which may remain undiagnosed if there is no presence of severe ischemic pattern in ECG signal. Therefore, biofluid dynamic studies through computational fluid dynamic (CFD) tools can produce patient specific simulation from non-invasive imaging for diagnosis. Further, CFD applied in qualitative coronary models representative of athletic population permits to study the vascular remodelling as well as the biofluid dynamic contribution to SCD, specifically the anomalous wave dynamics and impaired perfusion probably behind SrSCD of unknown causes at the autopsy (SrSCD that occurs in the absence of an evident structural or electrical cardiac disorder).

The first aim of this Master Thesis is to study the mechanoelectric phenomena contributing to sport-related sudden cardiac death. Then to investigate the potential resources provided by wearable sensor technologies for continuous monitoring and by computational fluid dynamic for coronary artery studies.

# **Introductory Section: Anatomy and physiology of the cardiovascular system**

## **1.1 The heart**

The heart is the central organ of the cardiovascular system, and it permits the blood circulation in vessels through rhythmic contraction [5][6].

### **1.1.1 Anatomy**

The heart is located in the *mediastinum*, an area from the sternum to the vertebral column and between the lungs. This area contains not only the heart but also blood vessels that reach and leave the heart and the esophagus. The heart is asymmetrically oriented into the chest: the apex is directed anteriorly, inferiorly and to the left, while the base is directed posteriorly, superiorly and to the right. The anterior surface, named sternocostal face, is close to sternum and ribs, the posterior-inferior surface, named diaphragmatic face, lies on the tendon centre of diaphragm [5][6].

The surface of the heart presents the sulci, which are grooves on the surface of the heart containing coronary blood vessels and fat [5][6]:

- coronary sulcus encircles the heart and marks the boundary between the atria and the ventricle;
- anterior interventricular sulcus marks the boundary between the ventricles anteriorly;
- posterior interventricular sulcus marks the boundary between the ventricles posteriorly.

The heart is surrounded by the pericardium [5][6]:

- Fibrous pericardium is the outer layer continues with the central tendon of diaphragm thus it anchors the heart. It is made of connective tissue and thus relative not distensible. Its rigid structure prevents rapid overfilling of the heart protecting the heart.
- Serious pericardium is under the fibrous pericardium and contains a parietal outer layer and a visceral layer (epicardium), between which the pericardial cavity with pericardial fluid are present. It lubricates the heart to prevent friction and freely move within the pericardium.



The other two layers of the heart are the cardiac muscular layer, *myocardium*, and the *endocardium*, which constitutes the lining of chamber and valves [5][6].

The heart has four chambers: two upper atria and two lower ventricles. The right and left sides of the heart are separated by the interatrial and interventricular septa and do not communicate. They are in communication through foramen ovale only during fetal period. After birth foramen ovale closes forming the *fossa ovalis*. Fossa ovalis is a depression on the septal wall of the atrial septum. It is located in the lower part of the septum, above and to the left of the orifice of the inferior vena cava. In this region the septum is less thick [5][6].

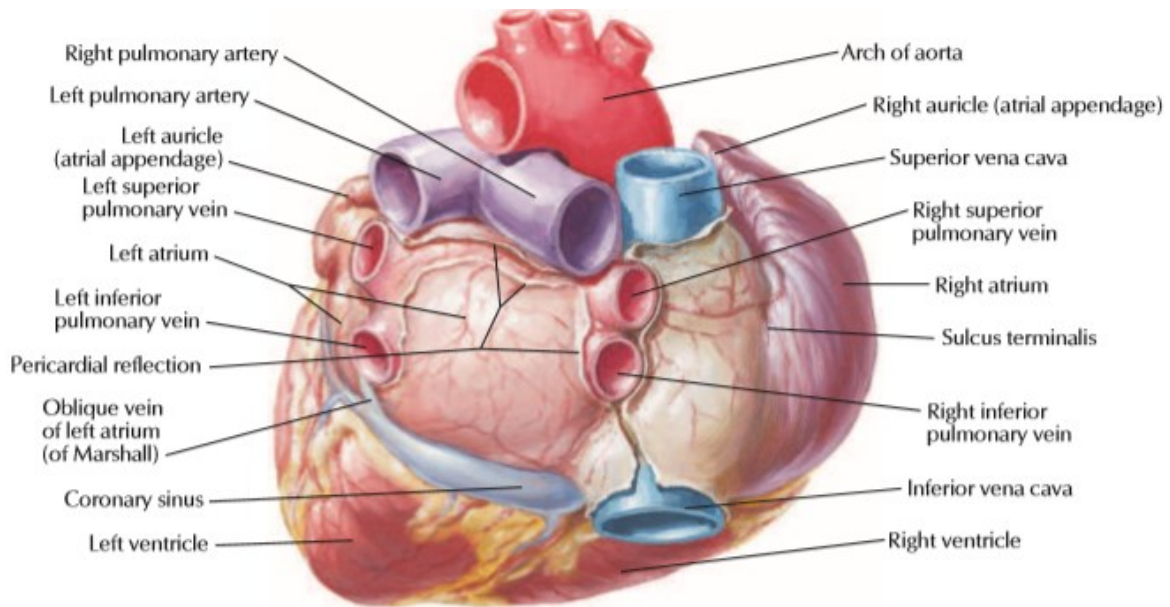
*Right atrium* receives blood from three sources, superior vena cava, inferior vena cava and coronary sinus. Through the tricuspid valve blood flows into the right ventricle. *Right ventricle* forms most of the anterior surface of the heart; this position is relevant both for imaging and electrocardiography since several electrodes are positioned close to the right ventricle than the left ventricle, receiving more information from it. Blood is ejected into the pulmonary artery through the pulmonary semilunar valve [5][6].

*Left atrium* receives blood from four pulmonary veins, two left and two right. Through the bicuspid valve blood flows into the left ventricle. *Left ventricle* forms the apex of the heart. It contains most of the cardiac muscle, for this reason, left ventricle predominates the electrocardiogram as it has more muscular tissue and so larger part of the current that is generated by the heart. Blood is ejected into the aorta through the aortic semilunar valve [5][6].

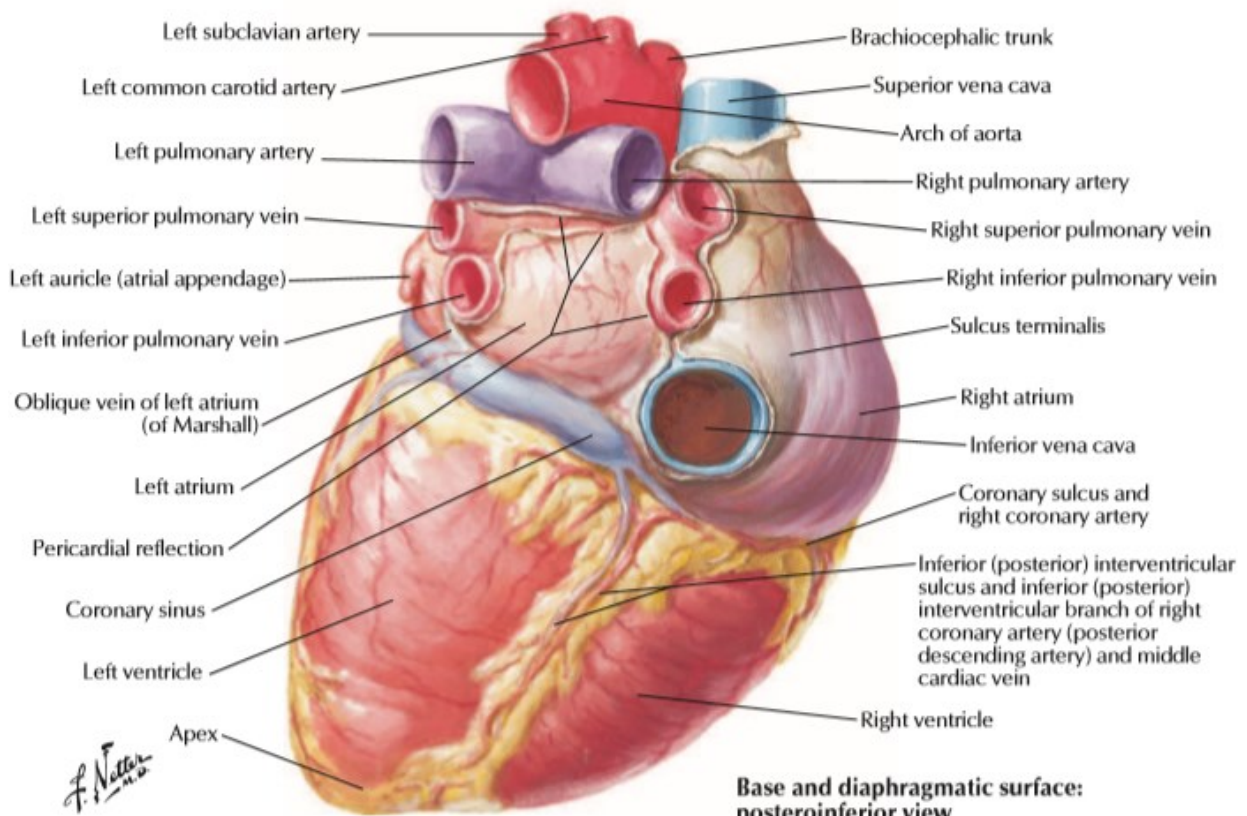
Both ventricles contain *papillary muscles* and *chordae tendinae*. Papillary muscles are cone shaped trabeculae. These raised bundles of cardiac muscle contract when the ventricles contract and help to maintain valves closed avoiding the blood backflow into the atria. Papillary muscles are anchored to the valve cusps by chordae tendinae [5][6].

Ventricular myocardium is organized in *ventricular myocardial band*. The muscle fibres in the ventricle are organized in wrapped muscle layers leading to preferential conduction direction. The heart is wrapped as a consequence of what happens during the embryonic phase. The myocardial band presents a basal loop and an apical loop and it can be divided into four segments: right (free wall RV), left (free wall LV), descendent (subendocardial), ascendant (subepicardial). Further, the ventricular myocardial band arrangement has a mechanical function enabling ventricles to produce great strength in every direction and specific ventricular movements: the right ventricular free wall moves shortens and moves towards the septum, while left ventricular chamber constricts and shortens [5][6].

Atria and ventricles are electrically isolated by the *fibrous skeleton*. Both myocardium, leaflets and cusps of the valve attach to the fibrous skeleton. It is responsible for the patency of atrioventricular (AV) and semilunar valves preventing their overdistension even if pressure rises too high [5][6]. Valves behaviour can be analysed during diastole and systole. During diastole AV valves are open and allow blood flow into ventricles from atria when ventricular pressure is lower than atrial pressure. Thus, it is a passive process for 80%, the remaining 20% of blood flow into ventricles is active and due to atrial contraction (atrial kick). During ventricular filling ventricle and papillary muscles are relaxed and so chordae tendineae are slack. During systole, semilunar valves close preventing blood from returning to ventricles by filling valve cusps with blood and so tightly closing semilunar valves. During systole, AV valves close preventing backflow of blood into atria. Chordae tendineae are pulled taut by contracted papillary muscles preventing cusps from reverting. Semilunar valves open with ventricular contraction because of the higher pressure into ventricles and the blood flows from ventricles into aorta and pulmonary artery trunk [5][6]. The anatomy of the heart is shown in Figure 1 (external view), Figure 2 (valves and fibrous skeleton) and Figure 3 (internal view).

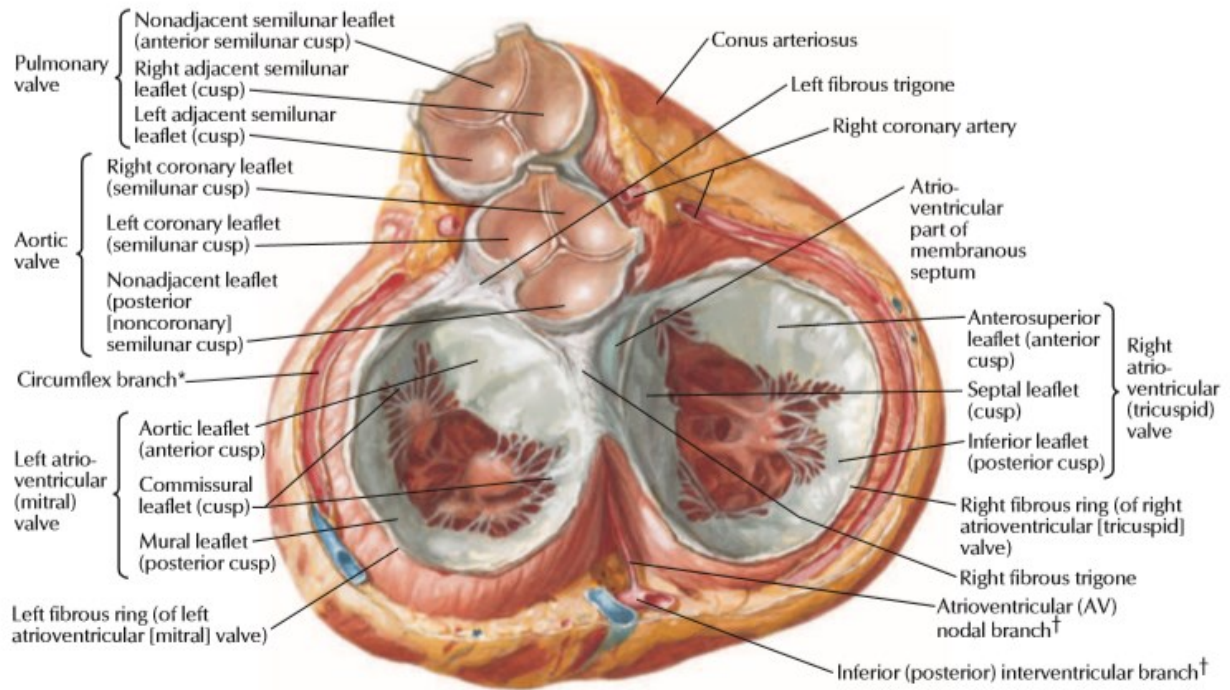


**Base of heart: posterior view**

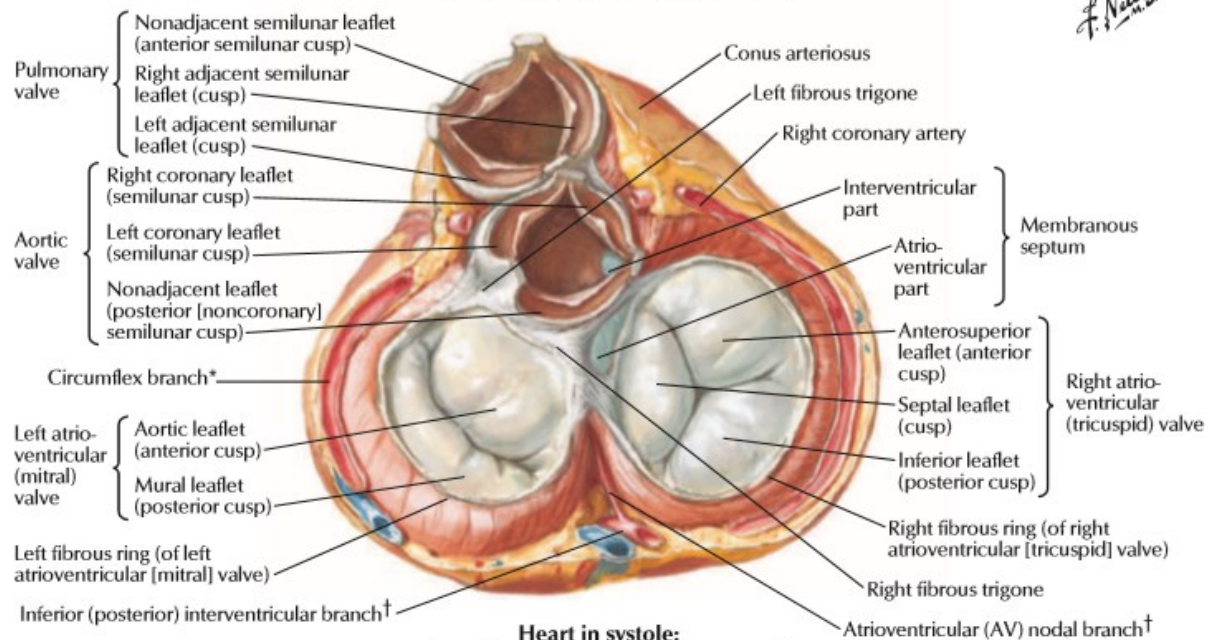


**Base and diaphragmatic surface: posteroinferior view**

Figure 1 Plate 218 shows external view of the cardiac anatomy, specifically the base and diaphragmatic structure. Atlas of Human Anatomy from Frank H. Netter 7th edition [7].



**Heart in diastole:**  
viewed from base with atria removed



**Heart in systole:**  
viewed from base with atria removed

\*Of left coronary artery  
†Of right coronary artery

Figure 2 Plate 226 shows the valves and the fibrous skeleton of the heart. Atlas of Human Anatomy from Frank H. Netter 7th edition [7].



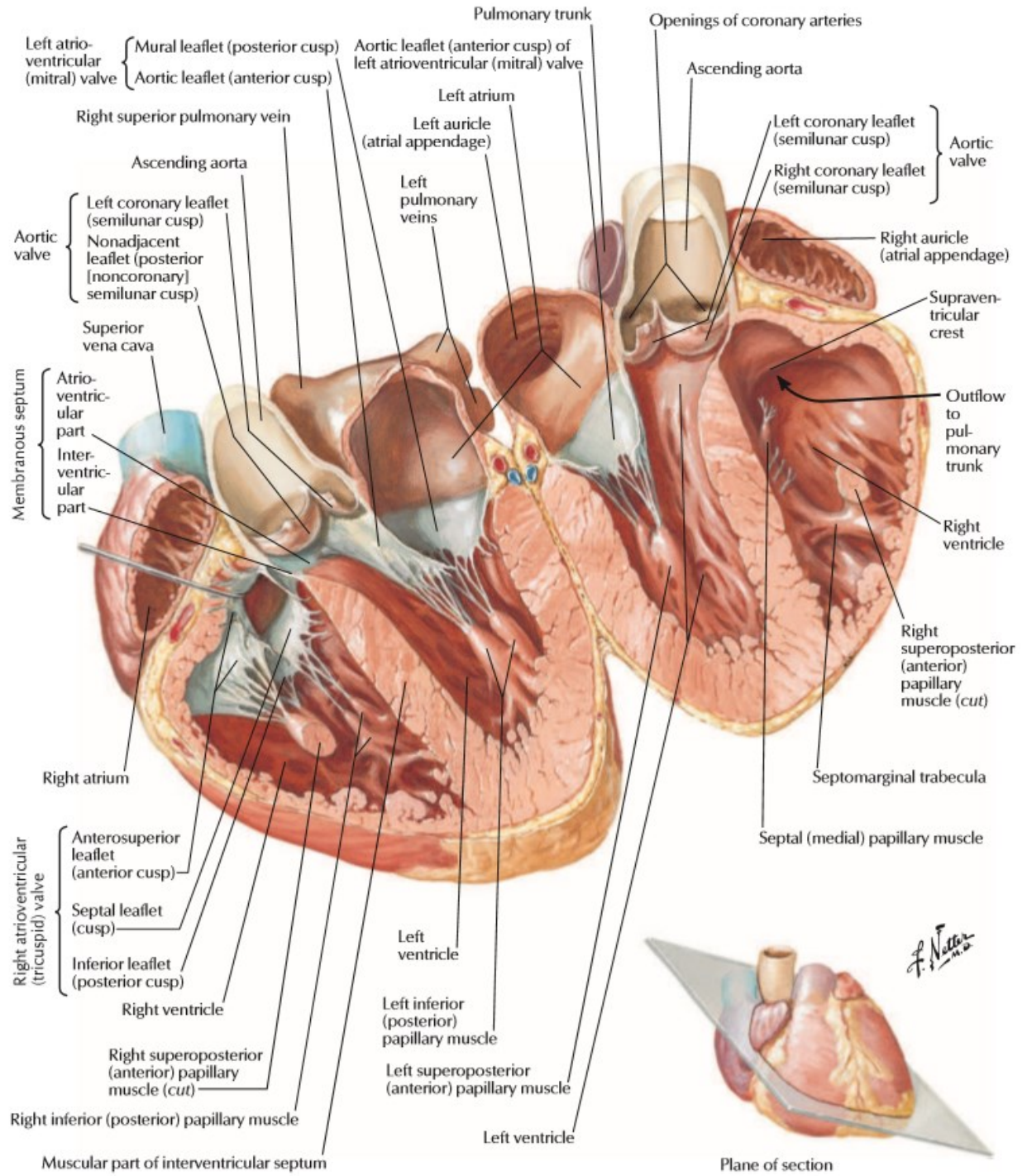


Figure 3 Plate 228 shows atria, ventricles and interventricular septum. Atlas of Human Anatomy from Frank H. Netter 7th edition [7].

### 1.1.2 Electrical physiology

Cardiac myocardium is composed by myocytes linked by intercalated disk. Intercalated disks consist of desmosomes and gap junctions. Desmosomes form mechanical connection between cells. Gap junction facilitate the exchange of ions between cells (so it facilitates the electrical communication). By this mechanism, action potential (AP) from an arbitrary site of the heart is conducted over the entire heart and cause a contraction in the entire heart muscle. Hence, the heart works as a functional syncytium. The electrical excitation of this functional syncytium is followed by a coordinated contraction, namely excitation-contraction coupling [5][6]. In this chapter, the electrical excitation is treated while the mechanical contraction is discussed in the following ‘Mechanical physiology’ section.

Pacemaking and conduction are fundamental process for the electrical activity of the heart (Figure 4).

The heart initiates its own action potentials into the pacemaker cells and it does not require neural input to trigger its contractions. However, autonomic nervous system does exert control over the rate of these contractions by altering the activity of the ion channels that determine the AP. Pacemakers cells with intrinsic automaticity are present in the sinoatrial (SA) node, atrioventricular (AV) node and conduction system (bundle branches and Purkinje fibres) . The firing rate is higher in the SA node (~70/min) than in AV node and conduction system (~50/min and ~15-30/min respectively), thus the faster pacemaker cells in the SA node dictates the rhythm of the heart [5][6].

In pacemaker cells the AP (Figure 5, panel (a)) do not present a resting stable potential [5][6]. The slow depolarization that occurs in the early stages of the pacemaker potential is due to closing of potassium channels and opening of funny channels [5][6]. Potassium channels open during repolarization of the action potential, and then close when the membrane returns to its polarized state [5][6]. Funny channels open after the cell repolarizes and allow sodium and potassium ions to cross the plasma membrane. The closing of potassium channels and the opening of funny channels during the early stages of the pacemaker potential have a net effect of decreasing potassium movement out of the cell and increasing sodium movement into the cell, causing the initial depolarization [5][6]. The funny channels are open for only a brief time, closing when the membrane potential approaches -55 mV. The initial depolarization triggers the opening of voltage-gated calcium channels called T-type channels (T stands for “transient”). This event raises calcium conductance, which depolarizes the cell even further. Although the T-type channels stay open for

only a short time before becoming inactivated, the resulting depolarization to threshold triggers the opening of a second population of voltage-gated calcium channels called L-type channels (L stands for “long-lasting”), which stay open longer and become inactivated only slowly [5][6].

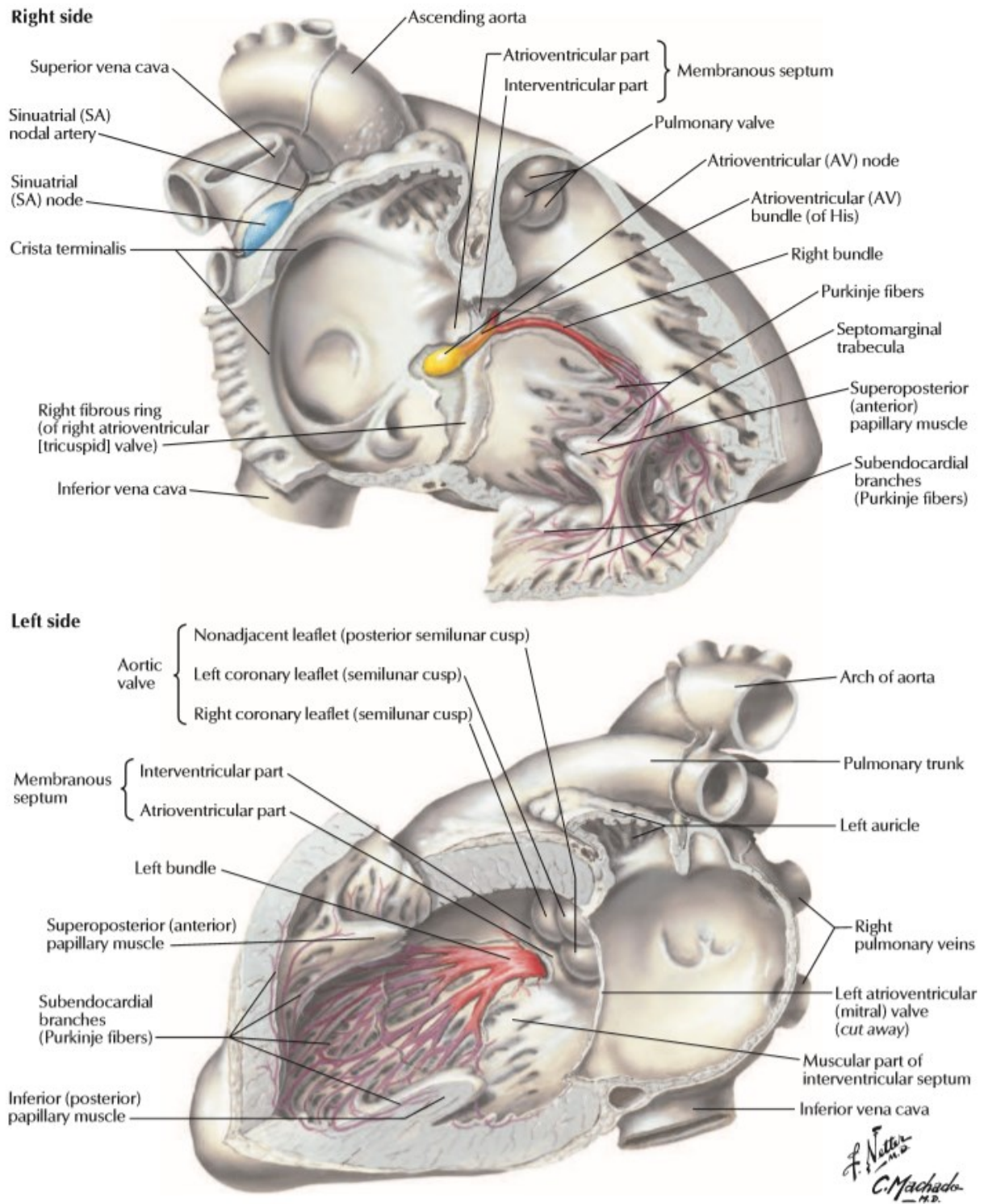


Figure 4 Plate 229 shows the conducting system of the heart. Atlas of Human Anatomy from Frank H. Netter 7th edition [7].

The result is a rapid depolarization characteristic of the upswing of the action potential. This depolarization triggers the opening of potassium channels and, consequently, a rise in potassium current; the result is to pull the membrane potential back down. The subsequent fall in potential removes the stimulus for calcium channel opening, allowing these channels to begin closing. This event reduces the flow of calcium into the cell, which works along with the increase in potassium current to repolarize the membrane and terminate the action potential [5][6].

The AP is conducted from SA node to AV node through the atrial myocardium. There are some preferential pathways, but they are not unique neither isolated. From AV node the excitation is transmitted to ventricles by His bundle, left and right bundle branches (LBB, RBB) and the Purkinje fibres [5][6]. The conduction through the AV node is slower because of the network of very fine fibres and the calcium type action potentials [5][6]. This fact produced a programmed delay between atrial and ventricular contraction that enable the complete filling of the ventricles and an efficient pump function [5][6]. Finally, the depolarizing current is transmitted from myocyte to myocyte working as a functional syncytium [5][6]. Myocytes are excitable cells and the AP spreads along them. At rest their membrane potential is about -90 mV. Voltage membrane is mainly determined by three ions sodium  $\text{Na}^+$  Potassium  $\text{K}^+$  and Calcium $^{2+}$ . Potassium ions are more concentrated inside the cells with respect to the outside, while sodium and calcium have a higher concentration outside the cell [5][6]. The rest membrane potential is maintained thanks to electrochemical forces and the potential is mainly determined by  $\text{K}^+$  ions given their higher relative conductance at rest. Ion conductance changes during the cardiac cycle determining the AP [5][6]. The heart work as a functional syncytium and the electrical excitation is transmitted from cell to cell through gap junctions [5][6]. Specifically, a depolarized cell has a more positive voltage than closer polarized (more negative) cell and current of  $\text{K}^+$  is generated through gap junction [5][6]. This current passively depolarizes the cell and if the voltage reaches a more positive threshold potential the action potential starts. AP has 4 phases and it is illustrated in panel (b) of Figure 5. In phase 0 of the cardiac AP, depolarization of the membrane triggers the opening of voltage-gated sodium channels, increasing the flow of sodium ions into the cell [5][6]. Consequently, the membrane potential becomes more positive, which triggers the opening of still more sodium channels, additional increases depolarization [5][6]. The result is a rapid rise in membrane potential that peaks between +30 and +40 mV. In phase 1, the sodium channels that were opened in phase 0 start to become inactivated, which reduces sodium conductance across the membrane [5][6]. This decreases the flow of sodium into the cell and causes the membrane potential to fall toward more negative values because potassium ions continue to move out of the cell [5][6]. The



membrane potential drops only a small amount, however, because the depolarization of the membrane that began in phase 0 has set into motion two additional events that are occurring at this time: (1) the closing of voltage-gated potassium channels, which reduces potassium conductance and decreases the flow of potassium out of the cell (2) the opening of L-type calcium channels, which raises calcium conductance and increases the flow of calcium into the cell [5][6]. Both these changes act to depolarize the membrane, thereby counteracting the effect of sodium channel inactivation [5][6]. During phase 2, which is also referred to as the plateau phase, most of the potassium channels that were closed in phase 1 stay closed and most of the calcium channels that opened in phase 1 remain open, keeping the membrane in its depolarized state [5][6]. During phase 3, potassium conductance increases, partly because of the action of a second population of potassium channels called delayed rectifier channels, which open in response to depolarization [5][6]. These channels begin to open during phases 1 and 2 but do not exert a significant influence on the membrane potential until phase 3 because they open slowly [5][6]. As potassium conductance rises, the flow of potassium out of the cell increases, which pulls the membrane potential down toward more negative values [5][6]. Furthermore, this fall in potential removes the stimulus that kept the inward rectifier channels closed in phase 2; as a consequence, these channels begin to open, which raises potassium current even further [5][6]. The fall in potential also removes the stimulus that kept the calcium channels open during phase 2 and allows them to begin closing, which lowers calcium current and reduces the flow of calcium into the cell. These phenomena repolarize the membrane, thereby terminating the action potential [5][6]. An important process in repolarization phase is the activation of sodium channels, which remain closed but their inactivation gate opens making them available for the generation of next AP. During phase 4, which corresponds to the stable resting potential, conductances of sodium, potassium and calcium are at their resting values [5][6]. During action potential ion currents move following gradient concentration. Instead in phase 4, an active process (ATP energy needed) restores the resting ion concentrations through the  $\text{Na}^+/\text{K}^+$  pump [5][6]. The calcium concentration is restored by  $\text{Ca}^{2+}$  ATPase pump and the  $\text{Na}^+/\text{Ca}^{2+}$  exchanger [5][6].

The cardiac AP presents an absolute refractory period, during which no further AP can be generated, followed by a relative refractory period. Further, the AP lasts as long as the contraction avoiding cardiac muscle tetanisation. In this way, ventricles can relax before the next AP is generated, enabling a complete filling and pumping of the blood [5][6].

The action potential shape is heterogeneous in different regions: endocardial AP are longer and have a flatter phase 2 than epicardial AP, which present a spike and doom in phase 2 [6].

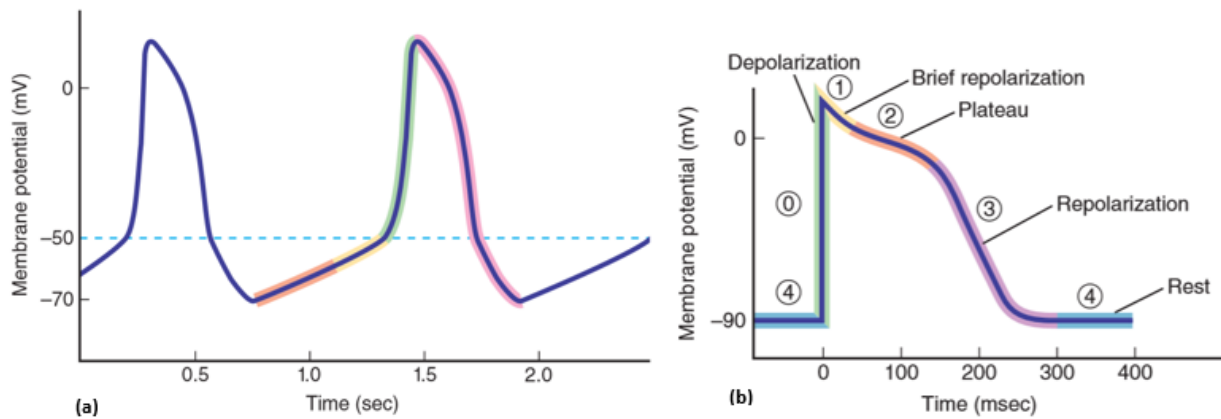


Figure 5 (a) Pacemaker potential. The two phases of spontaneous depolarization in orange and yellow, rapid depolarization in green, the repolarization phase in pink. (b) The cardiac action potential. Phase 0 in green, phase 1 in yellow, phase 2 in orange, phase 3 in purple and phase 4 in blue. The pictures are taken from the book 'Principle of human physiology' Cindy L. Stanfield [5].

The conduction velocities of AP throughout the heart have large regional differences, being slower in atrial and ventricular muscles and higher in conduction system. Conduction speed depends on steepness of phase zero of AP, amplitude of AP, fibre diameter and direction of conduction longitudinal or transversal. Conduction is faster in thick fibres along their longitudinal direction, and in  $\text{Na}^+$  type action potential with steeper upstroke than  $\text{Ca}^{2+}$  type action potential [5][6].

### 1.1.2.1 Electrocardiography

Electrical activity of the heart can be measure through electrocardiography. Surface electrocardiogram (ECG) records the spatial summation of time-dependent changes in electrical activity within the heart during depolarization and repolarization of the myocardial tissue. Depending on the leads and the lead system used the ECG morphology is different, the typical waveform will be here described (presented in Figure 6) to highlight the relation of waves with the cardiac cycle and the normal values of an ECG for health subjects.

P wave represents the wave of depolarization that spreads from the SA node throughout the atria; it is usually from 80 ms to 100 ms in duration [5][6][8]. P wave characterizes the intra atrial conduction that can change because of conduction disturbances and atrial enlargement [5][6][8]. The isoelectric period after the P wave (PQ segment, between the offset of the P wave and the onset of Q wave) represents the time in which the atrial cells are depolarized and the impulse is traveling within the AV node, where conduction velocity is greatly reduced [5][6][8]. The period of time from the onset of the P wave to the onset of the QRS complex, the PR interval, normally

ranges from 120 ms to 200 ms [5][6][8]. This interval represents the time between the onset of atrial depolarization and the onset of ventricular depolarization [5][6][8]. It is measured to assess the integrity of atrium/ventricular conduction [5][6][8]. The atrial repolarization is not visible because covered by the higher ventricular depolarization voltage [5][6][8]. The QRS complex represents ventricular depolarization and characterizes the intra ventricular conduction [5][6][8]. The duration of the QRS complex is normally 60 ms to 110 ms in duration, indicating that ventricular depolarization occurs rapidly [5][6][8]. If the QRS complex is prolonged (>120 ms), conduction is impaired within the ventricles [5][6][8]. The isoelectric period (ST segment, between the offset of the S wave and the onset of the T wave) following the QRS is the period at which the entire ventricle is depolarized and roughly corresponds to the plateau phase of the ventricular action potential [5][6][8]. The ST segment is important in the diagnosis of ventricular ischemia [5][6][8]. The T wave represents ventricular repolarization (phase 3 of the action potential) and lasts longer than depolarization [5][6][8]. During the QT interval (interval between the onset of the QRS complex and the offset of the T wave), both ventricular depolarization and repolarization occur [5][6][8]. QT interval can range from 200 ms to 400 ms depending on heart rate (HR, bpm) [5][6][8]. At high heart rates, ventricular action potentials are shorter, decreasing the QT interval. For this reason, QT measurement is usually corrected for HR [5][6][8]. There are different formulas, the most diffused is the Bazett equation, formula (1):

$$QTc = \frac{QT}{\sqrt{RR}} \quad (1)$$

where RR is the average RR interval in seconds, equal to 60/HR [8].

ECG can sometimes present U wave but its origin is not certain. It seems to be associated to the ventricular repolarization together with the T wave [5][6][8].

Cardiac rhythms (atrial and ventricular rates of depolarization) can be determined in ECG from the frequency of P waves and QRS complexes by recording a rhythm strip. A rhythm strip is usually generated from a single ECG lead (often lead II). In a normal ECG, a consistent, one-to-one correspondence exists between P waves and the QRS complex; that is, each P wave is followed by a QRS complex. This correspondence indicates that ventricular depolarization is triggered by atrial depolarization. Under these normal conditions, the heart is in sinus rhythm, because the SA node is controlling the cardiac rhythm. Normal sinus rhythm can range from 60 to 100 bpm at rest [5][6][8].

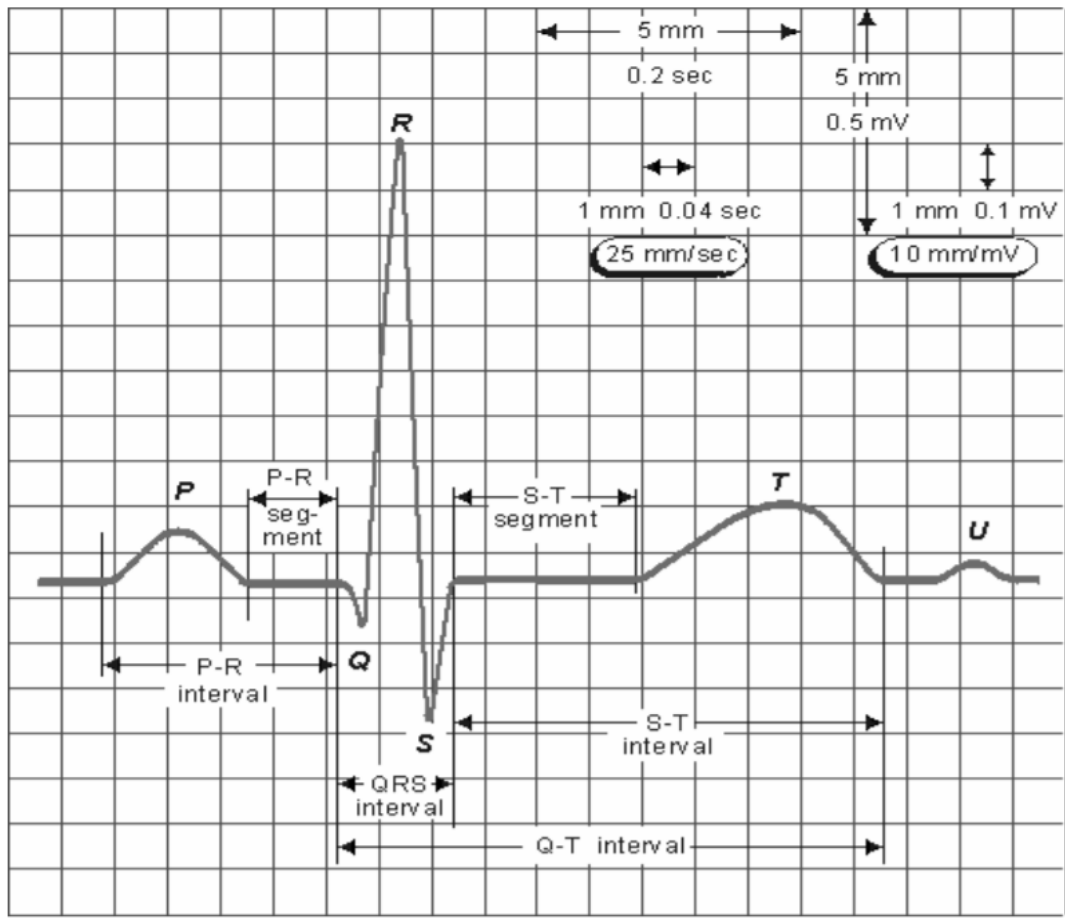


Figure 6 Typical ECG waveform [9].

### 1.1.3 Mechanical physiology

Myocardium is composed by striate muscular fibers. From the microscopic point of view, the myofilaments of contractile proteins are arranged into the sarcomere, the contractile unit. Contractile proteins are actin (thin filament) and myosin (thick filament). Sarcomeres form myofibrils that in turn constitute myocytes. Myocytes are connected at the level of intercalated disk by desmosomes (mechanical connection) and gap junctions (electrical connection). Myocytes connects into myofibers which form the myocardium [5][6].

Thin filaments consist of actin a spherical protein, tropomyosin and regulatory troponin complex. Thick filaments are formed by 300 to 400 myosin molecules which have heads and tails [5][6]. When  $Ca^{2+}$  binds to TnC of the troponin complex, the latter change conformation moving the myosin into actin grooves and unmask the myosin head binding site on the actin molecules [5][6]. Then myosin heads can bind to actin, forming cross bridges [5][6]. The cross bridge cycle is illustrated in details in Figure 7, while the cross bridge cycle in the contest of excitation-contraction

coupling is shown in Figure 8. The  $\text{Ca}^{2+}$  that initiates cross-bridge formation is released from the sarcoplasmic reticulum when the ryanodine receptors (RyR) sense the inflow of  $\text{Ca}^{2+}$  from the L type  $\text{Ca}^{2+}$  channels at the level of T tubules [5][6]. Calcium ions return into the SR through SERCA (sarco-endoplasmic reticulum calcium ATPase) at the end of contraction to enable relaxation of fibers. Sarcomeres contains Titin, a giant protein that anchors M-line to the Z-line. Titin has passive elasticity and it is the main responsible for the passive tension developed during the passive ventricular filling phase of the cardiac cycle [5][6].

Myocytes contain mitochondria that produce ATP, essential for contraction and relaxation, through oxidative phosphorylation. Energy production in normal healthy heart depends on oxidative phosphorylation for 95%, as glycolytic metabolism is capable of generating no more than 5% required for normal contractile performance [5][6].

The cross bridges cycle is mainly determined by  $[\text{Ca}^{2+}]$  and ATP.  $\text{Ca}^{2+}$  molecules make myosin binding site free on actin by attaching to the regulatory troponin complex, thus high  $[\text{Ca}^{2+}]$  leads to contraction while low  $[\text{Ca}^{2+}]$  characterizes relaxation. ATP instead attach to myosin to enable the passage from the attached state to the released state of the cross-bridge cycle, so relaxation. The same ATP molecule is used by myosin as energy for the next cycle [5][6].

As for skeletal muscles, sarcomeres have an optimal length thus an optimal myosin-actin overlap that enable the generation of maximum force. Frank Starling mechanism is the main mechanism of self-regulation of the heart: cardiac stroke volume (SV, mL) increases with increased filling before contraction starts. The mechanism is such that an increase in venous return leads to an increased stretching of the ventricles hence to a better contraction and to a stronger pumping function [5][6]. Sarcomere force-length relationship is at the base of Frank Starling law; the possible mechanisms behind it are [5][6]:

- optimal myosin-actin overlap;
- reduced lateral spacing between thin and thick filaments;
- orientation of myosin head;
- increased  $\text{Ca}^{2+}$  sensitivity with stretch.

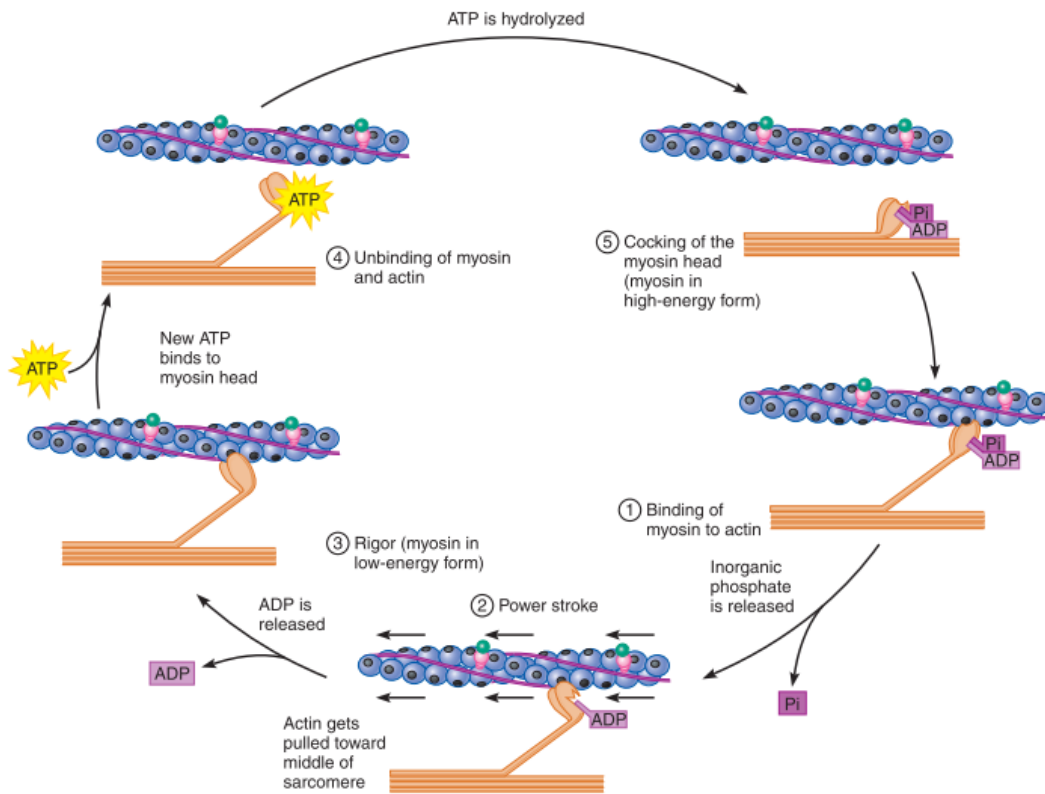


Figure 7 Crossbridge cycle [5].

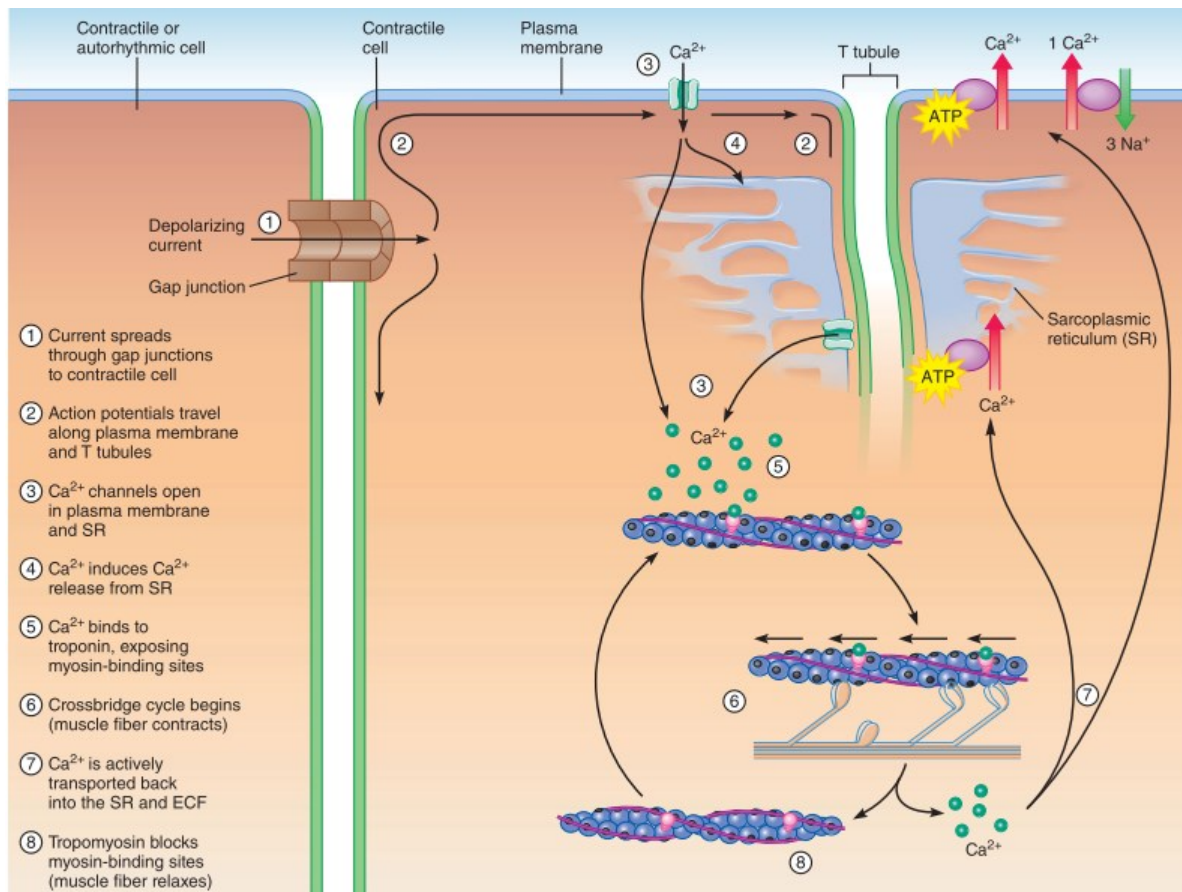


Figure 8 Crossbridge cycle in excitation-contraction coupling process[5].

Mechanical contraction of the myocardium results in the pump function of the heart repeated each cardiac cycle. Wiggers diagram describes the pump function along the cardiac cycle Figure 9. Wiggers diagram contains pressure curves of atria, ventricles, aorta and pulmonary artery, ventricular volume curves. The Wiggers diagram represents the 4 phases of cardiac cycle: filling phases, isometric contraction, ventricular ejection, isometric ventricular relaxation. Right and left heart pump the same amount of blood following the same cardiac cycle events. The main differences regard pressures, which are higher in the left side compared to the right side. For simplicity only left heart cycle is described since the same steps are applicable to the right heart [5][6].

Left ventricle filling phase starts with the situation that aortic valve is closed and the mitral valve is open. At the beginning there is a rapid filling phase in which the pressure is going down very fast when the mitral valve opens and the ventricle starts to fill (attraction of blood from the atrium create a negative pressure). Then a minor filling phase occurs because the pressures in left atrium and ventricle are almost the same (~8 mmHg). The early filling phase is passive and accounts for the ~80% of ventricular filling. During the late ventricular filling, a little pressure wave occurs, that represents the contraction of the atrium contributing to ventricular filling, it is also called atrium kick. Atrial kick contributes to ~ 15-35% to the blood volume in the ventricle. This extra volume in turn increases cardiac output (CO, L/min) by a similar ~ 15-35%. With aging, atrial kick tends to be a more significant contributor to cardiac output. In ventricular filling phase, the aorta pressure lower steadily because it spreads the blood to the systemic circulation and nothing enter the aorta, reaching ~80 mmHg [5][6].

LV isovolumetric contraction: the heart starts to contract because there was an electrical activation that interrupts the filling situation at the late of the phase 1. The pressure in ventricle is higher than pressure in atrium and the mitral valve closes. When the mitral valve close, there is a period in which the left ventricular volume curve shows a constant trend that is called isovolumetric contraction, no blood entering no blood leaving, until the moment that the left ventricular pressure became higher that the aortic pressure. When the heart starts to contract, the pressure in ventricle is going up until the point in which the ventricular pressure became equal to the aortic pressure and then higher that aortic pressure. At that point the aortic valve opens and the ejection phase starts [5][6].

During LV ejection, the ventricular pressure is higher that the aortic pressure and this pressure is needed to realize the flow of blood from the heart to the aorta against the afterload. In this phase

the left ventricle volume curve decreases (empty phase). This phase occurs until the aortic valve becomes close because LV pressure is lower than aortic pressure. During phase 3, the left atrium already starts to fill when the left ventricle is still emptying. A rapid ejection and a decreased ejection can be considered for the left ventricle. In the rapid ejection the left ventricular pressure is higher than aortic pressure and during the decreased ejection the pressure values reverse. During ejection phase the normal maximum LV and aortic pressure is around ~120 mmHg [5][6].

LV isovolumetric relaxation: the ventricle is now relaxing that is manifested by a decrease in pressure. In the aortic pressure curve the incisura and the dicrotic wave are present, the incisura is given by the closure of aortic valve, while the dicrotic wave by the back reflection of pressure wave. When the left ventricular pressure became lower than atrial pressure the mitral valve opens and this terminate phase 4 [5][6].

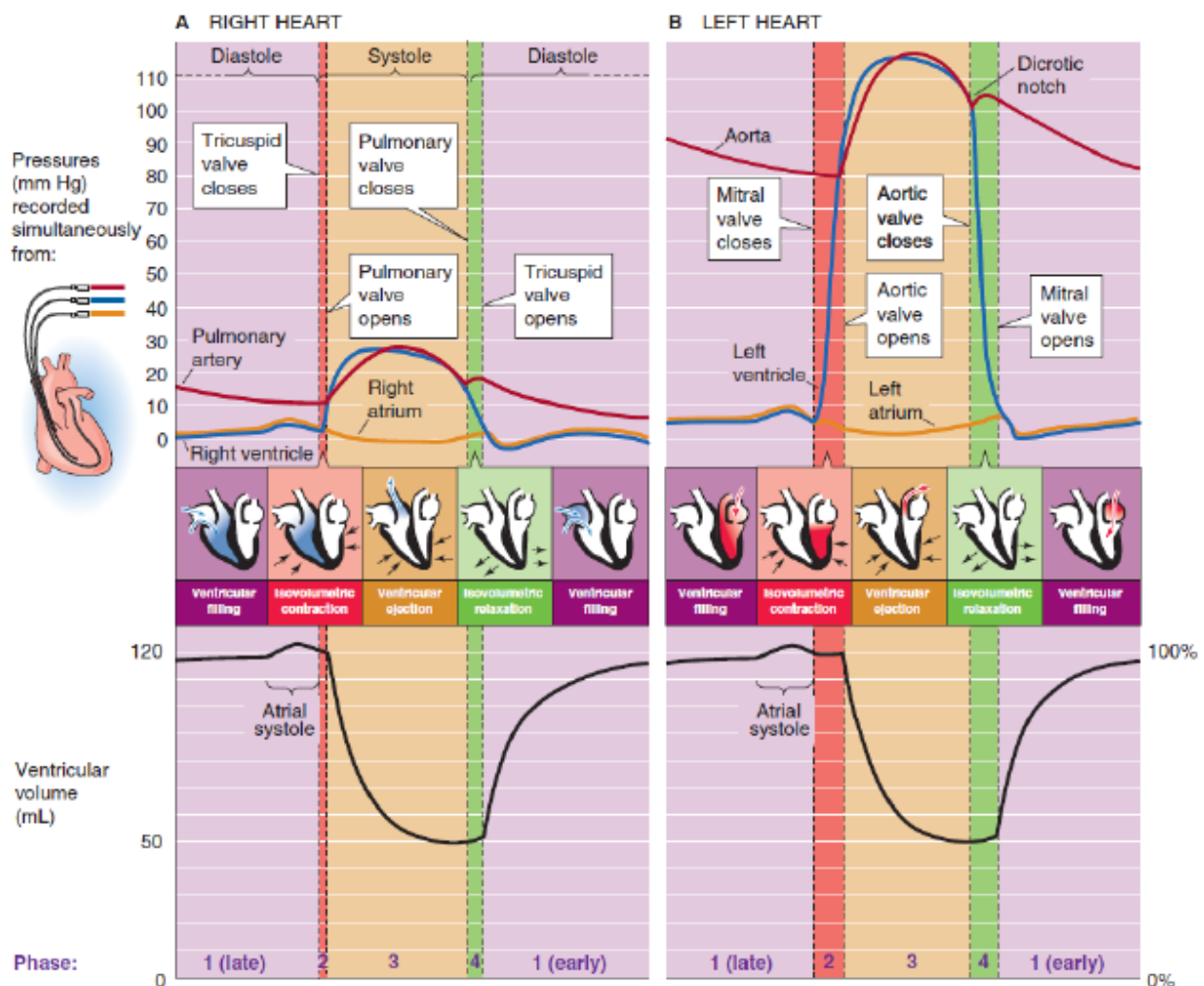


Figure 9 Wiggers diagram. Picture taken from Boron & Boulpaep: Medical Physiology, 3<sup>rd</sup> Edition [10].



The heart pump function is also described by the Pressure-Volume (PV) loop of LV (Figure 10). The two main parameters computed from it are SV and ejection fraction (EF). SV is the quantity of blood ejected in each beat and is given by the difference between end diastolic volume (EDV) and end systolic volume (ESV) [5][6]. Multiplying the SV by the HR, the cardiac output (CO) is obtained. EF is a measurement, expressed as a percentage, of how much blood the left ventricle pumps out with each contraction, with the formula (2) [5][6]:

$$EF = \frac{EDV - ESV}{EDV} \quad (2).$$

SV is influenced by contractility, preload and afterload [5][6]:

- increasing contractility without changing preload and afterload condition leads to a lower ESV and thus to an increase in SV;
- increased preload (filling) means that increases the fillings and the contraction starts with higher EDV, leading to increased SV for Frank Starling mechanism;
- increased afterload (aortic pressure) leads to an earlier closure of the aortic valve, so to a lower SV.

EF is an important parameter in predicting cardiac risk. Normal EF should range between 50% - 60%. When EF is < 30% - 35% , it is indicator of arrhythmia and risk for SCD [5][6].

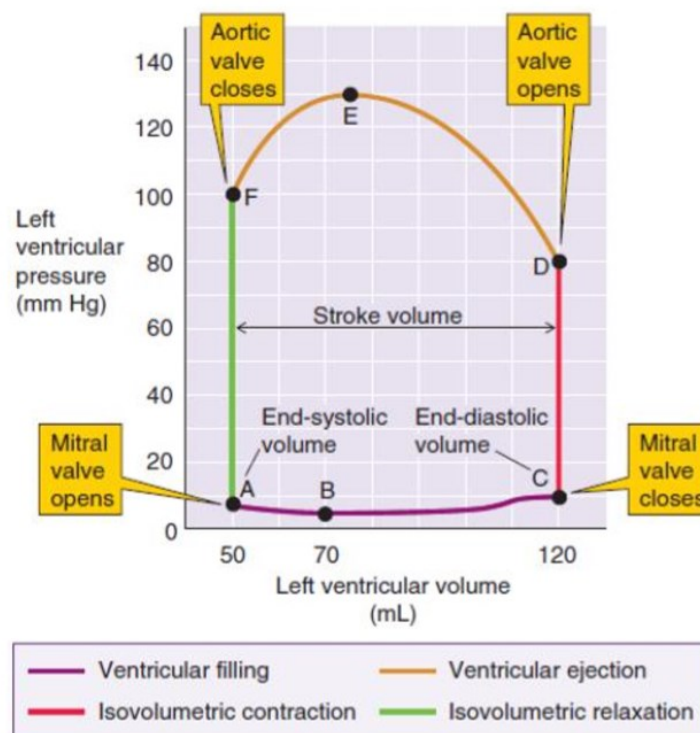


Figure 10 Pressure Volume (P-V) loop [10].

The last described mechanical characteristic is compliance, which defines the filling characteristics of the heart. The more compliant heart the easier is to fill the heart. Compliance is equal to the ratio  $dV/dP$ . The more the heart is filled, the more the pressure increases. In the increased compliance more filled can be the heart at the same pressure respect the normal compliance; it is a bad sign because the heart is enlarged and thus the contraction is not very good. Thus, heart cannot expel much blood because the contraction is corrupted. Indeed, it is not correct to relate simply EDV volume to sarcomere length (a determinant of contractility). *e.g.*, in a remodelled heart with structural dilation, new sarcomeres may have formed that have a quite normal length. Stretched hearts are not necessarily stronger. In the other hand, in the decreased compliance, the heart is hypertrophic, and it reaches higher pressure in very small volume. Increased or decreased compliance can be considered as pathological conditions [5][6].

## 1.2 Circulation

Blood leaves the heart through aorta and pulmonary artery. From the aorta, blood travels into the systemic circulation bringing oxygen and nutrients to tissues and organs through arteries, arterioles and capillaries. Deoxygenated blood comes back to the right atrium through venous system (venous capillaries, venules and veins). Pulmonary circulation starts from right ventricles and pulmonary artery, which brings deoxygenated blood to the lungs. After being oxygenated, blood enters into the left atrium through four pulmonary veins [5].

Coronary arteries bring oxygenated blood to the heart. Deoxygenated blood is drained by coronary veins and return to the right atrium through coronary sinus. Coronary veins run parallel to the coronary arteries. The following section focuses on the description of coronary system since it is the vascular structure treated in this work, specifically in the biofluid dynamic section [5].

### 1.2.1 Coronary arteries anatomy

Coronary arteries are the arterial vessels that bring oxygen-rich blood to the myocardium. They arise from the aortic root, more precisely from the sinuses of Valsalva (Figure 11). The main branches are two: left coronary artery (LCA) and right coronary artery (RCA) [5]. Depending on their distribution, coronary dominance can be defined. In clinical practice, coronary dominance is determined by the coronary that gives rise to the posterior interventricular branch that supply blood to the posterior and inferior wall of the left ventricle (LV) and the posterior interventricular septum:

- Right dominance, the posterior branch originates from the RCA (80-90 % of cases)
- Left dominance, the posterior branch originates from the LCA (10-15 % of cases)
- Codominance, the posterior branch originates from RCA while the posterior wall of left ventricle is supplied by LCA (5% of cases).

The anatomy of coronary arteries is visible in Figure12 and Figure 13.

#### Left coronary artery

The main stem (LM) of the left coronary artery originates from the left sinus of Valsalva and travels anteriorly and to the left towards the sternocostal surface of the heart, being positioned between the left atrial appendage and the pulmonary trunk [11]. It usually divides after about 1 to 2 cm into the circumflex artery (LCX) and anterior interventricular or descending, artery (LAD) [11]. These major branches supply most of the left ventricle, the ventricular septum, and the left

atrium, and in two fifths of the population give rise to the artery to the sinus node from LCX [11]. In some individuals, the main stem gives rise to a third branch, the intermediate artery. The intermediate artery runs in an intermediate position between LAD and LCX, on the anterolateral wall of the left ventricle and it supplies the area normally covered by the diagonal and/or obtuse marginal arteries [11].

- *Anterior Interventricular (Descending) Artery* , after gently curving around the pulmonary trunk, it enters the anterior interventricular groove then coursing up to the apex of the heart [11]. It then typically (in left dominant population) passes around the apex, ascending within the inferior interventricular sulcus towards the crux, and supplying branches to the apical surfaces of the inferior walls of both ventricles [11]. It gives rise to the diagonal arteries and the deep septal perforators; both sets of vessels vary in their number and course [11]. The diagonal arteries course along and supply the parietal wall of the left ventricle [11]. The deep septal perforators originate at right angles to the LAD and supply the anterior muscular ventricular septum [11]. The left descending septal artery is the most prominent branch of the septal perforators, it supplies moderator band, before terminating at the anterior papillary muscle [11].
- *Circumflex Artery* branches at an angle perpendicular to the main stem, entering and coursing through the left atrioventricular groove [11]. In most individuals who are right dominant, LCX terminates as the left obtuse marginal artery in the obtuse heart margin [11]. While in left dominant subjects, when LCX is dominant (one tenth of individuals), LCX reaches to the cardiac crux and gives rise to the artery to the atrioventricular node and the inferior interventricular artery [11]. Significant branches of LCX supply the posterior and lateral walls of the left ventricle and the supero-lateral papillary muscle [11]. Smaller branches of LCX are instead responsible for supplying the root of the aorta and ventricular myocardium adjacent to the atrioventricular groove [11]. A variable branch, known as the left atrial circumflex artery, may arise from the circumflex artery early in its course, and travel parallel to its parent artery [11].

#### Right coronary artery

RCA originates from the right sinus of Valsalva and enters directly the atrioventricular groove, descending anteriorly and inferiorly to the right border of the heart [11]. RCA irrigates the right ventricle and in right dominance cases, carries blood to the lower and posterior walls of the left ventricle. In fifty percent of population, the first branch departing from RCA is the infundibular,

or conal, branch [11]. In the other half of subjects the infundibular branch arises directly from a second orifice within the right sinus of Valsalva [11]. The right marginal artery is the largest branch of the RCA, and starts proximal to the acute margin coursing to the apex of the heart [11]. Moreover, when the LCX does not irrigates the sinus node, the artery to the sinus node originates from RCA [11]. The greatest percentage of population has a right coronary arterial dominance, RCA continues beyond the crux of the heart to the inferior interventricular artery and it provides the primary supply to the infero-septal papillary muscle and the diaphragmatic surface of the left ventricle [11]. In these cases the artery to the atrioventricular node also arises from the RCA [11].

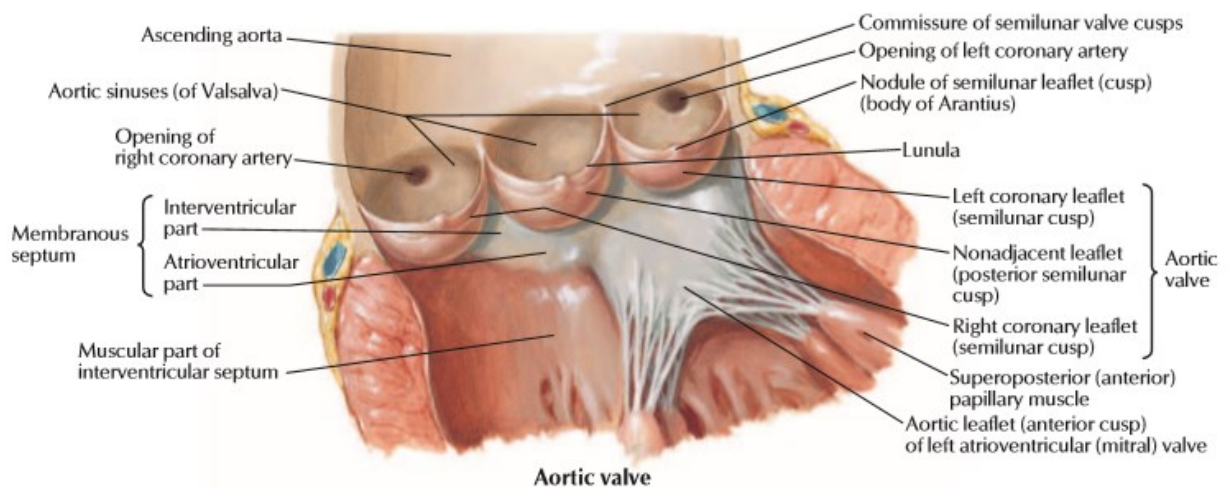
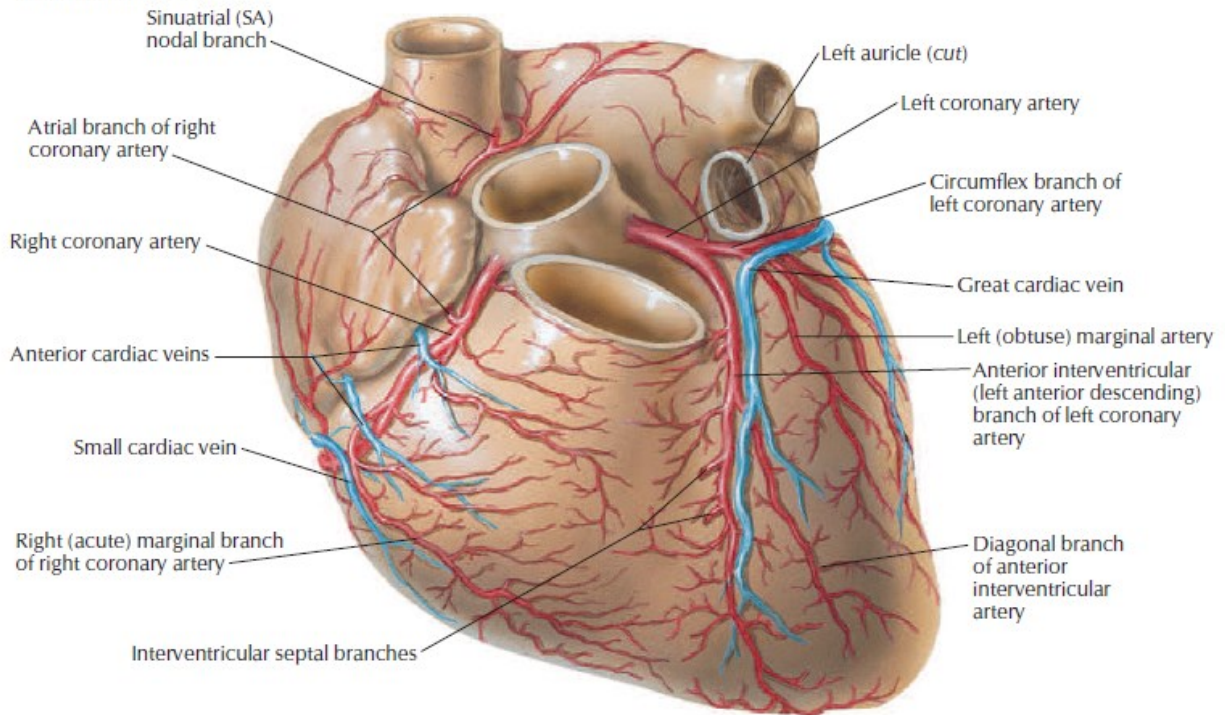


Figure 11 Plate 227 shows the aortic valve and the sinus of Valsalva. The representations are taken from the Atlas of Human Anatomy from Frank H. Netter 7th edition [7].

**Sternocostal surface**



**Diaphragmatic surface**

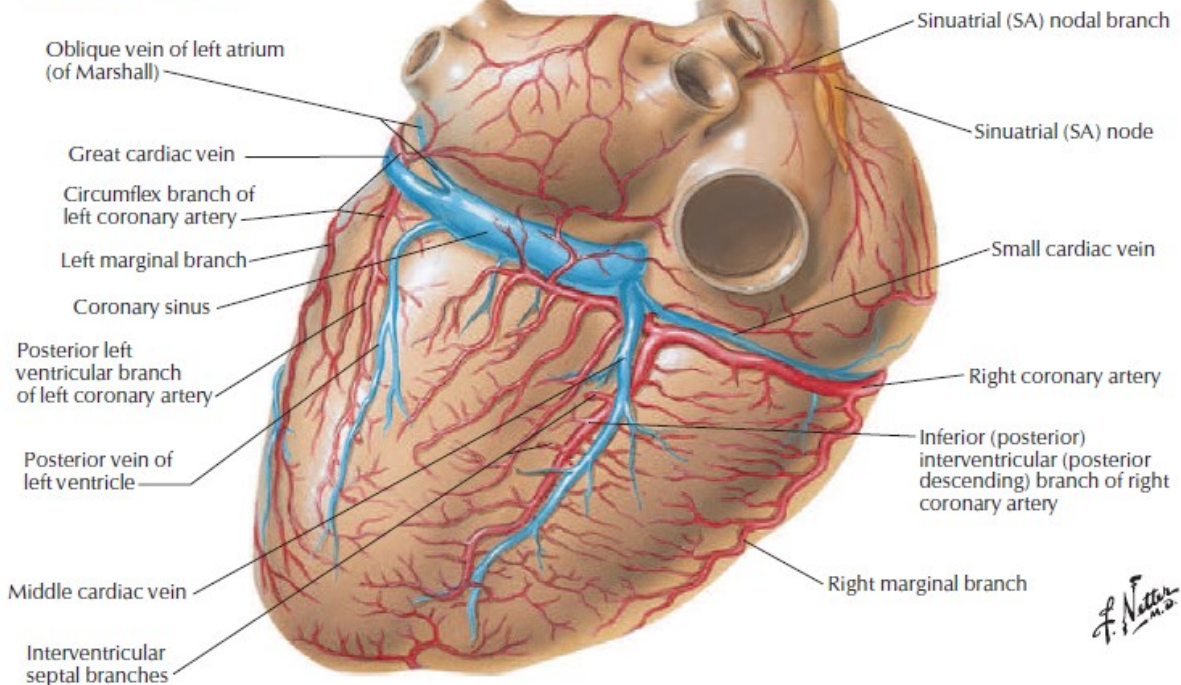


Figure 12 Plate 222 shows coronary arteries in red and cardiac veins in blue on the sternocostal surface (upper panel) and on diaphragmatic surface (bottom panel) of heart. The representations are taken from the Atlas of Human Anatomy from Frank H. Netter 7th edition [7].



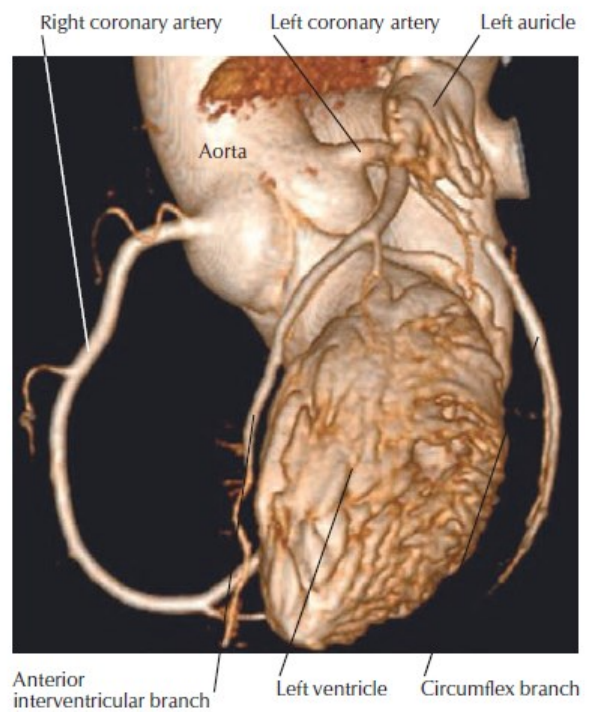
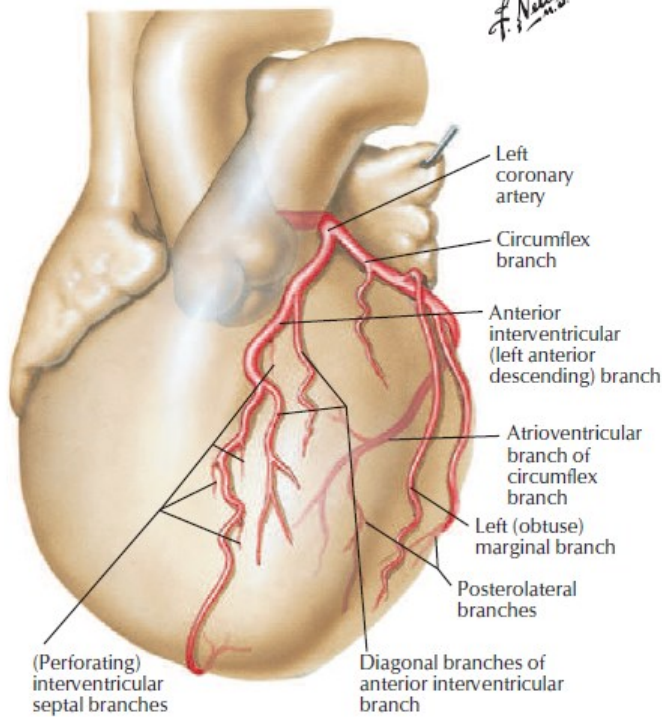
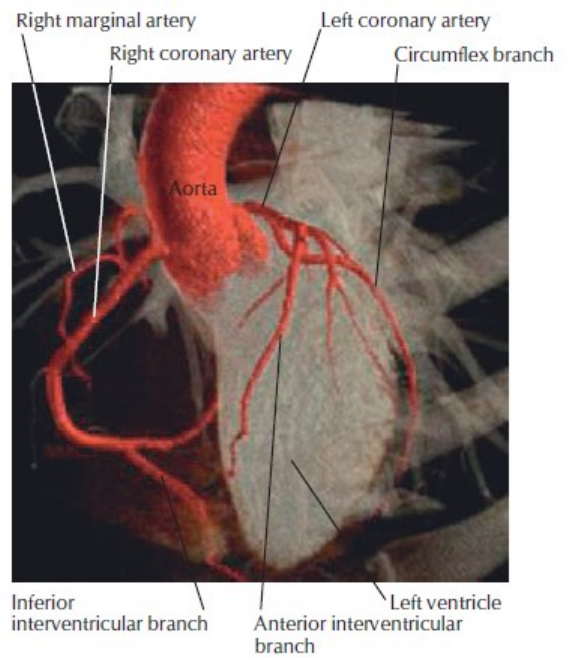
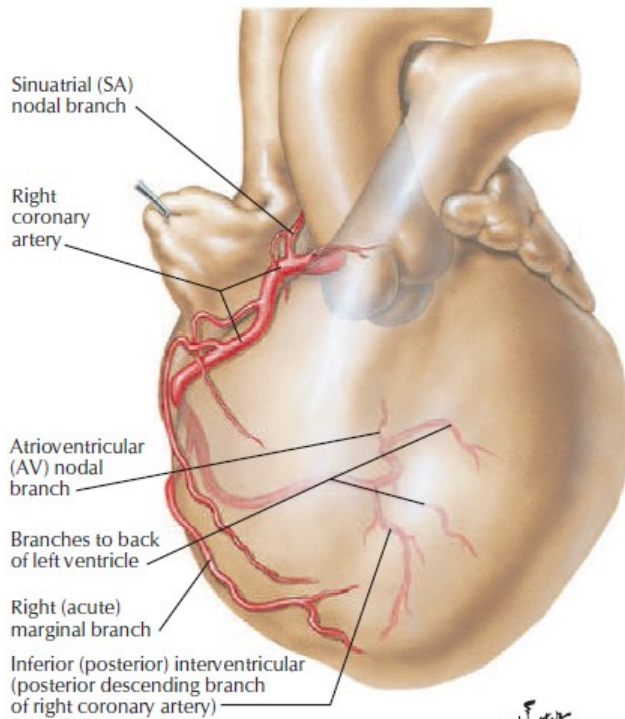


Figure 13 Plate 223 shows separately the right and left branches of coronary arteries respectively the upper and the bottom panel of the left part of the figure. Picture of coronary arteries from volume rendering imaging are present in the right side. The representations are taken from the Atlas of Human Anatomy from Frank H. Netter 7th edition [7].

### 1.2.2 Vessel structure

The coronary artery (muscular artery) wall consists of three layers. The inner layer (covering the luminal surface of vessel) is called intima, the middle layer is called media, and the outer one is called the adventitia [12].

The intima layer has a layer of endothelial cells plus connective tissue, namely few collagen bundles and basal lamina. Subendothelial area contains bundles of longitudinally arranged muscle cells, which is consistent with the longitudinal arrangement of inner media muscle cells. The intima is very thin and does not contribute to the mechanical properties of the vessel wall. The intima has a variable thickness, which is expressed as a ratio of media thickness. Ratios of 0.1–1 are considered normal [12].

The media consists of connective tissue, collagen, elastin, other elastic fibers and smooth muscle cells. Smooth muscle cells are responsible for vasodilation and vasoconstriction. Thus, the media layer has a fundamental role at physiological conditions under normal hemodynamic load. The thickness of a normal media layer is between 125 and 350  $\mu\text{m}$  (average 200  $\mu\text{m}$ ). However, the media layer in an atherosclerotic site is thinner and ranges between 16 and 190  $\mu\text{m}$  (average 80  $\mu\text{m}$ ) [12].

The adventitia layer protects the vessel wall from over-stretch as well as to mechanically couple to the surrounding tissues. It consists of fibrous tissue, fibroblasts and hydrophilic macromolecules (including glycosaminoglycans, proteoglycans and glycoproteins). Adventitia has many collagen bundles and a few elastin fibers. Elastin and collagen fibers form concentric densely packed fiber sheets in inner adventitia, and collagen fibers largely orient towards the axial direction of the artery. Elastin is parallel with collagen fiber but with secondary direction forming a netlike structure. Collagen bundles gradually become thicker and distributed randomly toward the exterior adventitia whereas elastin fibers were largely absent [12].



### **1.2.3 Mechanical properties of normal coronary arteries**

The arterial vessels behave as anisotropic materials due to the presence of fibers that exert mechanical resistances only along preferential directions. From the microscopic point of view, they are non-homogeneous materials due to their composition and each component has a different mechanical property.

In arteries, elastin fibrils have relatively lower stiffness and larger deformability, which helps to support blood vessels at low pressure, whereas collagen fibers are undulated and do not withstand for the low pressure loads. At high pressure, collagen fibers become straightened and engaged to carry most of the load. Engaged collagen fibers are much stiffer than elastin fiber, leading to a rapid increase in strain-stress curve of blood vessel. The modulus of elasticity of collagen is approximately 400 times greater than that of elastin [12].

The mechanical response of individual coronary layers is a direct result of microstructure. Largely longitudinal alignment of elastin and collagen fibers of adventitia layer induce a larger axial stress than circumferential stress, while media layer presents a higher circumferential stress than adventitia, since the smooth muscle cells orient towards the circumferential direction of coronary arteries [12].

Contraction of smooth muscle cells provides active response to physiological loads by altering circumferential as well as longitudinal mechanical properties of blood vessels [12]. Regarding active mechanical properties of coronary arteries, many studies showed that blood vessels present a uniaxial vasoconstriction; i.e., contracting only in the circumferential direction with no axial response. Other analysis suggest a biaxial response of coronary arteries in which smooth cardiac muscle contraction induced vessel stiffer in both circumferential and axial directions [12].

It can be inferred that an elastic, homogeneous and isotropic model is not enough to describe vessel wall in hemodynamic models and a more complex model including anisotropic characteristic should be chosen [13].

### 1.3 Regulation of cardiovascular system

Several mechanisms regulate the cardiovascular system.

Regarding neuronal control, both sympathetic and parasympathetic autonomic nervous system innervates the heart and the vasculature. Innervations are presented in Figure 14. The vagus nerve preferentially innervates the SA node and the AV node. Atrial muscle is also innervated by vagal efferents; ventricular myocardium is only sparsely innervated by vagal efferents. Vagal activation of the heart decreases heart rate (negative chronotropy), decreases conduction velocity (negative dromotropy), and decreases contractility (negative inotropy) of the heart. Vagal mediated inotropic influences are moderate in the atria and relatively weak in the ventricles. Activation of the sympathetic nerves to the heart increases heart rate (positive chronotropy), increases conduction velocity (positive dromotropy), and increases contractility (positive inotropy) of the heart. Sympathetic system influences both SA and AV nodes, atrial and ventricular myocardium [5][6][10].

The vasculature is subjected to extrinsic and intrinsic controls. The extrinsic system are neural and humoral controls, while the intrinsic system includes tissue metabolites, local hormones, myogenic and endothelial factor. The major target for control mechanisms is the vascular tone, an increase in vascular tone determines vasoconstriction while a decrease in vascular tone determines vasodilation. The sympathetic stimulation causes vasoconstriction while parasympathetic stimulation causes vasodilation on arteries and arterioles. The vasodilation by parasympathetic system affects only coronary arteries and genital vessels, in which muscarinic M<sub>2</sub> receptors are present. Only the sympathetic system affects the veins and venules by increasing the vascular tone and thus decreasing their capacitance [5][6][10].

Humoral control is the other extrinsic control on vasculature and it is exerted by several hormone [5][6][10]:

- circulating sympathetic neurotransmitters, mainly epinephrine (E), produced by the adrenal medulla under sympathetic stimulation, but also norepinephrine (NE);
- hormones produced by the renin-angiotensin- aldosterone system (RAAS);
- Atrial natriuretic peptide (ANP);
- Hormones produced by the hypothalamic-pituitary axis, e.g., vasopressin, also called antidiuretic hormone, ADH.

The autonomic nervous system exert an instantaneous control, while the humoral system has a slower action. The effect of neurohumoral activation on blood volume, cardiac output and arterial pressure are summarized in Table 1.

*Table 1 Effect of neurohumoral activation on blood volume, cardiac output and arterial pressure*

	Blood volume	Cardiac output	Arterial pressure
Sympathetic activity	↑	↑	↑
Parasympathetic activity	--	↓	↓
Circulating epinephrine	↑	↑	↓↑
Angiotensin II	↑	↑	↑
Aldosterone	↑	↑	↑
Atrial natriuretic peptide	↓	↓	↓
Arginine vasopressin	↑	↑	↑

↑= increase

↓= decrease

↓↑= dependent on plasma epinephrine concentration. Low concentration leads to vasodilation , high concentration to vasoconstriction

Finally, vasculatures are locally regulated concentration of tissue metabolites (high concentration of metabolites induces vasodilation of arterioles and arteries, as well as of capillary sphincter), myogenic and endothelial factors, extravascular compression and autoregulation [5][6][10].

For the scope of the present discussion about coronary arteries, it is important to highlight the nitric oxide NO among the endothelial factors and the extravascular compression mechanism. NO is the most potent vasodilator present in the body and produced under the influence amongst other of shearing forces. This mechanism is found in coronary arteries. Thus, if the heart is working harder (during exercise) and flow increases the coronary arteries dilate and allow more flow [5][6][10].

Extravascular compression mechanism explains how a muscle can block its own perfusion by contracting. This happens for the small branches of coronary arteries that run into the ventricular muscle and determines the coronary blood flow. Details about the mechanism in the biofluid dynamics section [5][6][10].

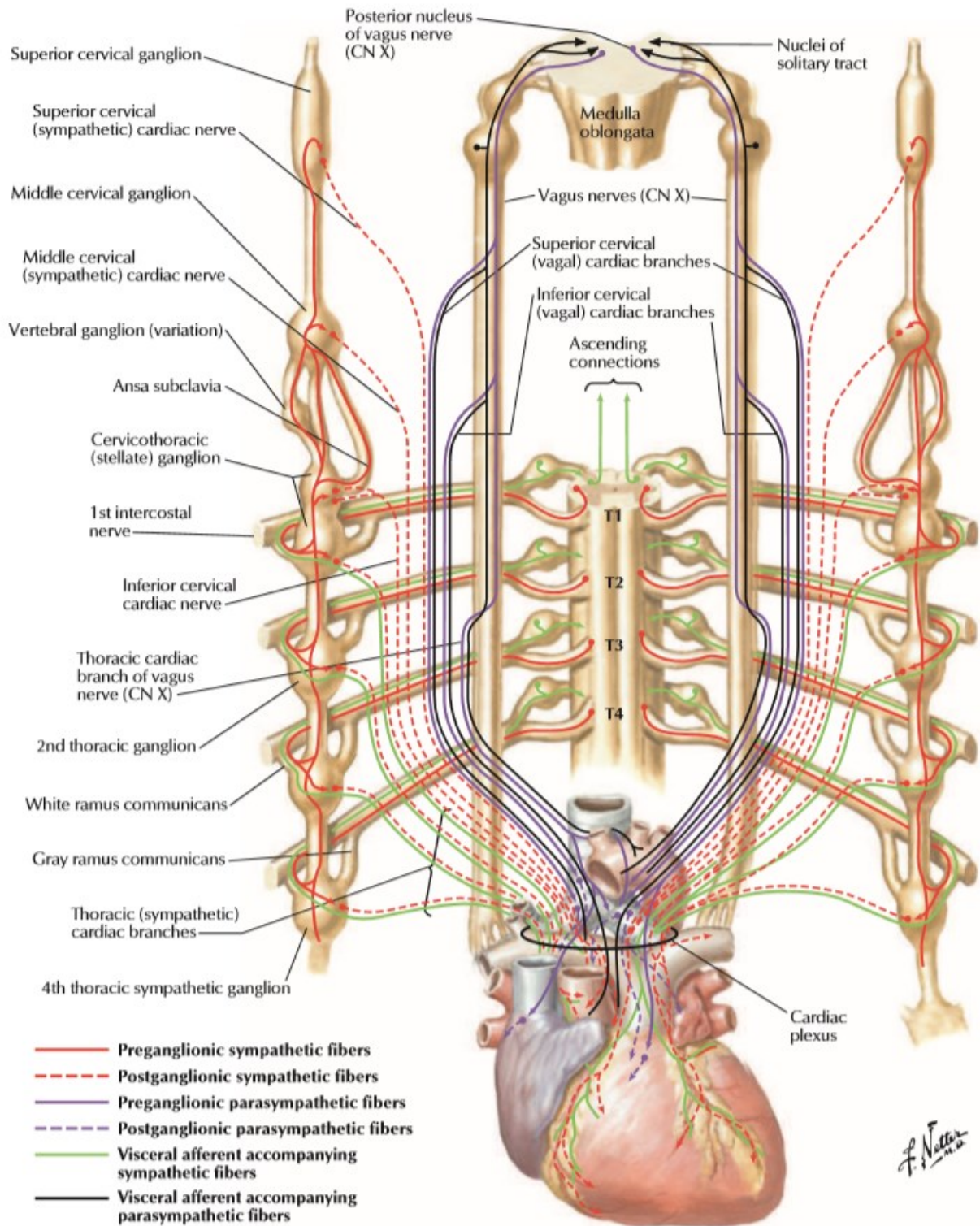


Figure 14 Plate 231 shows Sympathetic and parasympathetic innervation of the heart. The representation is taken from the Atlas of Human Anatomy from Frank H. Netter 7th edition [7].

### 1.3.1 Regulation of heart rate

The sinus node has an intrinsic HR without the influence of the autonomic nervous system. Intrinsic HR is different from the HR measured at rest, which is determined by the sympathovagal balance. SA node generates impulses at varying rate, 10% of rhythm variability is normal and mainly influenced by the natural mechanism of respiration. During expiration, HR slowed down and during inspiration HR faster again. Respiration interferes with cardiac filling determining blood pressure variability sensed by baroreceptors. The activation of the baroreflex mechanisms adjust HR and determines the HR variability. Normally in the negative feedback of baroreflex, an increase of pressure leads to a decrease in HR while a decrease of pressure leads to an increase in HR. thus fluctuations in blood pressure result in HR fluctuations with a certain delay. HR is dynamically adjusted by autonomic nervous system during daily activities. Informations about physical activity, skin temperature, respiration, blood pressure are sent to the cardiovascular centre in the brainstem by afferent fibres. The cardiovascular centre generates the appropriate sympathetic or parasympathetic responses. Temperature changes can change intrinsic heart rate. If body temperature raises by one degree °C there is an increase of about seven beats per minute in intrinsic heart rate. The central venous pressure (the right atrial pressure) by stretching the sinus node speeds up the intrinsic rate by about 6 percent for every mmHg pressure increase [5][6][10]. Autonomic nervous modulation of HR happens by modulating phase 4 of AP in pacemaker cells. Pacemaker cells have  $\beta$  adrenergic receptors and cholinergic receptors (muscarinic receptors). The first one is sensitive for epinephrine and norepinephrine neurotransmitters of the sympathetic nerves and the second one for acetylcholine (Ach) neurotransmitters of the parasympathetic nerves. There is a complex interaction between sympathetic stimulation and parasympathetic one. Sympathetic stimulation of  $\beta$  adrenergic receptors by epinephrine/norepinephrine enhances inward funny current  $I_f$  and calcium current  $I_{Ca}$ . These increased currents make the depolarization rate faster by making AP upstroke steeper and lower the threshold potential, thus increasing rate of pacemaker. This effect is inhibited by parasympathetic stimulation. Vagal stimulation of muscarinic M2-receptors by acetylcholine enhances outward potassium current  $I_K$ . This causes a more negative transmembrane potential at the beginning of phase 4 (longer time to reach the threshold at which the cell is going to fire), and hence decreases rate. Further, it makes depolarization rate slower (less steep upstroke of AP) and increases threshold potential by inhibition of sympathetic effect [5][6][10].

### 1.3.2 Regulation of myocardium contraction and relaxation

Most inotropy-regulating mechanisms affect calcium handling of the cell. There are six mechanisms [6]:

- L-type  $\text{Ca}^{2+}$  channel regulation by cAMP pathway; there are  $\beta$  adrenoreceptor sensitive for epinephrine and norepinephrine and they increase  $\text{Ca}^{2+}$  current through L-type channel, thus contractility. Muscarinic and adenosine receptors are also presented and they bind Ach and adenosine, inhibiting the cAMP pathway and thus decreasing contractility.
- Increase of  $\text{Ca}^{2+}$  release from SR (increase of contractility) by an intracellular transduction pathway that react to stimulation by Norepinephrine (NE), Angiotensin II (AII) and endothelin (ET-1)
- Calcium binding to TnC is important because it frees the myosin binding site on actin molecules. It is positive influenced by intracellular calcium concentration and it is negatively influenced by acidosis that occur during ischemia.
- Cyclic AMP pathway (amongst others elevated by catecholamines, so it plays a role when there is stress or exercise involved) increases phosphorylation of the myosin heads and may thus increase contractility.
- Modulation of SERCA activity. Elevated intracellular  $\text{Ca}^{2+}$  increases SR sequestration and subsequent release of  $\text{Ca}^{2+}$  in the cytosol during next action potential, thus enhancing contractility. Of course when sufficient ATP is present.
- $\text{Ca}^{2+}$  efflux from the cell by mechanism in the sarcolemma. It regards the ATP dependent pumps and the exchangers in sarcolemma. If there is a lack of ATP, there is a calcium overloading of the cell but it will not increase contractility because for contractility ATP is needed.

Concentration of  $\text{Ca}^{2+}$  regulates also relaxation (lusitropy). Lusitropy is increased by all mechanisms that move out  $\text{Ca}^{2+}$  from the cytosol at the end of action potential. ATP-pumps and exchanger in the sarcolemma (put calcium out of cell) as well as the SERCA pump that moves calcium in the sarcoplasmic reticulum. Impairment of these processes decreases lusitropy. Relaxation is fundamental because increased lusitropy increases cardiac filling ability and for the Frank Starling mechanism it increases cardiac output [5][6][10].

### 1.3.3 Regulation of cardiovascular function during exercise

During exercise there are cardiovascular adjustment. Mechanoreceptors and Chemoreceptors in muscle sense the forces that are provoked in skeletal muscle and metabolites concentration respectively. This ergo information is sent to the central nervous system and cardiovascular center in the brainstem [5][6][10]. As consequence, the following systems activates:

- Baroreflex resetting, it is necessary because the baroreflex buffer blood pressure tending to keep blood pressure constant, but in exercise the blood pressure needs to rise to contribute to an increase to cardiac output;
- Sympathetic outflow increases heart rate, contractility, arteriolar and venous constriction;
- Production of vasodilators in working muscle, this is given by chemoreceptors that sense metabolites;
- Enhancement of venous return through muscle pump and respiratory pump.

During exercise the cardiovascular system has to cope with an increased metabolic demand, which normally leads to an increase in sympathetic tone and a reduced vagal tone. One reflex that leads to that condition is the *exercise pressor reflex*. During exercise, mechanoreceptors and chemoreceptors signal exercise forces and metabolism and they activate the sympathetic outflow. Ergoreceptors afferent pathway passes through the spinal cord and then enter the medulla oblongata and arrive up to the higher levels. In the medulla, specifically in rostral ventrolateral medulla (RVLM), where sympathetic branches originate, the afferent ergo information stimulates the sympathetic system increasing sympathetic outflow. At the same time, this information travel to the level of the baroreflex in nucleus tractus solitarii (NTS) and inhibits the input of baroreceptors partly. The input of baroreceptors normally decreases the sympathetic outflow. Thus, the ergo information inhibit this inhibitory pathway. This is the way heart and vasculature receive sympathetic efferent info as consequence of afferent ergoreceptors information [5][6][10].

The result of these adjustments is the increase of cardiac output, which increase linearly with the level of exercise from low to heavy. Thus, HR and SV also increase. At heavy exercise, HR is changing steeper than before and the SV decreases. When the HR is increasing, it is more difficult to maintain the same filling thus the SV can go down under the influence of a further increased HR. Anyway, because CO is HR times SV, the CO is changing linearly at high level exercise. The mean arterial blood pressure (MAP) is slowly and linearly rising. Net systemic vascular resistance (SVR) goes down. This has to be seen in the perspective of the fact that there is vasoconstriction

in non-working muscle. Thus, it means that the vasodilation in the working muscle gives a change in the resistance (decrement) that is larger than the change in resistance (the increment) due to vasoconstriction in other tissue and finally there is a net decrease of systemic vascular resistance. The different vasoconstriction or vasodilation state of non-working and working muscles determine the redistribution of CO towards the exercising muscles. Thus, coronary circulation is increasing because heart's work can increase of 5-fold during physical activity. Increase in coronary flow is the principle mechanism for increasing myocardial O<sub>2</sub> supply; consequently, coronary flow shows a tight correlation with myocardial O<sub>2</sub> consumption. During intense exercise, the 5- to 6-fold increase in coronary blood flow results from a 20% - 40% elevation of mean arterial pressure in combination with a 70% - 80% reduction in coronary vascular resistance from resting levels [14].



# **I Section: Review on athlete's heart and mechanoelectric contribution to sport-related sudden cardiac death**

## **2.1 Introduction**

Regular physical activity has a proven beneficial role for cardiovascular health. Although, physical exercise is a potential trigger for sudden cardiac death (SCD). SCD was defined as a sudden unexpected death due to cardiac causes, or a death without evidence of structural heart abnormalities but with manifestation similar to cardiac-related death [1][2]. SCD occurred within 1 h from symptom onset (chest pain, fatigue and shortness of breath [3]) in a person without known cardiac disease or within a time frame of 24 h in a person having been seen alive and symptom free [1][2]. SCD is the leading medical cause of death across all sports. Increased cardiovascular load during exercise in people with an underlying cardiovascular abnormality can trigger SCD and it is known as sport-related sudden cardiac death (SrSCD) [1][2][3]. SrSCD could occur not only during sport activity but also after exercise at rest or during sleep [1]. It is worth clarifying that physical activity is not responsible for the greater incidence of SrSCD, rather it may be the combination of intense exercise and an underlying cardiovascular disease that triggers arrhythmias leading to cardiac arrest [2].

Given the growing sport participation among general population, SrSCD is recognized as a public health concern [4]. Therefore, prevention of SrSCD have been the subject of considerable scientific attention. Pre-participation screening of all subjects practicing sport activity has the potential to identify asymptomatic subjects at increased cardiovascular risk, both for competitive athletes and individuals engaged in leisure-time sports [15]. During pre-participation screening, under-diagnosis of pathology may lead to life-threatening events, and over-diagnosis may result in unnecessary disqualification. Thus, there is a growing interest in developing effective risk stratification algorithms for the early identification of sport participants with underlying cardiovascular disease and potentially reduce mortality [15]. One main challenge of sport cardiology is to differentiate accurately pathological changes seen in inherited or acquired cardiomyopathies that phenotypically overlap to physiological cardiac adaptation caused by exercise (athlete's heart). Indeed, many changes occur at the electrical, cellular, and structural level, all of which play a role in the physiological and functional adaptations to make the heart more efficient. Expected physiologic changes have variability by age, sport, gender, and ethnicity

[4]. Both European and American cardiology associations have proposed different pre-participation screening programs and interpretation guidelines. Yet these protocols were mainly based on result from Caucasian young adult athletes participating in competitive sports, thus excluding the magnitude and complexity of athlete population. Nowadays, professional sports teams employ thousands of young athletes but the number of veterans athletes and of older athletes involved in leisure sport is increasing and difficult to estimate [16]. As well as the mean age of athletic population is increasing, also the gender gap has been smoothed since women have been always more involved in competitive disciplines [16]. The variety of sports has also dramatically increased with the creation of extreme sports, e.g. Crossfit [16]. The ethnic diversity of the athlete population is increasing but also may be sport and region specific [16]. Therefore, the existent pre-participation screening programs are not extensively adaptable to the heterogenic athletic population. Furthermore, during our literature research, we have not found a review that treat aetiology and risk stratification for SrSCD in relation to all the influencing factors. These factors are all equally important for the discussion of cardiovascular adaptation in the athlete, as adaptation will be dependent on both the characteristics of the sport (intensity, duration and relative aerobic and anaerobic component) and the participant characteristics [1]. Besides, these influencing factors determine the developing of cardiovascular pathologies.

The aim of this work is to review the athlete's heart and the mechanoelectric phenomena leading to SrSCD. The discussion is stratified by the factors affecting physiological adaptation and pathological condition of the heart. The review covers also the importance of pre-participation screening to early detect anatomical or physiological substrate for SrSCD and the stratification risk based on age, gender, ethnicity and level of sport with the scope of targeted prevention through tailored and individualized pre-participation screening.

## 2.2 Methods for literature review

The material was collected from PubMed (<https://pubmed.ncbi.nlm.nih.gov/>), Scopus (<https://www.scopus.com/>) and Elsevier Science direct (<https://www.sciencedirect.com/>) databases. The following keywords were used: *sport related sudden cardiac death, incidence, athlete's heart, ECG interpretation, sport and ventricular remodelling.*

Firstly, the selection was based on screening protocol, meta-analysis on normal reference values and most recent interpretation guidelines. Then important references in the fields were selected based on the bibliography of the selected material. At the end, 115 papers were included in the review.

### **2.3 The determinants of athlete's heart**

Most data assessing the accuracy of screening in identifying cardiac pathology in athletes were derived from relatively unselected cohorts of subjects involved in competitive sports, predominantly young adult Caucasian male athletes. To improve the specificity, the factors affecting physiological adaptation and pathological condition of the heart should be accounted: sport, age, gender, ethnicity and level of sport activity [17]. These factors are fundamental to define a standardized framework for the definition of an association between exercise training and the resulting changes in cardiac structure [18][19].

Firstly, since leisure sport activity is increasing among general population, the discrimination of individuals who engage in competitive sport versus leisure sport is fundamental. According to the scientific statement of the American Heart Association/American College of Cardiology (AHA/ACC), a competitive athlete is defined as one who participates in an organized team or individual sport that requires regular competition against others as a central component, places a high premium on excellence and achievement, and requires some form of systematic and usually intense training. [15]. In general, professional competitive athletes have an high impact of stress and emotion given by the pressure to perform by teammates, coaches, and spectators [20]. Of note, it is important to recognize that several people who practice sports only for recreational purposes achieve training levels comparable to those of professional athletes [15]. Furthermore, each discipline has unique demands on the cardiovascular system, so the division should not be between professional athletes and leisure activity but based on the different combination of aerobic (dynamic) and anaerobic (static) component and the level of training.

The task force for sport classification is based on the different combination of aerobic and anaerobic component [21]. It was developed to discern whether it is reasonably safe to help in the definition of eligibility of an athlete for a particular competitive sport. This classification is based on peak static and dynamic components achieved during competition. The increasing dynamic component is defined in terms of the estimated percent of maximal oxygen uptake (MaxO<sub>2</sub>) achieved and correspond to an increasing cardiac output (CO). The increasing static component is related to the estimated percent of maximal voluntary contraction (MVC) of muscles reached and correspond to an increasing blood pressure (BP) load [21]. The classification is reported (Figure 15) as in the task force [21]: the lowest total cardiovascular demands, lowest CO and BP, are shown in green and the highest in red. Blue, yellow, and orange depict low moderate, moderate,

and high/moderate cardiovascular demands. Sport with danger of bodily collision are identified by the sign \* and sport related to increased risk for syncope occurrence by the sign †.

Although, the myocardial adaptation to exercise is expected to result from the intensity of exercise, whose magnitude determines the volume and pressure load, and the amount of time in which that hemodynamic stress is acting on the cardiovascular system. The stimulus for myocardial adaptation equals the hemodynamic stress (sport intensity) times the time in which that stress is applied (duration times the weekly frequency of training):

$$\text{volume of training} = \text{intensity} \times \text{amount} \quad (3).$$

It can be defined through the Metabolic Equivalent Test (MET-h/week = METS  $\times$  duration) [18][19]. In MET, low- intensity exercise is defined as corresponding to 1.8–2.9 METS, moderate intensity is defined as corresponding to 3–6 METS and high-intensity exercise is defined as >6 METS [19]. Exercise intensity is measured by oxygen consumption ( $\text{VO}_2$ ) which represents the metabolic need imposed by exercise. HR can be an alternative index of sport intensity but in highly trained athletes usually have lower HR than less trained individuals at the same submaximal level of exercise. Thus, HR as intensity index is dependent on the level of sport-related cardiac adaptation.

In this way, the myocardial stimulus estimation is more focused upon the individual activity rather than sporting disciplines, recognizing the wide range of training that athlete may undertake in a given sport and the presence of subjects practicing more than one sport disciplines. Thus, Beaudry et al. proposed the schema in Figure 16 to relate the intensity of training and the amount of training with predictable cardiac adaptations [18]. The influence of number of training hours on structural remodelling was shown by different studies, *e.g.* Finocchiaro et al. observed that a significant proportion of athletes involved in dynamic, static, or mixed training and with significantly higher training hours per week, showed concentric remodelling/hypertrophy of LV [22]. A further example is progressive endurance training program in untrained individual, which result in progressive adaptations in cardiac mass, left ventricle end diastolic volume (LVEDV) and finally compliance [23]. The relationship between dose of training and adaptation should be taken it account when designing a study, since cross-sectional approach does not allow for definite

conclusions regarding the temporal nature and link between dose of exercise and cardiac remodelling, and a longitudinal approach should be preferred [23][24].

Regarding age, population should be firstly divided in  $\leq 35$  years old and  $>35$  years old since the causes of SrSCD change between young and middle age / older athletes, with a greater prevalence of cardiomyopathy and congenital coronary artery in the first group and coronary atherosclerosis in the second one. The different pathological incidence reflects also in the different pre-participation screening needed [25] [26][27]. The under 35 years population can be further divided in paediatric ( $<14$  years old), adolescent ( $\geq 14$  years old and  $\leq 18$  years old) and young adult ( $>18$  years old and  $\leq 35$  years old). Paediatric/adolescent population especially is characterized by numerous cardiac changes due to growth, maturational age and hormones [28]. This reflects in more recurrent strange ECG findings and different ECG phenotype of most diseases leading to SCD with respect to adults, making ECG-based screening programs less specific and sensitive in children [28]. Of note, these age limits are not sharp threshold and may be not strictly respected when selecting population for studies, although cardiac changes with aging and the peculiarity of paediatric/adolescent population should be always central.

Gender differences reflects in lower cardiac remodelling and electrical adaptations in female with respect to male, as well as lower incidence of SrSCD. It may be explained by hormonal differences and the lower amount of physical exertion reached by female [2][29].

The last factor is ethnicity; three major ethnic group can be defined Caucasian, Afro-Caribbean and Asian. Afro-Caribbean population showed to have the higher cardiac remodelling and greater cardiac risk. While high prevalence of coronary disease resulted in Asian population with corresponding higher mortality and morbidity [30].

The classifiers and the classes are summarized in Table 2. Of note, inside the same class there is a high individual variability in cardiac remodelling and pathology, anyway an accurate classification of studied population can result in increased specificity and accuracy of screening protocols. Thus, in this review, every aspect is accounted for sport, age, gender and ethnicity when possible, depending on data availability.

<b>Increasing Static Component</b> 	<b>High</b> <b>(&gt;50% MVC)</b>	Bobsledding/Luge*†, Field events (throwing), Gymnastics*†, Martial arts*, Sailing, Sport climbing, Water skiing*†, Weight lifting*†, Windsurfing*†	Body Building*†, Downhill skiing*†, Skateboarding*†, Snowboarding*†, Wrestling*	Boxing*, Canoeing/Kayaking, Cycling*†, Decathlon, Rowing, Speed-skating*†, Triathlon*†
	<b>Moderate</b> <b>(20-50% MVC)</b>	Archery, Auto racing*†, Diving*†, Equestrian*†, Motorcycling*†	American football*, Field events (jumping), Figure skating*, Rodeoing*†, Rugby*, Running (sprint), Surfing*†, Synchronized, swimming†	Basketball*, Ice hockey*, Cross-country skiing (skating technique), Lacrosse*, Running (middle distance), Swimming, Team handball
	<b>Low</b> <b>(&lt;20% MVC)</b>	Billiard, Bowling, Cricket, Curling, Golf, Riflery	Baseball/Softball*, Fencing, Table tennis, Volleyball	Badminton, Cross-country, Skiing (classic technique), Field hockey*, Orienteering, Race walking, Racquetball/Squash, Running (long distance), Soccer*, Tennis
		<b>Low</b> <b>(&lt;40% Max O<sub>2</sub>)</b>	<b>Moderate</b> <b>(40-70% Max O<sub>2</sub>)</b>	<b>High</b> <b>(&gt;70% Max O<sub>2</sub>)</b>
		<b>Increasing Dynamic Component</b>		

Figure 15 Sport classification based on the dynamic and static component. The sign \* identifies the sport with danger of bodily collision and the sign † identifies sport related to increased risk for syncope occurrence [21].

<b>Intensity of training</b> 	<b>Fittest</b> <b>Greatest cardiac remodeling</b>
	<b>Moderate fitness</b> <b>Moderate cardiac remodeling</b>
	<b>Least fit</b> <b>Least cardiac remodeling</b>
	<b>Amount of training</b>

Figure 16 Combination of intensity and amount of training and expected cardiac remodeling [18].



Table 2 Scheme for classification of collected data based on the factors that affect the physiology and the pathophysiology of the athlete's heart: sport, age, gender, ethnicity.

<b>CLASSIFIER</b>	<b>CLASSES</b>			
<b>Sport</b>	Aerobic activity		Anaerobic activity	
<b>Age</b>	≤35 years		>35 years	
	<18 years			≥18 years
	Paediatric <14 years	Adolescent ≥14 years		
<b>Gender</b>	Female		Male	
<b>Ethnicity</b>	Caucasian	Afro- Caribbean	Asian	

## 2.4 Incidence of sport related sudden cardiac death

It is widely acknowledged that SrSCD is the leading medical cause of death among athletes although its exact incidence remains unclear. Variability in estimation of incidence rates is due to differences in methodology including the population being examined and the cases which are excluded or included (i.e. sudden cardiac arrest (SCA) victims that survived), the reliability of case registration and identification [1][2]. Mandatory system for reporting sport related death are the most reliable source but few of these exist [31][32][33][34], and cases of SrSCD are primarily identified from media reports, registries and insurance claims [1][2][3]. All these factors lead to bias and underestimation of SrSCD incidence rates [1][2][3]. Regarding the inclusion or exclusion of SCA victims should be noted that increasing public access to defibrillation (PDA) programs and availability of automatic external defibrillator (AED) have improved survival rates after SCA, which may decrease the overall incidence of SCD [29][35]. However, because primary prevention programs should identify all athletes at risk for SCA, the incidence of both SCA with survival and SCD would be preferred.

Several variables influence SrSCD incidence: age, sport, gender, geography and ethnicity.

It was estimated that SrSCD accounts for 15000 cases annually among general population in North America and in Europe [29]. Overall, among all SrSCD, only from 0.5 to 6% occurred in young competitive athletes, while more than 94 % among recreational sport participants [1][2][31][29]. The higher incidence rate for recreational sport participants could be justified by the more numerous of recreational sports participants as compared with competitive athletes [31][34].

Rate of SrSCD varies considerably with age, 35 years age is a cut off to divide population between young and old athletes since some cardiomyopathies and atherosclerosis present phenotypically when an athlete is older leading to different aetiology for SrSCD [1][35]. A study by Marijon et al. on general French population (age from 10 to 75) revealed that the age of subjects affected by SrSCD was relatively young ( $46 \pm 15$  years) with a predominance of men (95%), and without any prior history of heart disease [31]. This result during recreational sport is confirmed by the data from a nationwide registry on sports-related sudden cardiac deaths in Germany [34].

Regarding the gender variables, incidence of SrSCD is higher in male than female athletes. The gender difference may be related to several factors, including hormonal factors, a lower prevalence of underlying cardiac abnormalities and/or different cardiovascular adaptations to intense exercise

training in women [2][29]. Furthermore, in a global context, women participate less in high-level competitive sports, which may explain part of the difference [2][29].

Some sports, such as running, cycling, basket and soccer, are mostly implicated in SrSCD probably due to the greater size of the athletic population practicing them [2][31][34]. Of course, sport requiring a greater exertion and level of cardiac work register the highest incidence rates [2]. The incidence has regional variations based on the different sport practiced in different world areas: in the USA, basketball is the sport most often associated with SrSCD whereas in Italy soccer and running are most often involved [2][31][34][33].

## 2.5 The athlete's heart: physiological changes with athletic training

To develop effective pre-participation screening program, experts in sport cardiology must first have knowledge the physiological adaptation related to physical exercise that are generally addressed with term 'athlete's heart'.

During exercise, the metabolic demand of skeletal muscle increases in proportion to the intensity of exercise, consequently  $VO_2$  and CO increase [36]. The Fick equation can be used to quantify the relationship between CO and  $VO_2$  :

$$VO_2 = CO \times \Delta(\text{arterial} - \text{venous } O_2) \quad (4).$$

Thus, CO, product SV and HR, may increase upward of 5- to 6-fold during acute maximal exercise effort [36]. During maximal exercise engaging a large muscle mass, CO may increase from ~5 L/min at rest to ~15 L/min in young females and ~20 L/min in young males and up to ~25 to 30 and ~35 to 40 L/min in elite female and male athletes [36]. This elevation in cardiac function is expected from a structurally and functionally improved heart in the trained state [23]. Exercise training induces cardiovascular changes at the electrical and structural level, bringing functional adaptations to efficiently encounter the increased metabolic demand [37][4]. Expected physiologic changes have variability by age, sport, gender, body size, and ethnicity [37][4].

Even if structural, functional and electrical cardiac adaptation are treated separately in this review, there is no sharp divider between them, and the three mechanism interact each other.

### 2.5.1 Structural adaptations

Several studies have shown a direct relationship between exercise training and cardiac structural remodelling. The effects of exercise is different on each chamber and cardiac adaptations vary according to the type of exercise, especially it is related to exercise capacity given its robust association with maximal  $VO_2$  [24].

Morganroth et al. hypothesized that morphological adaptations in athletes correspond with the type of haemodynamic overload imposed on the heart during exercise [38]. Both dynamic (endurance or isotonic) and static (strength or isometric) exercise result in increased myocardial oxygen demand, but this distinction is relevant for the different types of haemodynamic burden on cardiovascular system and induced cardiac adaptation.

Dynamic exercise requires greater aerobic power, accomplished by an increase in maximum oxygen consumption and CO, with normal or reduced peripheral vascular resistance (PVR) favouring muscular perfusion by higher vascular conductance [23][38]. Increase in CO is due to an increase in SV (both at rest and during exercise with prolonged exercise training), by contrast, the maximum HR does not significantly increase [37][24]. The elevation of CO affect all 4 cardiac chambers and the increased volume overload leads to dilation that affects equally both ventricles and atria [36]. On left ventricle (LV), EDV overload and increased diastolic wall stress lead to eccentric left ventricle hypertrophy (LVH). It manifests with increased LV dimension measured as increase in LV end-diastolic diameter, LVEED, and a proportional LV mass increase, with minimal if any increase in LV wall thickness (LVWT) [22].

On the contrary, during static exercise, CO remains relatively stable but blood pressure increases due to marked rise in peripheral vascular resistance (PVR) [36][4]. The high PVR and LV afterload lead to repetitive pressure overload and increased systolic wall stress in LV. This state increases LV wall thickness (LVWT) with unchanged LV chamber size, consistent with concentric LVH pattern [36][4][22]. However, the other three chambers are relatively unaffected.

A meta-analysis of 59 echocardiographic studies on sport related cardiac adaptation confirmed the divergent changes occurring with dynamic and static sport [39]. Although, this dichotomous distinction between endurance and static training is a relative concept, since every sport discipline mixes aerobic and anaerobic exercise [39][21]. Further, every form of endurance training lead to an increase in blood pressure, as static training implies HR and CO increment [39]. Indeed, athletes involved in sports combining high aerobic and high anaerobic components usually show the most marked cardiovascular remodelling with remodelling patterns consistent with both static and dynamic exercise [36][39][40].

Regarding structural remodelling and dimensions of the heart, it should be noted that body size has a large influence on heart size, e.g. women in general have smaller cardiac dimensions and remodelling compared to men. Thus, cardiac measurements should be indexed for body surface area (BSA), especially RV parameters have a positive correlation with BSA [24]. Further, it was

proved that body size is a major determinant of LA size and gender differences in LA size are nearly completely accounted for by variation in body size [41].

### 2.5.1.1 Left ventricle

LV is the most studied chamber in highly trained athletes. Independently of age and gender, they generally show normal LV geometry [22][42]. Although, main LV geometrical parameters, LVEDD and LVWT (computed as septal thickness or relative wall thickness RWT), are greater in athletes than in age-matched non-athlete population. Athletes have 10-15% greater LV size, up to an increment of 15-20% in septal thickness, compared to age-matched non-athletes [37]. LV structural parameters are greater both in adult young athletes and paediatric/adolescents athletes, but the range of LV septal thickness differed between adolescent and adult athletes (independent of gender), with an upper limit of 16 mm in adults and 14 mm in adolescents [37][43].

Independently of gender, the mean LVEDD is 47 mm for paediatric/adolescent athletes while in adult athletes the mean LVEDD is 54 mm [43][20]. It is evident that cardiac enlargement increases with chronological age, but it is dramatically affected by maturational status during childhood and adolescence with adolescent measurements more near to adult values [43]:

- mean LVEDD =44.2mm for <14 years vs mean LVEDD =51.1mm for  $\geq$ 14 years;
- mean RWT =0.35 for <14 years vs mean RWT =0.36 for  $\geq$ 14 years.

Structural remodelling of LV is more pronounced among male athletes than female athletes with similar age and training intensity. Indeed, mean LVEDD is 49 mm [24] and 45 mm [43] for female adult and paediatric/adolescent athletes respectively while mean LVEDD is 55 mm [24] and 48 mm [43] for male adult and paediatric/adolescent athletes respectively. In extreme cases athletes can have LVEDD  $\geq$ 60 mm, and it can reach 70 mm in men [44]. The most extreme cavity dimension and/or wall thickness have been reported in elite male rowers, cross-country skiers, cyclists and swimmers with large body size [23]. RWT is 0.34 [43] for female paediatric/adolescent athletes while RWT is 0.36 [43] for male paediatric/adolescent athletes. While for young adult athletes, RWT is 0.35 and 0.36 for female and male respectively [22].

Eccentric LVH that results from endurance exercise training is typically more pronounced than the concentric LVH that derives from strength training [23]. LVH is reduced both among paediatric/adolescent and young adult female athletes, the reason might be in hormonal (lower

testosterone level in female) and genetic differences with men [37][43]. As shown by Finocchiaro et al. [22], a small proportion of females shows concentric hypertrophy/remodelling respect to males (12% vs. 7%). Conversely, a significant percentage (21%) of females adapt by developing eccentric hypertrophy, particularly those engaged in dynamic sports [22].

Regarding ethnicity, Afro-Caribbean athletes have increased LVH with greater concentric remodelling pattern in response to constant training loads compared with Caucasian athletes. Different studies suggested that LV geometry and the main physiological remodelling are principally related to ethnicity, independently from gender and age [37][43][45]. Taking as reference dimension the LV septal thickness, it does not overcome normal limit of 11 mm in white adult female athletes while for a small, but not negligible, proportion of black female athletes (3%) the thickness is up to 13 mm [46]. Additionally, Basavarajaiah et al. reported LV septal thickness > 12 mm in 18% black male athletes compared to 4% in white male athletes [47]. The same trend is confirmed for paediatric and adolescent athletes by a meta-analysis on paediatric athlete's heart [43]:

- mean LVEDD =49.5mm for black paediatric athletes vs mean LVEDD =48.2mm for white paediatric athletes;
- mean RWT =0.39 for black paediatric athletes vs mean RWT =0.36 for white paediatric athletes.

The amount of training, measured as number of training hours per weeks could also affect structural remodelling. Finocchiaro et al. observed that a significant proportion of athletes involved in dynamic, static, or mixed training and with significantly higher training hours per week, showed higher remodelling with more pattern of concentric LVH [22].

### **2.5.1.2 Right ventricle**

Most studies focus on LV adaptation and limited number of data are available for RV [23][48]. However, during strenuous endurance exercise, RV is highly stressed by pulmonary pressures, which increase almost linearly with increasing CO. RV wall stress is higher than LV wall stress, given the less thickness of right ventricular wall and the absence of a reduction in vascular resistance in pulmonary circulation compared in the peripheral circulation during exercise [48]. In trained endurance athletes, RV measurements commonly exceed standard reference ranges for



untrained individuals with increased right ventricle mass (RVM), right ventricle end diastolic volume (RVEDD) and RV free wall thickness [4] [49].

Endurance exercise of moderate to high intensity requires that both the LV and RV handle larger CO. Biventricular increase in CO lead to a balanced and parallel enlargement of RV and LV, with similar increase in mass as note by CMR [23] [37][24]. RV commonly show an eccentric hypertrophic pattern [24].

Although, the decrease in vascular resistance is less pronounced in the pulmonary circulation. The mismatch between increased CO and resistance in pulmonary circulation may result in an increase of pulmonary artery pressure and RV afterload [37]. In the comparison between dynamic and static training, pulmonary artery systolic pressure is higher in endurance ( $26.3 \pm 6.6$  mmHg) than strength athletes ( $19.7 \pm 8.1$  mmHg) [50]. This may explain the relative unchanged RV dimensions in response to strength activities with respect to the significantly greater RV dimensions in elite endurance-trained athletes both in general and when the two athletic populations are matched for age and gender [4][24][50].

Ethnicity is an established determinant of left ventricular remodelling. Physiological RV enlargement is commonly observed in both black and white athletes, but impact of ethnicity is minimal, which obviates the need for ethnic-specific RV reference values [51]. However, Afro-Caribbean athletes showed frequent ECG repolarization abnormalities (see electrical adaptation chapter), which if combined with RV enlargement compatible with arrhythmogenic right ventricle cardiomyopathy (ARVC) may lead to a prevalence of erroneous ARVC diagnosis in this ethnic group [51].

Zaidi et al. [51] observed large differences in absolute RV dimensions between male and female; hence, they proposed gender-specific reference value. Further, given the positive relation between BSA and RV dimensions, indexed reference values are also recommended. The proposed upper limits for RV remodelling with respect to gender are reported in Table 3. Age was only weakly associated with RV dimensions and they suggested that these upper limits may be applied to adolescent athletes, because studied cohort was aged between 14 and 35 years with 33% of subjects being  $\leq 18$  years old [51].

Table 3 Reference upper limits of cardiac structural remodeling for right ventricle [51]. The absolute value of measurements is reported out of brackets while the value indexed for BSA is reported into the brackets.

<b>RV measurements</b>	<b>Female</b>	<b>male</b>
Basal RVEDD (RVD1), mm (mm/m <sup>2</sup> )	49 (28)	55 (28)
Middle ventricle RVEDD (RVD2), mm (mm/m <sup>2</sup> )	43 (25)	47 (24)
Base to apex RVEDD (RVD3), mm (mm/m <sup>2</sup> )	100 (57)	109 (56)
RVWT, mm (mm/m <sup>2</sup> )	5 (3)	6 (3)
RVOT proximal (RVT1), mm (mm/m <sup>2</sup> )	40 (23)	43 (22)
RVOT distal (RVT2), mm (mm/m <sup>2</sup> )	29 (16)	32 (17)
RVOTP, mm (mm/m <sup>2</sup> )	37 (21)	40 (20)
RVEDA, cm (cm <sup>2</sup> /m <sup>2</sup> )	32 (18)	39 (19)

### 2.5.1.3 Left atrium

LA is subject to remodelling with physical activity because of volume and pressure overload after long term training. LA is enlarged in highly trained athletes compared with sedentary controls, regardless of whether their sport activity requires predominantly endurance or strength exercise, of course a sport combining high endurance and high strength components results in the greatest impact on LA enlargement [4][24][37][41] [52]. On average athletic population has greater antero-posterior LA diameter of 4.2 mm (95% CI: 0.9 to 7.6) [41]. Echocardiographic patterns of paediatric athletes confirm also the LA diameter increment with respect to the paediatric non-athletes (30.2 mm vs 26.5 mm) [43]. Antero-posterior LA diameter was the first parameter used to quantify LA remodelling by echocardiographic measurements [53]. In that study antero-posterior diameter was assessed in 1777 competitive athletes engaged in 38 disciplines. The normal upper limits of LA diameter for athletes were signed at 45 mm in woman and 50 mm in man [53]. Gender seems to affect LA diameter growth, in men it was in average 2.3 mm (95% CI: 0.8 to 3.7) greater than in women [41].

Although, LA enlargement in the antero-posterior dimension is constrained by the aortic root anteriorly and the tracheal bifurcation posteriorly, forcing the LA to expand predominantly in the superior-inferior and medial-lateral dimensions [41]. This alters LA geometry such that the antero-posterior dimension may not accurately represent LA size [41]. LA volume provides a more accurate and reproducible estimate of LA size compared with reference measurement from cardiac magnetic resonance (CMR) [41]. LA volume also has a stronger association with adverse cardiovascular outcomes than LA diameter or area [41]. For this reasons American Society of Echocardiography (ASE) recommendations suggest always to determine LA volume and LA volume indexed to BSA, called LA volume index (LAVi), which has an higher sensitivity in

determining LA enlargement [24][41]. Mean LAVi was 30.8 ml/m<sup>2</sup> (95% CI: 26.1 to 35.5) in male elite athletes and 24.5 ml/m<sup>2</sup> (95% CI: 21.6 to 27.5) in male controls. LAVi revealed to be on average 7.0 ml/m<sup>2</sup> greater than volumes in the general population [41]. In healthy athletes A LAVi  $\geq 34$  mL/m<sup>2</sup> was found, but this value coincide with cut-off value to establish LA enlargement in general population from ASE/EAE recommendation [24][54]. Therefore the cut-off point of  $\geq 34$  mL/m<sup>2</sup> of 2D LAVi for establishing LA enlargement in general population from ASE/EAE recommendation could leads to sport exclusion of dilated LA cavities in normal athletes [24].

Significantly different LA volumes between men and women is present [24]. However, these differences did no longer persist after indexing for body size regardless of the method used to calculate them [55]. No statistically significant differences between the genders when indexed LA volumes were present [41]. Therefore, LAVi index has less need for checking for age-gender-specific references [55][56]. Therefore, from data pooled from both genders, weighted mean LAVi for BSA was 30.9 ml/m<sup>2</sup> (95% CI: 28.1 to 33.7) in male and female elite athletes and 24.1 ml/m<sup>2</sup> (95% CI: 22.1 to 26.1) in controls [41]. Anyway, a CMR study on LA volume measured found only a small difference between female controls and female athletes independently of sport discipline, suggesting a less pronounced LA remodelling in female than male athletes [52]. The same CMR study further found that when indexing LA volume to total heart volume (THV), the result did not differ between athletes and controls indicating a balanced enlargement in healthy athletes [52].

LA remodelling may be one of the mechanisms associated with supraventricular arrhythmias and atrial fibrillation in athletes, but the relation remains not completely understood and sometimes controversial [37][24]. Several possible mechanisms, alone or together, could contribute to atrial fibrillation (AF) in habitual athletes. Vagal tone and bradycardia are more prevalent in athletes, and bradycardia has been associated with AF in patients with structurally normal hearts. Inflammatory changes with excessive training and LA remodelling and dilation are also possible causes, e.g. structural remodelling of athlete's heart, with larger atria and a more stretched postero-septal region can lead to unusual arrhythmia substrates due to increased tissue anisotropy [48][41][57].

#### **2.5.1.4 Right atrium**

Few studies have focused on the quantification of RA size in athletic population. Due to its irregular shape and the impossibility of biplane recording, usually RA dimension is measured as an area by using the apical 4-chamber view and minor axis dimension is often used to estimate RA size [58]. As for RV and LA, RA dimensions should be indexed to BSA [58]. Zaidi et al. proposed a reference upper limit for the RA area, also indexed to BSA: 24 cm<sup>2</sup> (13 cm<sup>2</sup>/m<sup>2</sup>) for female and 28 cm<sup>2</sup> (14 cm<sup>2</sup>/m<sup>2</sup>) for male [51]. Another study [58], suggested a slightly higher upper limits for RA area of endurance male athletes 14.5 cm<sup>2</sup>/m<sup>2</sup> and 2.9 cm/m<sup>2</sup> for the RA minor axis. Thus, training activity with increase in blood volume can lead to RA dilatation, indeed RA dimensions appeared to be greater in elite endurance-trained athletes than in age- and gender-matched strength trained athletes and sedentary controls [50]. RA volume measurements from CMR imaging, result in greater volumes both in male and female athletes compared to non-athletes even when volume were indexed for BSA. As for LA, male population is characterized by a more pronounced RA enlargement but it is proportional to THV [52].

#### **2.5.2 Vascular adaptation**

Starting from the aorta, a pair of studies show that sport related adaptation are not present, considering the association of exercise and aortic root dilation inconsistent. Dilated aortic root is uncommon among competitive athletes:  $\geq 40$  mm in 1.3% of males and  $\geq 34$  mm in 0.9% of females (99th percentiles). Dilatation of the aortic root is most likely to represent pathology rather than a sport-related adaptation. Greater diameters were reported in strength-trained athletes compared to endurance-trained athletes, but also with a low prevalence of dilated aortic root [37] [59].

Sport-related vascular adaptation regards mainly small resistance and large conduit arteries. This process of arterial remodelling refers to the increase or decrease of diameters of small resistance and large conduit arteries and to the thickening of arterial wall by altering the composition in terms of the amounts of cellular (vascular smooth muscle and endothelium) and extracellular matrix constituents [60]. Arterial remodelling may be associated with the specific haemodynamic condition and load within each vessel during exercise given by the type of sport, intensity and duration of exercise [59][61]. Changes in shear stress and transmural pressure, can lead to physiological adaptations in arteries and arterioles. Shear stress, which is the force applied by the

blood to the endothelial cells, is the main cause of changes in arterial dimensions, and growth of arterioles and capillaries. Comparing dynamic and static type of sports, the former appears to promote arterial function and remodelling to a greater extent [61].

During endurance exercise, muscle perfusion is enhanced of many fold and consequently the shear stress is higher. Shear stress is sensed by mechanosensors on the endothelial cells leading to an acute vasodilation so a reduction of vascular resistance, but it also influences the expression of proteins important for vascular function and vascular growth [23]. Indeed, a structural remodelling is present to accommodate the higher perfusion rates in muscles, arteries diameter increases and wall thickness decreases and the volume of arteriolar network grows [62].

Concerning the coronary circulation, adaptive growth of the coronary circulation is a response to exercise in the healthy heart [60]. Exercise training induces increases in coronary transport capacity through adaptations in the coronary microcirculation including increased arteriolar diameters and/or densities and changes in the vasomotor reactivity of coronary resistance arteries. Exercise-related increase in coronary blood flow enhances also basal coronary size and compliance in main coronary arteries [63]. Stimuli related to increase in blood flow – shear stress and wall tension – and to mechanical deformation of the myocardium – stretch and compression – are the main triggers of coronary artery adaptation [60]. Arterial remodelling is most common among endurance athletes and concern an increase in vascular smooth muscle after long period training. At the capillary level, angiogenesis is present; it is the growth of new capillary vessels from the terminal circulation. The process involves only endothelial cells [60]. As these exchange vessels increase in number, some may be enlarged and transformed at their proximal ends into supplying arterioles or small arteries by a process described as ‘arteriolarization’ [60]. Finally, highly trained endurance athletes show a higher myocardial oxygen extraction thanks to the lower HR, a physiological adaptation that enable to reach longer blood mean transit time, improving oxygen extraction [23] [24].

### 2.5.3 Functional adaptations

In fully strength sport disciplines, the CO remains relatively stable but increasing the dynamic component CO increases along with the increment of peripheral oxygen demand. The capacity to produce a very high aerobic power for prolonged time is essential for endurance athletes and thus the heart must generate a high CO that is achieved by a large SV. This increase in SV is mediated predominantly by a large left ventricle end diastolic volume (LVEDV). LVEDV is determined by diastolic filling, which in turn is influenced by HR, intrinsic myocardial relaxation, ventricular compliance, ventricular filling pressures, atrial contraction, pericardial and pulmonary constraints. Endurance training leads to enhanced early diastolic LV filling and a more rapid filling of the heart during high-intensity exercise due to an increase restorative forces and diastolic suction. Indeed, an increment of the transmural intraventricular pressure gradient rapidly attract blood from the LA to the apex of LV. This increased diastolic suction and hence rapid filling of LV is likely to explain the continuous rise in SV in highly trained endurance individuals as opposed to less active and sedentary subjects. In addition, cardiac chamber compliance has also been shown to be enhanced in athletes, resulting in a large LVEDV and a greater use of the Frank-Starling mechanism with increase of ventricular contractile forces [23]. Sustained endurance training preserves ventricular compliance with age, potentially preventing heart failure in the elderly. This enhancement of LV diastolic function is essential to preserve SV thanks to the ability of the LV to relax at high heart rates. The process is aided by the functionally lower HR reached by highly trained athletes at a submaximal level of exercise with respect to less trained subjects. In contrast, strength training appears to not affect LV relaxation, which could result mildly impaired due to the concentric LVH pattern characteristic of adaptation to pure strength disciplines [37].

Regarding systolic function, it is assessed by left ventricle ejection fraction (LVEF). LVEF is generally normal among athletes and the rate of ventricular emptying plays only a modest role in the augmentation of SV during exercise [23]. However, a transient reduction in LVEF has been demonstrated after prolonged strenuous exercise, termed ‘cardiac fatigue’ and it is secondary to an extreme LV dilatation [37]. Thus, LVEF is highly dependent on load and it is limited in the assessment of ventricular systolic function.

However, new advances in echocardiography, including strain imaging and speckle tracking, suggest that intense exercise may lead to changes in LV systolic function that are not detected by echocardiography at rest. Even if LVEF remains unchanged, other systolic parameters may change

significantly with increased peak systolic tissue velocities, equally increased radial strain in all segments, increased longitudinal strain with a base-to-apex gradient and increased circumferential strain in the LV free wall [37].

Endurance training causes a biventricular CO increment, therefore RV presents improved early diastolic RV function and increased right ventricle stroke volume (RVSV). While systolic functions have minimal changes and are comparable between athletes and not athletic subjects [4][49][50]. Intense endurance exercise may cause acute RV dysfunction that recovers in the short term, but chronic structural changes and reduced RV function are evident in some athletes. This hemodynamic imbalance may promote transient RV injury or incomplete recovery, with possible long-term structural consequences [37].

Increase in ventricular filling, so in SV and cardiac preload, is significantly affected by the increase in blood volume as response to exercise training. Exercise training leads to an expansion of blood volume (hypervolemia) by aldosterone-sodium retention mechanism and increased plasma albumin content. Erythrocyte volume expansion is also observed. Plasma and erythrocyte volume increase from 8% to 10% above the pre-training level, resulting in a haematocrit ~1% lower than sedentary control level. The hypervolemia associated with exercise training reflects a larger total body water volume, which increases interstitial fluid available to the sweat glands and allows greater plasma volume to perfuse skin to enhance conductive heat exchange for evaporative cooling during exercise. In addition, hypervolemia and the lower haematocrit lower blood viscosity, which in turn may be responsible for a decrease of heart workload combined with a greater filling of the heart and a lower peripheral resistance [23].

In trained endurance athletes, the increase in CO is not correlated to an increase of HR, although increase in HR is responsible for the majority of CO augmentation at the onset of exercise. The increase in HR following exercise onset is mediated by a combination of vagal withdrawal and  $\beta$ -adrenergic stimulation. CO at a given absolute submaximal workload is not significantly different following exercise training as oxygen demand is also unaltered. The unchanged CO is the result of a larger SV and lower HR increasing the evidence that higher heart volume lowers intrinsic HR. Maximal HR is decreased by 3% to 7% with training. From a functional perspective, a lower maximal HR will allow for increased filling time, which is likely to be important for preservation of a large EDV and SV, of which the latter may exceed that of sedentary subjects by ~60% to 70% during maximal exercise [23].



#### 2.5.4 Electrical adaptations

Physical exercise acts as an arrhythmic trigger. More than 80% of competitive athletes have changes in resting ECG reflecting physiological adaptation to exercise training; changes potentially confounded with cardiovascular (CV) pathology are present in 10-12% [64][65]. Electrical adaptation in athletes result from conditioning of the cardiac autonomic nervous system (increased vagal tone and/or sympathetic withdrawal) and structural remodelling [37]. Increased vagal tone is responsible for findings such as bradycardia, sinus arrhythmia, early repolarization, first degree AV block and Mobitz type I second degree AV block, alteration that disappear with increased heart rate during exercise. Structural remodelling is responsible for criteria of increased cavity size, e.g. increased QRS voltage due to LVH [66], and changes in the mechanical environment of the heart are capable of influencing both the initiation and spread of cardiac excitation through pathways [67]. The extent of these changes depends on the athlete's ethnicity, age, gender and level of training, as well as the type of training and the type of sport. All these factors should be considered when looking at an athlete's ECG [68]. Normal exercise-related ECG changes are mostly present in male black-African athletes, both adolescent and adult, engaged in endurance sport than in West-Asian and Caucasian athletes, which have comparable rates of 'uncommon' ECG changes (7.9% vs 5.8%,  $p>0.05$ ) [64][69]. In a study on ECG changes frequency between sport with high endurance component and sport with prevalent static component [70], training-related ECG changes were more common in the first group with respect to the second one regardless of gender. Recent studies show that gender has a significant effect on ECG patterns in athletes [71]. In general, ECGs of female athletes show less alteration than ECGs of male athletes [72]. This difference could be related to the lower cardiac remodelling in women since changes in expression of cardiac remodelling (increased R/S-wave voltages suggestive for LVH, early repolarization pattern, or marked sinus bradycardia) are far less common in female than male athletes [71]. While anterior T wave inversion (TWI) is the only pattern more common in female than male athletes [71][72].

Electrocardiographic pattern representative of cardiac adaptations, which need to be differentiated clinically from pathologic sign, include the following:

- **Resting bradycardia:** present in 60%-80% of highly trained athletes, especially those engaged in sports with high endurance component [64][69]. Resting Bradycardia has similar and higher prevalence in African and Caucasian athletes than in Asian ones [64][69]. Systemic oxygen

demand and hence CO at rest is largely unaffected by exercise training, and the bradycardia is, therefore, likely secondary to the increased SV due to training [23]. In well-trained athletes resting bradycardia seemed to result from functional increased vagal tone [73] [48]. However, it has recently shown that there is also a correlation between fundamental intrinsic change of sinus automaticity and the decreased expression of the pacemaker current by a downward regulation of funny current [48]. Sinus bradycardia is not fully reversible after cessation of sport practice leading thus it could be also caused by structural changes during the cardiac remodelling [48]. In absence of symptoms (fatigue, syncope or dizziness), a HR should be considered normal if it is  $\geq 30$  bpm and/or pauses of  $\geq 3$  s during sleep hours due to increased vagal tone [37][68]. Although, very long pauses, e.g.  $>4$  s during sleep, even when associated with abruptly increased vagal tone, may predispose to develop pause-mediated polymorphic ventricular tachycardia (VT) or ventricular fibrillation (VF) [48]. Marked sinus bradycardia, a waking HR  $< 30$  bpm, is rarely observed and it may arise clinical concern. Regardless intensity of training, current guidelines suggest a repeat ECG after exercise or Holter ECG during exercise to ascertain the physiological features of such bradycardia [73].

- **Sinus arrhythmia:** represent HR variation during respiratory cycle as consequence of increased vagal tone: rate increases during inspiration and decreases during expiration [68][73]. An exaggerated response to inspiration and expiration is found in  $>50\%$  of athletes [37].

- **Ectopic atrial rhythm:** P waves with different morphologies compared to the sinus P waves (known as a ‘wandering atrial pacemaker’ if there are more than two different morphologies) are normal in athletes and are most easily seen when P waves are negative in the inferior leads [37][73].

- **Junctional escape rhythm:** resulting from a faster AV rate than the resting sinus rate; can be found in athletes with marked bradycardia [37]. Typically the rate is less than 100 bpm with narrow QRS complex unless the baseline QRS is conducted with aberrancy [73]. However sinus rhythm resumes with increasing HR [68].

- **First-degree AV block and Mobitz type I AV block (Second-degree AV block):** these are considered normal findings in asymptomatic athletes [74]. The former type is the most common especially among endurance athletes (up to 10%), the second one is frequent among Caucasian endurance athletes (up to 5%) [37][64][67][69]. First-degree AV block is considered normal in athletes when PR interval ranges between 200 ms and 400 ms, while in Mobitz type I AV block PR interval progressively lengthens until there is non-conducted P wave with no QRS complex

and the first PR interval after the dropped beat is shorter than the last conducted PR interval [73]. Higher degrees of AV block (Mobitz Type II 2nd degree AV block or complete heart block) are not a feature of athletic adaptation and are indicative of further cardiac investigation [73]. It is also unusual to see profound PR lengthening  $>400$  ms in healthy athletes and current guidelines recommend further evaluation [73].

• **Incomplete right bundle branch block (iRBBB)**: it is observed in healthy athletes up to 15% or 20% depending on the studied population, and it is considered a normal finding. It has a prevalence lower of Afro-Caribbean and Asian athletes than Caucasian athletes, particularly involved in endurance disciplines. It reflects prolonged conduction time resulting from increased RV size secondary to regular training [64][69]. iRBBB, in ECG, is defined as an rsR' pattern in V1 and qRS pattern in V6 with a QRS duration  $<120$  ms [73]. Sometimes Brugada ECG pattern mimics IRBBB, they can be distinguished by the absence of reciprocal S-wave in leads I and V6 for Brugada ECG. This right ventricular conduction delay is possibly caused by enlarged RV cavity size and RV remodelling, resulting in increased conduction time, and not by a delay within the specialized conduction system and it could be reversible with deconditioning [68]. Particular attention should be paid to the simultaneous presence of iRBBB sign and ST-T abnormalities because ARVC may present with iRBBB with TWI in the mid-precordial leads beyond V2, low limb-lead voltages and premature ventricular beats with a left bundle branch block (LBBB) pattern [68]. Most recent expert consensus guidelines suggest that complete RBBB without TWI is a borderline finding which should only prompt further investigation if accompanied by other borderline or abnormal ECG findings [73]. However, complete RBBB is rare in healthy athletes, with an incidence of 0.5– 2.5% [73]. Thus, some studies suggest to perform further investigation to exclude structural heart disease when complete RBBB pattern is present in ECG [74].

• **Isolated QRS voltage criteria for left ventricle hypertrophy** ( $SV_1 + RV_5$  or  $V_6 > 3.5$  mV) are found in approximately one third of athletic population, and in Africans - Caribbean individuals the percentage of athletes with physiologic LVH can be  $>80\%$  [37]. This sign is usually isolated in normal athletes or can be found in combination with sinus bradycardia and minor conduction delay, features suggesting physiological hypertrophy [73]. While in subject with hypertrophic cardiomyopathy, pathological LVH is usually indicated by the presence of additional ECG features such as T-wave inversion, ST-depression, pathological Q waves, left axis deviation or left bundle branch block (LBBB) [75]. Similarly, isolated voltage criterion for right ventricular hypertrophy (RVH) ( $RV_1 + SV_{5/6} > 1.10$  mV) is observed in more than 10% of healthy athletes [76], and, in

isolation, does not appear to correlate with the presence of cardiac pathology [73][74]. As predictable, isolated QRS voltage criteria for LVH, as well as RVH criteria [76], are less frequent in female gender given the lower ventricular remodelling. Indeed, Finocchiaro et al. [22] showed that Sokolow-Lyon (SL) voltage criteria for LVH as well as left axis deviation are less common in female than in male elite athletes in a study including more than 1000 highly trained athletes. The SL criteria for LVH were present in 14% of females compared with 42% of males [71].

- **Early repolarization:** 60% of highly trained Caucasian young athletes present it in resting ECG, reaching 80-90% in Afro-Caribbean athletes [37][69][77][78]. Early repolarization is associated with the increased vagal tone observed in athletes and is a reversible phenomenon that disappears with deconditioning [68]. Early repolarization is more common in young male athletes with increased QRS voltage, interventricular septal thickness and slower HR [78]. The most common pattern in Caucasians is an elevation of the J-point (QRS-ST junction) of at least 0.1 mV followed by a peaked and tall positive T-wave in the inferior and/or lateral leads [79]. Although anterior J-point elevation is also commonly observed in conjunction with inferior and/or lateral J-point elevation, the anterior ECG leads V1-V3 have been excluded from the most recent guidelines for early repolarisation recognition in order to avoid confusion with the Brugada pattern [74]. In fact, anterior early repolarization pattern (elevated and convex ST-segment preceding a negative T-wave in leads V1–V4) is common in Afro-Caribbean athletes and shares many similarities with the type 1 Brugada sign in ECG [80]. In order to distinguish early repolarization from Brugada syndrome (BS), the 2010 ESC criteria proposed that a down-sloping ST segment elevation is typical of BS whereas an up-sloping ST segment elevation is characteristic of early repolarization, with a sensitivity of 97% [80][81]. All patterns of early repolarization (with the exception of a spontaneous Brugada Type 1 ECG pattern) are considered benign variants in asymptomatic athletes [73]. Although the ECG pattern of QRS slurring (J-wave) without ST-segment elevation in the infero-lateral leads is more frequent in athletes affected by SCD than in healthy athletes, however this pattern appears not to indicate a significant risk for recurrent malignant ventricular arrhythmias in the general athletic population [77].

- **Repolarization in black athletes:** more than two-thirds of Afro-Caribbean athletes exhibit domed ST segment elevation often combined with TWI [69][82]. Afro-Caribbean athletes showed a higher prevalence of anterior TWI than non-athletes of the same ethnic group and Caucasians [83]. The combination of domed ST segment elevation and TWI in leads V1-V4 is frequent in Afro-Caribbean athletes without any association to structural disease, and it does not require

further clinical assessment in the absence of symptoms, positive family history or abnormal physical examination, [37] [80]. This can be considered an ethnicity-related response to physical exercise since it is uncommon in Caucasian group [77]. Normal repolarization changes in African-Caribbean athletes do not extend beyond V4 towards lateral leads (V5-V6) [68]. Thus, T-wave inversion in the leads V5-V6 is always considered an abnormal finding and requires additional evaluation to exclude the presence of cardiomyopathies such as hypertrophic cardiomyopathy (HCM) [68]. In anterior leads the combination of ST segment elevation (J point elevation > 0.1 mV) and TWI is most frequently observed in male athletes of Afro-Caribbean origin, but this combination is rarely observed in highly trained female athletes [71] [84].

• **Juvenile pattern:** TWI in leads V1, V2 and V3 is a normal ECG finding in paediatric/adolescent athletes, because of RV dominance and repolarization polarity directed posteriorly [83]. The prevalence of TWI in leads V1, V2 and V3 resulted inversely correlated with age (8.4% in those younger than 14 years old versus 1.7% in those older than 14 years) [85]. More precisely, pubertal development stage rather than age was independently associated with precordial TWI and can clinically explain it [85]. TWI in leads V1, V2 and V3 should be regarded in the context of age and primary of pubertal development, suggesting additional clinical testing only if this ECG pattern persists beyond puberty [77]. After pubertal age, TWI can be considered an ethnicity-related response to exercise in Afro-Caribbean athletes and usually it is combined with ST segment elevation indicating early repolarization, as explained in the previous section [77]. Regarding gender differences, anterior TWI alone was more prevalent in female athletes (9% in females vs 4% in males in a study by Finocchiaro et al.) [22][86]. This electrocardiographic abnormality did not demonstrate any relation with LV geometry patterns in female[22]. Moreover female athletes of Afro-Caribbean descent exhibit more frequently anterior TWI than white counterparts [46].

## **2.6 Aetiology of sport related sudden cardiac death**

Athletes encounter extreme physiological conditions, both during physical activity and at rest, with high adrenergic tone, potential for ischemia, ionic disturbances and high wall stress during physical activity, and high vagal tone, bradycardia, and dispersion of repolarization at rest. All these structural and functional changes may predispose the athlete's heart to develop arrhythmias, at the atrial, nodal and ventricular levels, thus the athlete's heart is a proarrhythmic heart [48]. The relation between sports and arrhythmias can have different faces. Firstly, physical activity may be the promoter of the underlying arrhythmic substrate, accelerating the development of the phenotype and of arrhythmic events. Further, even in the absence of underlying genetic predisposition, physical exercise leads to cardiac structural remodelling which can induce a substrate for arrhythmias. Secondly, an athlete with an underlying and pre-existing condition (structural or electrical, inherited, or acquired) may develop an arrhythmic event, because physical activity sets the stage for an arrhythmia to occur [48]. This is the most widely held view on the association between sports and arrhythmias [48].

### **2.6.1 Physical activity as a promoter of cardiac damage and arrhythmic substrate**

Extreme physical activity may be the promoter of the underlying arrhythmic substrate both in presence or absence of a genetic predisposition, e.g. structural remodelling of athlete's heart, with larger atria and a more stretched postero-septal region in LA can lead to unusual arrhythmia substrates due to increased tissue anisotropy [48]. A U-shaped correlation was found between the incidence of atrial fibrillation and atrial flutter with the level of endurance activity. Thus, regular mild-to-moderate exercise seems to provide strong protection from atrial fibrillation, while long-term intensive endurance exercise constitutes a risk factor, albeit small. The modest risk for AF given by extreme endurance training may be consequence of left atrial dilatation, enhanced vagal tone, possibly micro fibrosis and increased atrial ectopic beat, which are part of the cardiac adaptations of athlete's heart. Even if it was proven that physiological dilatation might create a progressive propensity for developing arrhythmias, there is no clearly defined threshold determining when intense cardiac remodelling may increase the risk for arrhythmias at the atrial and ventricular level. This leads to many grey zones, where there are high clinical debates on when continue or stop sport practice.

Further to the intensity of physical activity on development of arrhythmic substrate, it depends also on severity of phenotypic substrate, which is highly influenced by gender. Females have an incidence of arrhythmias being from 5 to 10 time lower than in male athletes maybe due to hormonal factors. A main issue of sport cardiology is to understand how large is the effect of cardiac remodelling on the development of arrhythmic substrate in individual cases to define the risk severe arrhythmias and improve the management and eligibility recommendation [48].

### **2.6.2 Physical activity as a trigger for arrhythmias in presence of underlying pathology**

Intensive physical training is known to add significant burden on cardiovascular system, particularly a combination of intense exercise and underlying cardiovascular disease could accelerate diseases progression and eventually increase the risk of SCD in athletes [2][87]. The risk for SrSCD is relative to the pathological substrate and appears to be greater in people with cardiomyopathies and congenital coronary artery anomalies [15]. Several factors, in the presence of an underlying cardiovascular disease, may contribute to the increased risk of SrSCD in athletes, including the high release of catecholamine, increased platelet aggregation/adhesion, dehydration and electrolyte disturbances associated with exercise, as well as the potential concomitant use of drugs/doping [2][15].

Heart diseases contributing to SrSCD in athletes generally fall into two categories: inherited and acquired. Inherited cardiac disorders, divided into structural and electrical, may be quiescent but can predispose the athlete to SrSCD primarily through ventricular arrhythmias. Cardiomyopathies and congenital coronary arteries anomaly are the primary cause of morbidity and mortality in young athletes  $\leq 35$  years of age. In older athletes, atherosclerotic coronary artery disease is the recognized dominant cause of SrSCD and comorbid states such as, obesity, hypertension, atrial fibrillation, may also impact their health status more than in young population [15].

The incidence of cardiac disease substrate for SrSCD varies depending on age, gender and ethnicity. It is difficult to determine a global incidence index and statistics should account for these influencing factors. For example accounting for ethnicity, some of the underlying cardiovascular abnormalities, such as HCM, are more common in the Afro-Caribbean population than Caucasians, as well as the associated ECG changes, suggesting that occurrence of HCM-related SrSCD is expected to be higher in Afro-Caribbean athletes [47]. There is also evidence that

Brugada syndrome may be more common in Asian than Caucasian populations, but systematic studies addressing the causes of SrSCD in Asian, African and South American populations are still lacking [88].

The causes of SrSCD are classified in Table 4. The main pathologies substrate to SrSCD, so related to higher incidence of SrSCD, are treated deeply in the following sections. The other less common structural cardiac abnormalities responsible for SrSCD in young athletes (accounting for 3–8% of SrSCD) include aortic dissection and rupture (usually in the context of Marfan syndrome), sarcoidosis, valvular heart disease (e.g. mitral valve prolapse or aortic valve stenosis) and atherosclerotic coronary artery disease [2].

Table 4 Classification of causes of sport related sudden cardiac death.

<b>Inherited</b>	<b>Structural cardiac abnormalities :</b>  <i>Cardiomyopathies</i> Hypertrophic Cardiomyopathy (HCM) Arrhythmogenic right ventricular cardiomyopathy (ARVC) Dilated cardiomyopathy (DCM) Left ventricular noncompaction cardiomyopathy (LVNC)  <i>Congenital coronary anomalies</i>  <i>Aortic diseases</i>
	<b>Electrical disorders:</b>  <i>Wolff–Parkinson–White syndrome</i>  <i>Channelopathies</i> Long QT syndrome (LQTS) Short QT syndrome (SQTS) Brugada syndrome Catecholaminergic polymorphic ventricular tachycardia
<b>Acquired</b>	<b>Structural:</b> Myocardial ischemia Myocarditis Cardiac Sarcoidosis Valvular heart disease
	<b>Other causes:</b> Commotio cordis Drugs and stimulants



### 2.6.2.1 Inherited structural cardiac abnormalities

#### **Cardiomyopathy:**

##### *Hypertrophic cardiomyopathy*

Hypertrophic cardiomyopathy (HCM) is an increase in LV wall thickness with reduce size of ventricular cavity (asymmetrical LVH) that leads to impaired diastolic function, dynamic left ventricular outflow tract obstruction and microcirculatory coronary disease with a consequent reduction in subendocardial flow causing failure to augment stroke volume during exercise and low peak oxygen consumption [89][20]. HCM is reported historically as the most common cause of SrSCD among  $\leq 35$  years athletes who have usually been asymptomatic (or only mildly symptomatic) [2][90].

In the presence of a pathologic substrate of HCM, intense exercise with consequent alterations in hydration, blood volume, electrolytes, acid-base imbalance, and catecholamine release can represent the trigger for the development of ventricular arrhythmias [91].

Differentiating physiological LVH due to exercise from morphologically mild HCM in the athletes is particularly challenging [89][20]. A wide array of clinical tools are available to create diagnostic algorithms to facilitate such differentiation, including clinical symptoms and family history, ECG, echocardiography and CMR, exercise stress testing and genetic testing [20][89]. It should be noted that HCM in athletes might be slightly different from that in sedentary patients with slightly different identification parameters.

Gersh et al [92] , in ACCF/AHA guideline, recommends electrocardiography as a I class imaging analysis in the screening algorithm for HCM. In ECG, abnormal TWI is the hallmark of HCM and observed in over three-quarters of athletes with HCM. TWI was found more common among athletes with HCM compared to sedentary individuals with HCM (96 % versus 84 %) with the lateral leads V5 and V6 most frequently involved. ST segment depression was observed in more than 50% of athletes with HCM and 25% demonstrated pathological deep Q waves [93]. Additionally, healthy athletes with physiological concentric LVH showed normal systolic and diastolic function at echocardiographic assessment, with absence of abnormal TWI, ST segment depression or pathological Q waves in ECG [22][93]. Further ECG changes indicating HCM may include left-axis deviation, excessive left ventricular voltage, and less commonly, arrhythmias may be observed, including premature atrial or ventricular contractions, AF, or even ventricular

tachycardia [20]. Afro-Caribbean patients with HCM showed the highest prevalence of TWI (82.7%) but involving mainly infero-lateral leads (78.8%) rather than the anterior leads (3.8%) where TWI plus J point elevation (convex ST segment elevation) is usually associated to physiological early repolarization [77]. Thus anterior TWI in healthy athletes is preceded by convex ST-segment elevation while HCM patients typically showed ST-segment depression [77].

Following the ACCF/AHA guideline [92] and the ESC guideline [94] regarding imaging echocardiographic measurements, the diagnosis of HCM can be made in adult patients with a left ventricular end-diastolic wall thickness  $\geq 15$  mm or z scores  $>9$  ( $>2-3$  z scores in adolescent and children) [94][95]. While, Sharma et al [96] determined that HCM should be considered in any male or female, both in athletic and not athletic population, with a left ventricular wall thickness of  $\geq 12$ mm. This threshold is more appropriate for female given their estimated maximal septal thickness of LV equal to 11 mm, but it can be used for Caucasian male athletes recognising that a small number of them has wall thicknesses  $> 12$ mm [20].

Athletes with HCM usually exhibit lower wall thickness than sedentary individuals with HCM (15.8 mm versus 19.7 mm,  $p < 0.001$ ) with asymmetrical hypertrophy pattern usually localised in the LV apex and/or septum [89][93]. Due to cardiac remodelling, approximately 2% of Caucasian athletes and up to 13% of Afro-Caribbean athletes (given their greater tendency to cardiac hypertrophy) have a left ventricular wall thickness ranging from 13 mm to 16 mm, falling in the grey zone of HCM diagnosis [97]. In these cases, the pattern of LVH should be analysed since a symmetrical increase in LV wall thickness with homogenous hypertrophic pattern is seen in athletes with physiological LVH. [89]. Moreover, the presence of normal or increased LVEDD, normal systolic and diastolic functions, normal atrial size, and the reduction in LV wall thickness after a period of detraining are related with sport-related remodelling [98][99]. Therefore, these other echocardiographic features can be used for the distinction of athlete's heart from HCM. A key echocardiographic feature is the LVEDD, which is normal or reduced in HCM, except towards the end stage of disease usually identified by LV dilation and reduced functional capacity in sedentary patients [20] [89]. Although, increased LVEDD is observed in most athletes with physiological eccentric LVH in response to an increased cardiac workload during exercise.

Further, the LVEDD in healthy athletes measures in average  $60 \pm 3$ mm reaching maximal value up to 70 mm as opposed to HCM patients who generally have a dilated LVEDD of  $< 50$ mm with an average dimension of 44 mm [20][89]. Another study [100] obtained similar results, comparing athletes in the grey zone and athletic patients with HCM. In addition, they reported that a cut-off

of 54 mm for LVEDD had a sensitivity and specificity of 100% to help distinguish physiological LVH from HCM [100]. However this results are questioned by another study, in which 14% of athletes with HCM revealed an LVEDD >54 mm with an upper limit of 60 mm [93].

During HCM diagnosis through echocardiography and/or CMR, the assessment of mitral valve and papillary muscle structures is suggested since they can result impaired, with elongated valve leaflets, abnormality of papillary muscles and chordae tendinae attachment to leaflets [20]. Moreover, Systolic anterior motion of the mitral valve against the inter-ventricular septum causing dynamic LVOTO is present in approximately 25 % of sedentary HCM individuals and up to 70 % of cases during exercise [101]. While athletes with HCM do not usually reveal baseline or dynamic LVOTO [89].

From a functional point of view, sedentary HCM patients usually present concomitant hyperdynamic systolic function, reduced myocardial relaxation and diastolic dysfunction due to myofibers disarray coupled with impaired sarcoplasmic calcium kinetics [89]. Most athletes with HCM, however, demonstrate normal diastolic function according to conventional parameters. Indeed, E prime 9 cm/s and E/E prime ratio >12 as a cut-off for pathology showed to have low sensitivity under 35% in athletic population [19]. Higher sensitivity and specificity, respectively of 43% and 84%, in identifying HCM in athlete was found using longitudinal function as a discriminating marker (S prime <9 cm/s).

Tissue deformation measurements through speckle tracking, specifically reduced longitudinal and circumferential strain, showed the greatest performance [20][89][102]. Global longitudinal strain (GLS) measurements more negative than -10 % resulted in a sensitivity of 87 % and specificity of 95 % sedentary HCM patient [102]. While in athletic population, a GLS more negative than -15% is suggested to identify pathologic hypertrophy [89]. Moreover, left ventricular tissue velocities, controlled through Tissue Doppler imaging, may be abnormal in HCM [20]. Thus, Tissue Doppler imaging and strain are promising diagnostic tools for the differential diagnosis between athlete's heart and HCM. However, diagnostic accuracy of echocardiographic parameters is currently limited by the lack of validated clinical cut-offs stratified by age, gender, ethnicity, and sport types. Furthermore, available reference ranges are largely restricted to relatively sedentary HCM patients and athletes with physiological ventricular hypertrophy [15]. Moreover, accuracy in measuring the left ventricular walls is important; and echocardiography measurements are more prone to errors that can falsely overestimate or underestimate wall thickness, e.g. when the septal measurement erroneously includes portion of RV muscle bundle septum) [20]. CMR imaging should be

considered when the electrocardiogram, family history, or personal history are concerning, but the echocardiogram is inconclusive. CMR performs better than echocardiography in diagnosis of atypical forms of cardiomyopathies, which can demonstrate hypertrophy localised in the apex or lateral free wall of the LV. Some HCM patients can have thickening of the lateral wall alone with a relatively normal septal thickness. The lateral wall cannot be seen through echocardiography because of air artefact. The addition of CMR can overcome this artefact and allow complete visualisation of the LV [20]. Further, tissue characterization using late gadolinium enhancement (LGE) allows identification of macroscopic replacement fibrosis. In HCM, myocardial fibrosis is usually patchy, occurring within maximally hypertrophied segments. On average LGE is present in only about 50% of HCM patients, thus the absence of LGE does not exclude HCM [15][97]. Further, non-specific small clustered patches of LGE are frequently encountered in the hearts of healthy athletes, due to LVH in response to elevated endurance training [15]. Further comparing athletes with HCM to sedentary HCM patients, there is no discernible difference in the presence of myocardial fibrosis from CMR (33 % versus 40.6 %,  $p=0.258$ ) [93]. New indexes derived from CMR have been shown to accurately confirm physiologic rather than pathologic LVH [103] [104]. These CMR derived parameters are: gender-specific RVEDV/LVEDV ratio (identifying balanced remodelling), LVEDV/mass ratio and LV diastolic wall / LV diastolic volume ratio [103] [104].

Finally, the usefulness of maximal oxygen uptake  $VO_2$  max in differential diagnosis has not been proved yet providing contradictory results in different studies and  $VO_2$  reference data are lacked for Afro-Caribbean athletes and athletes with HCM [15][89].

A characteristic of athlete's heart, not seen in HCM, is the recovering of normal dimensions of remodelled LV after a period of detraining (deconditioning). Deconditioning for 6 to 8 weeks has been shown to reverse some of the structural and electrical changes associated with exercise, including normalization of TWI on the resting ECG and, more importantly for recognition of athlete's heart, the regression of physiological LVH [98][99]. However, reversal of the LVEDD did not always occur [98][99]. In contrast, an athlete with HCM will continue to demonstrate a pathological phenotype irrespective of whether they have undertaken a period of detraining or not [98][99].

### ***Arrhythmogenic right ventricular cardiomyopathy/dysplasia***

Arrhythmogenic right ventricular cardiomyopathy/dysplasia (ARVC) is an inherited heart muscle disease that predominantly affects the RV and, less commonly the LV. Pathologically, ARVC is characterised by progressive death of myocardial cells with subsequent fibro-fatty replacement, and, clinically, by electrical instability leading to ventricular tachycardia and fibrillation responsible for SCD. In patients with ARVC, the risk of SCD is 5.4 times higher for competitive athletes than sedentary subjects. Triggering mechanisms include increased afterload during exercise, which stretches the diseased myocardium resulting in ventricular arrhythmia and/or favouring reentrant arrhythmic mechanisms. Also, “super sensitivity” to catecholamines due to damage of sympathetic nerve trunks by fibro-fatty replacement may contribute to ventricular arrhythmias [2]. ARVC accounts for 4% to 22% of SrSCD in athletes [97]. The disease is more malignant in men than in women, a finding that can be explained either by a direct influence of sex hormones on the mechanisms involved in the phenotypic expression of the disease or by gender-related differences in the amount and intensity of exercise [105].

The diagnosis of ARVC is based on findings from a combination of echocardiography or CMR, electrocardiography, 24-hour ambulatory rhythm monitoring, signal averaged electrocardiography, and family history. Typically, no single test can make the diagnosis of ARVC alone [15][20]. In ECG, TWI in anterior leads V1, V2 and V3 and ventricular premature beats arising from the RV outflow tract are the commonest type of ECG abnormalities identified in patients with ARVC [20][97]. Resting echocardiography still represents the first-line imaging technique for the evaluation of the RV in symptomatic athletes or with ECG findings suggestive of ARVC, even if it may fail to identify subtle RV wall motion abnormalities [15][97]. Patients, with quite normal ECG and Holter monitoring and concomitant unclear or suboptimal echo findings, should be further evaluated with CMR. CMR is more accurate than echocardiography in identifying regional RV wall motion abnormalities, volumes and function, and allows assessment of fibrosis and signs of fibro-fatty replacement/infiltration [15]. CMR findings consistent with ARVC diagnosis are the following: reduced RVEF (<45%), unbalanced RV enlargement with RVEDV/VLEDV ratio > 1.15, RV wall motion abnormalities and the presence of LGE [15][103]. The latter is also useful in the identification of early and/or predominant LV involvement, which is increasingly being recognized by advances in the molecular genetics of arrhythmogenic cardiomyopathy (AC) [15][97] [106].

This disease is not usually confused with athlete's heart, although both entities may share right ventricular outflow tract enlargement, a reduced resting RVEF and a borderline low RV fractional area change [97]. Anyway, in athletes, physiologic RV enlargement mainly involves the inflow tract, it is usually associated with balanced LV enlargement, and RV diastolic function results normal [15]. The most confusing elements may be found in ECG, indeed 14% of healthy endurance athletes shows TWI in V1, V2 and V3 and ventricular premature beats arising from the RV outflow tract, usually identified in patients with ARVC [20][97]. Although iRBBB pattern typical of athletes is uncommon in ARVC, particular attention should be paid if all these abnormalities are encountered together in athlete's ECG. In fact, ARVC may present with iRBBB plus TWI in leads beyond V2, or with low limb-lead voltages, and with premature ventricular beats with a LBBB pattern. Zalidi et al. derived that, in patient with repolarization abnormalities, balanced biventricular dilatation was likely to represent a benign manifestation of training in asymptomatic athletes without a relevant family history of cardiomyopathy or SCD [106].

### ***Dilated cardiomyopathy***

Dilated cardiomyopathy DCM is a myocardial disorder characterised by left ventricular dilatation, impaired systolic function (LVEF in the lower normal range or depressed), reduced SV and increased end-diastolic chamber pressure. It can be familial or genetic in origin, secondary to infection, inflammation, toxic substances or metabolic disorders, or related to long-standing uncontrolled hypertension. Morphologically, the left ventricular cavity is disproportionately increased in size and round-shaped. Life-threatening ventricular and supraventricular tachyarrhythmias usually represent the clinical presentation of this disorder, before left ventricular dysfunction is clinically evident, and SCD is most common in young people with DCM engaged in physical exercise and sport [2]. However, SrSCD due to DCM is relatively rare in competitive athletes as compared with other cardiomyopathies since systolic function impairment preventing adequate CO during exercise is not generally compatible with professional sports practice. There could exist a structural overlap between early-stage DCM and endurance athlete's heart with significant chamber dilation due to long term volume and pressure overload and concomitant decreased LVEF at rest [15]. In athletes with extreme LV dilation (LVED  $\geq$ 60 mm up 70 mm in men [44]), correct assessment of LVEF and exclusion of wall motion abnormalities are fundamental. CMR permits accurate assessment of LVEF and detection of fibrosis, usually by presence of LGE in the mid wall of the LV which is indicative of underlying cardiomyopathy in a

patient with an increased LV volume and reduced EF, but the absence of LGE does not necessarily exclude a DCM [37][97]. An LVEDD > 60 mm that persisted after a period of deconditioning, and associated with impaired LVEF < 45% and reduced SV is suggestive of DCM [107]. However, as morpho-functional adaptations typical of the athlete's heart have been described to persist over the long term, a brief period of detraining may not be sufficient to achieve a clear differential diagnosis [15]. This scenario may require downstream evaluation by stress imaging, or repeated assessment after long detraining. Stress echocardiography and CMR are often effective in identifying abnormalities of both systolic and diastolic function that become more apparent on exercise, and to detect abnormal tissue characterization [15]. It was demonstrated that highly trained football players with reduced resting systolic function showed normalization of LV function with exercise [108]. In contrast, patients with DCM rarely demonstrate the ability to augment CO in response to increased metabolic demands during training [97]. Simultaneous measurement of gas exchange during a cardiopulmonary exercise testing is able to identify DCM patients with reduced exercise capacity, reflected in low maximum VO<sub>2</sub> [37]. Although, peak VO<sub>2</sub> consumption values do not revealed a discriminative power between athletes with physiological LV enlargement and athletes with DCM [109].

### ***Left ventricular noncompaction or excessive trabeculation cardiomyopathy***

Left ventricular noncompaction cardiomyopathy (LVNC) is characterized by a double-layered LV myocardial wall structure comprising a thin epicardial layer and a trabeculated inner endocardial layer [15][97]. LVNC has been associated with increased risk of heart failure, ventricular arrhythmias, SCD, and thromboembolic events [15]. The diagnosis of this condition requires personal and family history, physical examination, 12-lead ECG, and cardiac imaging [15]. Electrocardiographic signs possibly found in case of LVNC are: TWI in lateral and inferior leads; ST segment depression; pathologic Q waves; LBBB and premature ventricular contraction (PVC) [73]. Echocardiography can detect the excessive endocardial trabeculation pattern and LV function abnormalities, but its spatial resolution does not allow accurate measures and the identification of crypts within the epicardium, especially when located in the LV apex. The most widely used echocardiographic diagnostic criteria fixed a threshold of end-systolic trabecular/ compact ratio  $\geq 2$  in adults and  $\geq 1.4$  in children [15]. CMR is often requested to confirm or exclude LVNC in symptomatic or positive family history patients with echocardiographic detection of a trabecular pattern. CMR with its superior spatial resolution provides a detailed assessment of the thin

epicardial layer and can differentiate endocardial trabeculation from apical HCM and crypts within the epicardium, which are rarely detectable with echocardiography [97]. Furthermore, CMR can confirm the pathology by detection of fibrosis pattern, it allows quantification of the LGE, which has been associated with a worse clinical status and outcome in excessive trabecular cardiomyopathy [15]. LVNC is often an unclassified cardiomyopathy for which the current imaging diagnostic criteria, based on echocardiography and CMR, reveal low specificity, leading to over diagnosis of this cardiomyopathy. Furthermore, the LVNC phenotype can overlap with other cardiomyopathies such as HCM and DCM, thus its true incidence and prevalence are not known [110].

Regarding the differentiation from athlete's heart, LV trabeculation without other features of noncompaction or repolarization changes could be a physiological response to increased preload during exercise in highly trained athletes [37].

Although, few competitive athletes with LVNC have been reported clinically, and therefore, the consequences of LVNC in athletic population are unknown and there is uncertainty on risk-stratification algorithm and athletic specific diagnostic criteria are not defined [110].

### **Coronary artery anomaly and disease**

Coronary artery anomalies (CAA) can be of congenital origins and can cause coronary insufficiency with consequent impaired myocardial perfusion and myocardial ischemia [111]. Anatomically, CCAs can feature an abnormal (1) coronary location/orientation of ostia with respect to the aortic wall, (2) course of the proximal or intermediate coronary segments, or (3) termination [111]. While coronary artery disease (CAD) is the narrowing or blockage of the coronary arteries, usually caused by atherosclerosis. CAA is mostly related to SrSCD in  $\leq 35$  years old athletes while CAD is mostly related to SrSCD in  $> 35$  years old athletes.

The CAAs most commonly responsible for SrSCD occur in the coronary arteries originating from the wrong sinus of Valsalva (the left coronary artery originating from the right sinus, or the right coronary artery originating from the left sinus) and it has an interatrial course between the aorta and the pulmonary artery [2].

The main cause of ischemia in patients with CAAs is generally the narrowing of the initial segment of the coronary artery at an intramural course by compression in between the inner and outer layers



of the aortic tunica media [111]. Myocardial ischemia is precipitated by exercise because of critically impaired coronary flow due to an abnormal, slit-like ostium of the anomalous coronary artery, compression of the anomalous artery between the pulmonary artery and ascending aorta or, possibly, coronary spasm triggered by endothelial dysfunction [2]. Young people with CAA may die suddenly as the first manifestation of their abnormality, although some may experience angina, syncope or palpitations [2]. The vast majority of these symptoms are related to exertion [2]. In an older population (>35 years) with congenital CAA, SrSCD is extremely rare, whereas symptoms of chest pain, shortness of breath or syncope are more prevalent [111].

Anomalies of the coronary arteries can be recognized through imaging analysis of anatomic and functional features [111]. Accurate exploration of proximal portion of coronary arteries by echocardiography may be useful in identifying athletes with anomalous coronary origin [24]. Although visualization of proximal LCA is possible in up to 97% cases, while identification of the origin of the RCA may not be possible in ~20% of athletes. The use of Doppler technique improves the precision of echocardiographic diagnosis since high flow velocity is a probable marker of stenosis [111]. Coronary artery disease may be diagnosed by exercise stress echocardiography by evaluating exercise inducible ischemia with moderate sensitivity and specificity (about 76 and 88%, respectively) [24]. However, in athletes with anomalous implantation of coronary artery, exercise stress echocardiography can be normal (absence of inducible ischemia), but this does not change the risk for SrSCD in such patients [24]. CMR has a greater sensitivity than echocardiography [111]. In adolescents or adults, CMR can yield a consistently specific diagnosis of high risk CAA type and the recognition of low risk CAAs [111]. Importantly for the patient, the analysis can be performed quickly and reliably without side effects or discomfort [111]. Stress perfusion CMR imaging allows for assessment of inducible ischemia and can help in the diagnosis of CAA in athletes as well as in the assessment of decisions relating to surgical intervention e.g. in asymptomatic right coronary origin from the left sinus of Valsalva [24][97]. CMR may also play an important role in depicting proximal coronary artery anomalies in athletes using coronary magnetic resonance angiography (MRA). Thus both stress CMR imaging and MRA can be used, as a less invasive tool with respect to coronary angiography, in asymptomatic young athletes with suspected CAA, as they have low risk of CAD [24]. Instead, electrocardiography has low sensitivity and specificity specifically in detecting CAA and premature coronary atherosclerosis. ECG signs representing impaired myocardial perfusion are more characteristic of an intense state of ischemia and in the ischemic cascade.

## **2.6.2.2 Inherited Electrical disorders**

### **Wolff–Parkinson–White syndrome**

Wolff–Parkinson–White (WPW) syndrome is a cardiac conduction system disorder characterized by abnormal accessory conduction pathways between the atria and the ventricles with anterograde conduction, causing ventricular pre-excitation [2][112]. Most patients with pre-excitation remain asymptomatic [2]. Symptomatic patients classically present with palpitations, pre-syncope, or syncope that results from supraventricular tachyarrhythmias, specifically orthodromic or antidromic atrioventricular reciprocating tachycardia (AVRT) [112]. SCD may be the first manifestation of underlying disease and occurs more frequently in exercising individuals [112]. SCD is a result of rapid anterograde conduction over the accessory pathway, when pre-excitation develops atrial fibrillation, which could lead to ventricular fibrillation [2]. The following ECG patterns characterize the diagnosis of WPW: delta waves, short PR interval and widened QRS complex. Utilization of the electrocardiogram as part of the pre-participation physical evaluation may allow for early identification of asymptomatic individuals with a WPW pattern [112]. WPW accounts for at least 1% of SrSCD. The risk of lethal arrhythmia appears to be higher in asymptomatic children than in adults, and SCD happens often at first manifestation [112].

### **Channelopathies**

Different arrhythmogenic diseases defined as channelopathies (long or short QT syndrome (LQTS, SQTS), Brugada syndrome (BS) and catecholaminergic polymorphic ventricular tachycardia (CPVT)) highly expose young subjects to risk of life-threatening arrhythmias. Pathophysiological mechanisms include mutations affecting genes associated with transmembrane ion channels (LQTS, SQTS, and BS) or proteins involved in intracellular calcium handling (CPVT) [2][113].

### ***Congenital long QT syndrome***

Congenital long QT syndrome (LQTS) is a group of disorders caused by mutations in channels that regulate sodium, potassium, and calcium currents and by a mutation in a cytoskeletal gene (ankyrin B) that affects sodium and calcium kinetics. There are three types of LQTS. The LQT1 type is mutation of KCNQ1 potassium channel (IKs) gene, LQT2 is the mutation of HERG

potassium channel (IKr) gene and LQT3 is the mutation of SCN5A sodium channel (INa) gene. These mutation result in prolonged ventricular repolarization and an increased risk for sustained ventricular tachyarrhythmias, characteristically torsade de pointes and ventricular arrhythmias during exercise or stressful circumstances [114][115]. The number of cases of SCD due to LQTS among young athletes is estimated to range from 0.5% to 8% [2]. LQTS manifest most commonly by syncope and electrocardiographic changes due to mutations in ion channels involved in cardiac action potential plateau and repolarisation. The diagnosis of LQTS relies on the measurement of the QT interval corrected for HR (QTc) using Bazett's formula on 12-lead electrocardiograms at stable HR at rest between 60 and 100 bpm [115]. Electrocardiographically it is difficult to define a clear cut off value for diagnosis: LQTS is defined as a corrected QT interval >440 ms in men and >460 ms in women, but intervals of >470 ms and >480 ms have been suggested [2]. Extreme QT prolongation (usually >500 ms) predisposes to torsade de pointes and ventricular fibrillation and therefore QTc>480 ms is sufficient to establish the positive diagnosis [115]. LQTS patients often present with additional ECG features including excessive bradycardia for the age, visible T-wave alternance or notches on the T-wave (suggestive for LQT2) and long sinus pauses that are common among LQT3 patients. Moreover, age and gender affect QTc measurements in both healthy individuals and patients with LQTS affecting the different genotype [116]. Therefore, other ECG and clinical factors are usually taken into consideration, using various scoring systems, for diagnosis. Score combining the age of the patient, clinical and family history, the QTc duration, T wave morphology, and previous history of Torsade de pointes has been created such as the 1993-2011 LQTS diagnostic criteria where a LQTS risk score >3 is already considered diagnostic for LQTS [115][117]. Stress exercise test allows exploring the adaptation of the QT interval to rapidly increasing heart rates, which has been demonstrated to be impaired in LQTS, especially LQT1[118]. LQT1 and LQT2 patients show an exaggerated QT prolongation after physical effort [118]. A QTc interval  $\geq$ 480 ms at the fourth minute of recovery from exercise stress has been recently suggested as a new criterion to consider in the LQTS risk score after demonstrating 100% specificity in identifying LQT1 and LQT2 patients [117][119]. QT interval also fails to adapt to sinus tachycardia after standing up quickly in LQTS patients and may elicit an exaggerated QTc prolongation; a QTc >499 ms at maximal nearness between the end of the T-wave and the beginning of the following P-wave shows a 90% sensitivity and 87% specificity for the diagnosis of LQTS [120]. Finally, ethnicity differences should be addressed with Africans having increased QT duration and shorter QRS duration; and such differences with Caucasians in QT duration did not fluctuate with HR variations during stress tests [45]. Definitely, 12-lead ECG and daily

monitoring are recommended to comprehensively evaluate the QTc interval in precordial leads at different times throughout the day, including the night when LQT3 patients exhibit the largest QTc prolongation [115].

### ***Congenital short QT syndrome***

Congenital short QT syndrome (SQTS) is characterized by a very short QT interval and predisposition to atrial and ventricular fibrillation [113]. Possible causes are mutations in potassium channels KCNH2, KCNQ1 and KCNJ2 or by mutations L-type calcium channel CACNA1C and CACNB2 [113]. During sport, no specific triggers for STQS arrhythmic events have been identified, and thus the consequences of strenuous physical activity in SQTS patients remain unknown. During electrocardiographic analysis, the diagnosis of SQTS is established in those patients with a shorter than normal QTc. Nevertheless, an accurate threshold to identify those patients with a short repolarization that pose at risk of SCD remains controversial. Current ESC guidelines propose a QTc  $\leq 340$  ms to diagnose SQTS [121]. Diagnosis should be considered in the presence of a QTc  $\leq 360$  ms in the secondary prevention setting as well as for patients with a familiar history of SCD or SQTS or in patients with a known gene mutation [115].

### ***Brugada syndrome***

BS is an autosomal dominant, sodium channelopathy, which clinically presents with syncope (due to polymorphic ventricular tachycardia) or less commonly as ventricular fibrillation leading to SCD [2]. Brugada syndrome is responsible for up to 4% of all SCD worldwide [122]. Increased vagal tone induced by chronic athletic conditioning may enhance the propensity to die at rest, and hyperthermia during exercise may potentially trigger arrhythmias during strenuous activity [2]. The disease has mixed phenotypic expressions: distinct repolarisation abnormalities, subclinical cardiac conduction defects, heterogeneity of repolarization and depolarization, particularly over the RT and the outflow tract, predisposing to arrhythmogenic substrate [115] [122].

Diagnosing BS should include both clinical history and ECG findings [122]. An ECG pattern of J-point and ST-segment elevation in the precordial leads V1 and V2 is typically seen and called Brugada Type I ECG pattern and it is considered sufficient for the diagnosis [115]. Classically, Type I ECG pattern has a coved ST segment elevation  $\geq 2$  mm, negative T wave and no isoelectric

separation of T wave. The coved Type I ECG pattern is considered diagnostic of the syndrome but its prevalence is very low [122]. There exist two more rare ECG pattern Type 2 and Type 3 but they are usually indicated both by the term Type 2. Type 2 ECG pattern has a saddleback appearance with an ST segment elevation of  $\geq 2$  mm, though that is still  $\geq 1$  mm ST elevation and a positive or biphasic T wave; Type 3 ECG pattern is also saddleback but has an ST segment elevation of  $\geq 1$  mm [122]. Distinguishing between a saddle back Type 2 Brugada pattern and one of many “Brugada-like” patterns presents challenges especially in athletes. Several criteria have been proposed to assess Brugada like ECG patterns in athletes, these were previously discussed in the section ‘early repolarization’ in chapter about ‘Electrical adaptation’ [122].

### ***Catecholaminergic polymorphic ventricular tachycardia***

This involves mutations in the ryanodine receptor, calsequestrin or the ankyrin-B protein, which predispose to arrhythmias and recurrent syncope typically provoked by exercise or stress [2]. Adrenergically mediated supraventricular arrhythmias (premature atrial contractions, runs of supraventricular tachycardia and bursts of atrial fibrillation) are also frequent in CPVT [115]. This adrenergically dependent arrhythmia is highly lethal, typically before the age of 20–30 years, and cases are estimated to comprise a substantial number of patients with familial arrhythmias without QTc prolongation or Brugada type ECG abnormalities [2]. According to the latest diagnostic criteria, CPVT is diagnosed in the presence of a structurally normal heart, normal ECG, and effort- or emotion-induced ventricular tachycardia [121]. Patients usually show normal resting ECGs, but the exercise test may show multifocal ventricular premature beats or ventricular tachycardia with alternating QRS axis [2].

### **2.6.2.3 Acquired Structural cardiac abnormalities**

#### **Myocarditis**

Myocarditis is usually caused by viral infections of the myocardium with a consequent transition to scar and DCM [110]. Myocarditis commonly presents with disproportionate shortness of breath on exertion, chest pain, and arrhythmias or acute myocardial infarction without antecedent symptoms [110]. The contribution of myocarditis to SCD varies significantly with age, causing

SCD in ~2% of infants, ~5% of children and higher rates of myocarditis related death are occasionally reported in general populations  $\leq 35$  years old [110]. Most SCD attributable to myocarditis occur in males [110]. Myocarditis accounts for 4 to 7.5% of arrhythmogenic SrSCD. Athletes, with fibrotic regions as consequence of sub-clinical myocarditis, seem to have a high susceptibility to develop ventricular arrhythmias. Fibrotic areas in the LV are more common among athletes proving the idea that intense exercise has a promoting effect on the development of this substrate. Maybe, intense exercise during a viral infection may make the heart more vulnerable to develop scar [51]. Myocarditis can present with electrocardiographic features of cardiac ischemia or unexplained high-degree AV block or other arrhythmias. Echocardiography or CMR imaging can detect wall motion abnormalities or pericardial effusion.

In addition, LGE findings in CMR imaging demonstrated to be a major predictor of mortality with septal and mid-wall pattern showing a correlation with major adverse cardiac events independent of symptoms, EF and LVEDV [97][110].

#### **2.6.2.4 Other acquired causes**

##### **Drugs and Stimulants**

Many doping substances commonly used (anabolic steroids, growth hormone, erythropoietin) have the potential to increase cardiovascular risk in athletes by inducing potentially lethal ventricular tachyarrhythmias, especially in extreme circumstances such as physical exhaustion, difficult environmental conditions and extreme stress [2].

##### **Commotio cordis**

Commotio cordis is caused by a blow or a small object forcefully hurting the chest, specifically to the precordium, can trigger ventricular fibrillation without causing structural injury to the heart and the overlying skeletal structure (ribs and sternum). Specifically, the collision should happen 10–30 ms before the T-wave peak (i.e., during the vulnerable phase of repolarisation) potentially inducing ventricular fibrillation. In sport setting, commotio cordis is typically caused by hockey pucks or lacrosse balls and other small objects forcefully striking the chest; or in bodily contact sport by blow or players colliding. Commotio cordis accounts for 20% of cases [2][3][123].

### **2.6.2.5 Sudden cardiac death of unknown causes**

A considerable subset of SCD, however, occurs in the absence of an evident structural or electrical cardiac disorder. In the study of Burke et al, 6/34 SrSCD were of unknown cause, and other studies found a percentage of 1–7% of SrSCD from unknown causes [2][123]. As channelopathies do not present any distinct morphological abnormalities, it is possible that these electrical disorders might be responsible for a number of SrSCDs previously considered as unexplained. From a biofluid dynamic point of view SCD of unknown causes could be caused by an impaired wave dynamics and flux in coronary arteries. Indeed worsening perfusion and oxygen delivering combined with increase myocardial load can lead to ischemia and myocardial infarction [124].

## 2.7 Screening

In sport cardiology, the goal for health care providers is to enhance prevention and management of SrSCD, guaranteeing safe sport participation. Accordingly, there is growing interest to promote effective risk stratification algorithms for the early identification of sport participants with underlying cardiovascular disease at risk of SrSCD or a pathological athlete's heart, creating targeted prevention through tailored and individualized pre-participation screening.

The cardiovascular screening of athletes could be applied at two levels:

- First level screening: pre-participation screening of asymptomatic competitive or leisure athletes,
- Second level screening: deeper assessment of athletes reporting specific symptoms, positive family history, and/or abnormal physical examination.

Pre-participation screening of all subjects embarking on sports activity has the potential to identify asymptomatic competitive athletes or asymptomatic individuals engaged in leisure-time sports activity at increased cardiovascular risk and potentially reduce mortality [15].

Differentiating between sport-related physiological adaptation of cardiovascular system and cardiovascular subclinical disease is the most challenging task. During pre-participation screening, under-diagnosis and over-diagnosis of pathology may lead to life-threatening events and unnecessary disqualification respectively [15].

Although much has been debated, different guidelines for the first level pre-participation screening include clinical and family history and physical examination to detect or raise suspicion of cardiovascular abnormalities, with 12-lead ECG as the first-line test for the diagnosis of heart disease in sport participants [15]. Athletes are eligible for competition if negative results are obtained from family history, physical examination and 12-lead ECG, otherwise additional tests are requested. Cardiovascular abnormalities potentially responsible for SrSCD are managed according to the available recommendations for sports eligibility [25].

When a second level screening is recommended, standard echocardiography has a central role because of its wide availability, relative low cost, and high diagnostic and prognostic power. One main limit of echocardiography is the poor spatial resolution, which is overcome by cardiovascular magnetic resonance. CMR allows precise assessment of cardiovascular anatomy, function, and



myocardial tissue characterization. Given its characteristics, CMR imaging is required when results from first level screening and echocardiography are equivocal or raise the suspicion of heart disease [15]. Even if most imaging studies continue to be performed at rest, the distinction between athlete's heart and cardiac pathology may be better appraised during exercise, when it would be easier to unveil reduced functional reserve in pathological situations. This involves the absence of reference values for morphologic and functional parameters under stress and uncertainties about the most effective stressor to be used [15].

Pre-participation protocols seem to not have the same efficiency on middle-aged/senior athletes engaged in leisure-time sports. Whereas ECG screening has been proven to be life-saving in young competitive athletes (<35 years), in whom SCD is mostly caused by ECG-detectable genetic cardiomyopathies, it appears to be a non-accurate test for detecting CADs, which are the most common cause of SrSCD in middle-aged/senior athletes engaged in leisure-time sports [26]. Nonetheless, most Associations of Cardiology and Sports Medicine as a prudent measure recommend cardiovascular medical evaluation before sport activity. The specific cardiovascular evaluations vary in relation to the individual risk profile (age, sex, blood pressure, blood cholesterol, and smoking history) and the type or intensity of physical exercise. Evaluations vary from self-check through questionnaire to maximal exercise testing and other cardiologic evaluations. The latter are usually reserved to those individuals with increased risk for adverse coronary events embarking on moderate/intense training [26][27]. As in older athletic population, also children require specific pre-participation screening. In fact, normal ECG in pre-pubertal age and the ECG phenotype of most diseases causing SCD differ notably from adults. These facts result in less specific and less sensitive ECG-based screening programs when extending the adult recommendation to children, without further studies. Therefore, history and physical exam should remain central component of pre-participation screening in paediatric population [28].

### **2.7.1 Electrocardiography**

In pre-participation screening, 12-lead ECG allows early detection of cardiovascular conditions distinctively manifesting with ECG abnormalities (electrical alteration), and pre-symptomatic diagnosis of cardiomyopathies such as HCM and AVRC, which manifest with ECG abnormalities in up 90% of affected individual [77].

During pre-participation screening both resting ECG and stress ECG are recorded. Resting ECG is a static track that can highlight coronary diseases, cardiac rhythm disturbances (extra systoles, arrhythmia and fibrillation), changes in heart volume due to hypertrophy and the electrical impulse conduction problems. Stress ECG is a dynamic track that can highlight latent heart diseases and establish the limits of physical activity for patients with coronary failure. Additionally, stress ECG after gentle exercise permits to identify as normal ECG findings such as low atrial rhythm, isorhythmic dissociation and junctional rhythms, which occur as result of increased vagal tone and/or intrinsic alterations to pacemaker cells and AV conduction tissue in highly trained athletes. Indeed in stress ECG after gentle exercise these ECG patterns are overcome at high HR [73].

Nevertheless, the ECG has been traditionally considered to be a poor screening test in athletes, because of its presumed low specificity and its potentially difficult interpretation that requires specialized expert to recognize the physiological ECG alteration characteristic of athlete's heart from the ECG abnormalities seen in cardiovascular diseases and so avoid high false positive rates [77].

Only few countries developed comprehensive pre-participation screening protocols including 12-lead resting ECG in addition to careful family history information and physical examination [15]. Currently, European Society of Cardiology (ESC), most European Cardiology Societies and Sports Medical Federations, and the International Olympic Committee ("Lausanne Recommendations") recommend the 12-lead ECG screening as a part of pre-participation screening of competitive athletes [25]. In the 2005, a consensus statement of the Section of Sports Cardiology of the European Society of Cardiology (ESC) proposed a common European screening protocol for prevention of SCD in young competitive athletes, which included ECG in addition to history and physical examination. However, the document listed the ECG abnormalities relevant to pre-participation screening but did not provide any specific guidelines for interpretation of athlete's ECG [25].

A new perspective in the interpretation of an athlete's ECG was first proposed in 2010 by a consensus document of ESC, with the aim to increase the specificity and sensitivity of the pre-participation ECG screening program, elevating its accuracy in detecting heart diseases and cost-effectiveness [81].

In this document, the athlete's ECG changes were classified into two groups: "common and training-related" (Group 1) and "uncommon and training-unrelated" (Group 2) [81]. The classification was performed according to four aspects: the prevalence of athlete's ECG changes,

their relation to exercise training, the association with an increased risk of cardiovascular disease and the need for further investigations [81]. According to the ESC recommendations, finding common (Group 1) changes should not cause alarm and the athletes should be considered eligible for competition; on the other hand, further clinical investigation should be reserved to athletes with Group 2 abnormalities, which may be associated with an underlying heart disease at risk of SrSCD [81].

In 2011, a group of experts coordinated of the Stanford University published a second international consensus document, which provided clearer definitions and cut-off values for LQTS and intra-ventricular conduction delay. In addition, the Stanford criteria suggested to include among sport-related ECG changes the anterior TWI associated with ST-segment elevation in black athletes [125]. In 2013 the ECG criteria were further refined, obtaining the “Seattle criteria”. The document provided a detailed description of ECG parameters with reference values for abnormality and included clinical recommendation for management and follow-up of athletes with pathologic ECG abnormalities [126]. The Stanford and Seattle criteria refined the existing guidelines for athlete's ECG interpretation improving successfully specificity, particularly among Afro-Caribbean athletes. However, they were largely based on experts' consensus and lacked supporting scientific data [77].

Most recently, the International Consensus Standards for ECG Interpretation in Athletes was published in the European Heart Journal, the Journal of the American College of Cardiology and the British Journal of Sports Medicine [73]. These recommendations provides refined diagnostic criteria for ECG interpretation in asymptomatic athletes or in the evaluation of athletes with cardiac symptoms or a positive family history for cardiac disease [73]. However, it should always be remembered that a normal ECG should not offer false reassurance in the assessment of an athlete in whom suspicion of cardiac pathology is high [74].

Further studies are needed to test the accuracy of ECG screening in relation to ethnicity, gender, age and different levels of training and/or type of sports, since refined diagnostic criteria were tested in cohorts of predominantly competitive male and young athletes [77]. The following Tables 5 and 6 report the international standards for ECG interpretation in athletes [73] and summarize the normal and abnormal ECG findings discussed in the previous sections. Each normal or abnormal ECG pattern is related to symbols that represents its higher recurrence within a group of the risk stratification classification. Table 5 contains normal training-related ECG alterations due to physiologic adaptations to regular exercise, which do not require further evaluation in

asymptomatic athletes with no significant family history. Table 6 contains abnormal ECG findings unrelated to regular training, these may suggest the presence of pathologic cardiovascular disease, and require further diagnostic investigation. Moreover, borderline ECG findings in athletes are reported. If present in isolation borderline ECG finding do not represent pathologic condition in athletes, but the concomitant presence of two or more of them requires additional investigation. The last two columns of Table 6 report also the potential diagnoses and the suggested second order screening [73].

Some observation regarding the abnormal ECG findings, specifically TWI, are needed. TWI >2mm in the inferior / lateral leads should raise the suspicion of ischemic heart disease, aortic valve disease, hypertensive cardiomyopathy, HCM or LVNC. This ECG pattern may identify athletes at risk for subsequent development of structural heart disease, suggesting for continuous clinical surveillance with ECG and echocardiograms [68]. Regarding biphasic T wave, if the negative portion of the T wave is >1 mm in depth in two or more leads (excluding leads aVR and V1), it is reasonable to consider this pattern as abnormal [68].

*Table 5* Normal ECG findings in athletes [73]. The symbols identify the population in which these normal ECG patterns are usually recurrent: Sport : **aerobic activity** ■ **anaerobic activity** ■ **mixed activity** ■ ; Gender: **female** \* **male** \*; Age: >35● <18<35● <14<18● <6<14● ; Ethnicity: **Caucasian** ◆ **Afro-Caribbean** ◆ **Asian** ◆

Normal ECG findings	Definitions
Resting sinus bradycardia ■ ◆ ◆	in absence of symptoms (fatigue, syncope or dizziness), a normal heart rate $\geq 30$ bpm and/or pauses of $\geq 3$ s during sleep hours due to increased vagal tone
Sinus arrhythmia	Heart rate variation with respiration: rate increases during inspiration and decreases during expiration
Ectopic atrial rhythm	P waves have a different morphology compared with the sinus P wave, such as negative P waves in the inferior leads
Junctional escape rhythm	QRS rate is faster than the resting P wave or sinus rate and typically less than 100 beats/minute with narrow QRS complex unless the baseline QRS is conducted with aberrancy
First-degree AV block	200 ms < PR interval < 400 ms
Mobitz type I second-degree AV block	PR interval progressively lengthens until there is a non-conducted P wave with no QRS complex; the first PR interval after the dropped beat is shorter than the last conducted PR interval
iRBBB ■ ◆	rSR' pattern in lead V1 and a qRS pattern in lead V6 with QRS duration < 120ms
Isolated increased QRS voltage * ◆	Isolated QRS voltage criteria for left (SV1 $\geq$ RV5 or RV6 > 3.5 mV) or right ventricular hypertrophy (RV1 $\geq$ SV5 or SV6 > 1.1 mV)
Early repolarization * ◆ ● ●	J point elevation, ST elevation, J waves, or terminal QRS slurring in the inferior and/or lateral leads
Early repolarization in black athletes * ◆ ● ●	J-point elevation and convex ('domed') ST segment elevation followed by T wave inversion in leads V1-V4 in black athletes
Juvenile T wave pattern * ◆ ●	T-wave inversion V1–V3 in athletes < age 16

Table 6 Abnormal ECG findings in athletes [73].

ECG abnormality	Definition	Potential cardiac disease	Recommended second level screening
T wave inversion	$\geq 1\text{mm}$ in depth in two or more contiguous leads; excludes leads aVR, III, and V1.		
	<u>Anterior</u> : V2–V4. excludes: 1) black athletes with J-point elevation and convex ST segment elevation followed by TWI in V2–V4; 2) athletes < age 16 with TWI in V1–V3; 3) biphasic T waves in only V3.	ARVC DCM	Echocardiography Exercise ECG test Minimum 24 h ECG monitor SAECG signal averaged ecg
	<u>Lateral</u> : I and aVL, V5 and/or V6 (only one lead of TWI required in V5 or V6).	HCM DCM LVNC ARVC (with predominant LV involvement) Myocarditis aortic valve disease	Echocardiography CMR Exercise ECG test Minimum 24 h ECG monitor
	<u>Inferolateral</u> : II and aVF, V5–V6, I and aVL.	HCM DCM LVNC ARVC (with predominant LV involvement) Myocarditis	Echocardiography CMR Exercise ECG test Minimum 24 h ECG monitor
	<u>Inferior</u> : II, III and aVF	HCM DCM LVNC Myocarditis aortic valve disease	Echocardiography
ST segment depression	ST $\geq 0.5\text{mm}$ in depth in two or more contiguous leads. ST $>0.5\text{ mm}$ below PR isoelectric line between J-junction and beginning of T wave in V4–6, I and aVL, or ST $\geq 1\text{mm}$ in depth in any lead.	HCM DCM LVNC ARVC Myocarditis CAD	Echocardiography CMR
Pathologic Q waves	Q/R ratio $\geq 0.25$ or $\geq 40\text{ms}$ in duration in two or more leads (excluding III and aVR)	HCM DCM LVNC Myocarditis CAD Prior MI	Repeat ECG for septal (V1–V2) QS pattern Echocardiography CAD risk factor assessment
Complete LBBB	QRS $\geq 120\text{ms}$ , predominantly negative QRS complex in lead V1 (QS or rS), and upright notched or slurred R wave in leads I and V6	DCM HCM LVNC Sarcoidosis Myocarditis CAD	Echocardiography CMR (with stress perfusion study)
Profound nonspecific intra-ventricular conduction delay	Any QRS duration $\geq 140\text{ms}$	DCM	Echocardiography
Epsilon wave	Distinct low amplitude signal (small positive deflection or notch) between the end of the QRS complex and onset of the T wave in leads V1–V3	ARVC	Echocardiography Exercise ECG test Minimum 24 h ECG monitor SAECG CMR

Table 6 Continue. Abnormal ECG findings in athletes [73].

Ventricular pre-excitation	PR interval < 120 ms with a delta wave (slurred upstroke in the QRS complex) and wide QRS ( $\geq 120$ ms)	WPW	Exercise ECG test Echocardiography
QTc interval	QTc $\geq 470$ ms <b>male</b> * QTc $\geq 480$ ms <b>female</b> * QTc $\geq 500$ ms (marked QT prolongation)	LQTS	Repeat resting ECG on separate day Review for QT prolonging medication Acquire ECG of 1st degree relatives if possible
	QTc $\leq 340$ ms	SQTS	Repeat resting ECG on separate day Review for QT prolonging medication Acquire ECG of 1st degree relatives if possible
Brugada Type I pattern	Coved pattern: initial ST elevation $\geq 2$ mm (high take-off) with downsloping ST segment elevation followed by a negative symmetric T wave in $\geq 1$ leads in V1–V3 Profound	Brugada syndrome	Referral to cardiologist or heart rhythm specialist Genetic testing and family screening
Profound sinus bradycardia	waking HR < 30 bpm or sinus pauses $\geq 3$ s	Myocardial or electrical disease	Repeat ECG after exercise (mild aerobic activity)
Profound first-degree atrioventricular block	PR interval $\geq 400$ ms	Myocardial or electrical disease	Repeat ECG after exercise (mild aerobic activity)
Mobitz Type II second-degree atrioventricular block	intermittently non-conducted P waves with a fixed PR interval	Myocardial or electrical disease	Echocardiography Minimum 24 h ECG monitor
Third-degree atrioventricular block	Complete atrioventricular block	Myocardial or electrical disease	Echocardiography Minimum 24 h ECG monitor
Atrial tachyarrhythmias	Supraventricular tachycardia, atrial fibrillation, atrial flutter	Myocardial or electrical disease	Minimum 24 h ECG monitor Exercise ECG test Echocardiography
PVC	$\geq 2$ PVCs per 10 s tracing	HCM DCM LVNC ARVC Myocarditis Sarcoidosis	24 h ECG monitor Exercise ECG test Echocardiography
Ventricular arrhythmias	Couplets, triplets, and non-sustained ventricular tachycardia	Myocardial or electrical disease	Exercise ECG test Minimum 24 h ECG monitor Echocardiography CMR
Left axis deviation *	$-30^\circ$ to $-90^\circ$	Two or more borderline ECG findings can be an index of myocardial disease (ARVD, Brugada syndrome, Congenital structural heart diseases), consider echocardiography and additional testing based on clinical suspicion.	
Left atrial enlargement	Prolonged P wave duration of $>120$ ms in leads I or II with negative portion of the P wave $\geq 1$ mm in depth and $\geq 40$ ms in duration in lead V1		
Right axis deviation	$> 120^\circ$		
Right atrial enlargement	P wave $\geq 2.5$ mm in II, III, or aVF		
Complete RBBB	Rsr' pattern in lead V1 and a S wave wider than R wave in lead V6 with QRS duration $\geq 120$ ms		

## **2.7.2 Imaging**

Cardiac imaging is not usually recommended as a first-line test, but it represents a very useful tool, both at rest and during stress imaging, in the assessment of athletes with a positive family history, symptoms, and/or abnormal resting 12-lead ECG.

### **2.7.2.1 Echocardiography**

Echocardiography is the first line and most available imaging tool used in case of suspected family history and ECG. It enables differentiation of physiologic and pathologic response to exercise, namely athlete's heart from pathologic LVH [24]. Combining different methods, such as 2D and 3D measurements of cardiac size, volumes, wall thickness, mass index, tissue velocity, and myocardial strain imaging, echocardiography allows comprehensive morphologic and functional evaluation of the heart [24]. Further echocardiography, with its high temporal resolution, permits diastolic function testing and valvular heart disease assessment. On the other hand, echocardiography has a low acoustic window, poor visualization of apical segments and RA and limited reproducibility.

In 2018, the British Society of Echocardiography (BSE) and Cardiac Risk in the Young (CRY) published a guideline update for the practice of echocardiography in the cardiac screening of sports participants [19].

### **2.7.2.2 Cardiac Magnetic Resonance**

In the presence of abnormal or uncertain findings from the upstream diagnostic analysis, CMR imaging can be helpful to perform diagnosis and distinguish between exercise-induced cardiac remodelling and cardiovascular pathology. CMR overcomes echocardiography for spatial resolution and it represents the current gold standard in the non-invasive assessment of cardiac morphology, quantification of volumes and flow, and advanced myocardial tissue characterization. Indeed it allows morphological and functional evaluation of cardiac chambers, with clear delineation of ventricular endocardial and epicardial borders [15], providing full ventricular

coverage with no interslice gap and the ability to image any plane [97]. Therefore it is the most accurate way to measure structural and cellular remodelling to long-life exercise such as in veterans athletes [97]. In morphological evaluation, native whole-heart CMR permits visualization of the origin and course of coronary arteries without the need for paramagnetic contrast agents [15]. This decreases the risk related to more invasive techniques and to potentially dangerous ionizing radiation or the administration of intravenous medicines and contrast. A further advantage for patient comfort is the fast data acquisition time 10–15 min [15].

Other CMR sequences of value include: stress perfusion for ischemia assessment; tissue-tracking module for measurement of strain and strain-derived parameters; LGE modality that is useful in evaluating presence of fibrosis and scar further providing clarification of a disease process in athletes with structural features overlapping cardiomyopathy [15][97].

The main limitations of this diagnostic tool are: expensiveness, limited availability, limited temporal resolution, use sometimes of contrast agent and artefacts [15].

### **2.7.2.3 Stress Imaging**

Stress imaging (stress echocardiography and stress CMR) represents a useful tool to unmask covert pathological changes that are not evident at rest, especially in athletes in whom arrhythmias and/or early-stage cardiomyopathies are suspected. Further, stress imaging permits the reproduction of exercise-induced ischemia and the evaluation of reduced cardiac functional reserve in stress condition. Either pharmacological stressors or exercise can induce stress. Exercise imaging has several advantages. Firstly, it avoids the administration of drugs, which, although generally well tolerated, may cause unwanted harmful side effects. Secondly, the use of dynamic exercise as a stressor permits to obtain real physiological activation of the cardiovascular system. Thirdly, exercise stress is the simplest modality that can induce both regional wall motion abnormalities in cardiac chambers and vasculature, and perfusion defects. Finally, exercise allows exercise related symptoms to be reproduced and their correlation with ECG and stress imaging findings [15]. On the other hand, it requires specific and sometimes expensive equipment. Moreover, motion artefacts may significantly limit the overall accuracy of the examination with both echocardiography and CMR during stress. To overcome motion limitation and obtain higher quality images, images could be acquired immediately after temporary exercise cessation.



However, the time period of exercise cessation allows partial recovery, limiting the detection of abnormalities unmasked mainly during effort. Stress echocardiography enables evaluation of cardiac structure, especially ventricles, and function combined with real-time electrocardiographic and cardiopulmonary exercise testing (CPET) data. Moreover, wide availability, low cost, and the absence of ionizing radiation also make it the ideal method in the evaluation of athlete's heart during exercise [15][24]. Technological improvements currently offer the possibility to perform exercise CMR imaging with high accuracy and reproducibility. The main developments are free-breathing real-time CMR imaging techniques and the availability of CMR-compatible exercise equipment [15]. Even if it is less available than stress echocardiography, stress CMR provided promise results in the assessment of athletes with mild ventricular dilation, mildly reduced LVEF or RVEF and when rest imaging is inconclusive [15][24]. Despite initial favourable results, further investigations are needed to assess cost-effectiveness and diagnostic benefits of stress imaging in distinguishing between early-stage cardiomyopathies and exercise- induced cardiac remodelling [15].

## **II Section: Cardiac monitoring through wearable sensors: normative electrocardiographic reference standards for athletes**

### **3.1 Background**

Regular physical activity has proven a general beneficial role for cardiovascular health. In few cases, although, increased cardiovascular load during exertion in people with an underlying, often unknown, cardiovascular abnormality can trigger SrSCD. As seen from the analysis of incidence in the first section, SrSCD is the leading medical cause of death across all sports [1][2][3].

Prevention remains the only weapon to contrast SrSCD. Pre-participation screening represents the first-line test for the diagnosis of cardiovascular pathology in sport participants. Although, its cost-effectiveness is widely debated with the main goal to balance among saved lives, economic costs and legal, ethical and psychological issues [127][128]. Thus the objective of health care providers should be to develop individualized pre-participation screening and effective risk stratification algorithms for the early identification of sport participants with underlying cardiovascular disease at risk of SrSCD. Currently, pre-participation screening include clinical and family history, physical examination and rest 12-lead ECG [15]. Unfortunately, most screenings are usually recommended for competitive athletes, while amateur athletes and people occasionally practicing sport are typically left to optional, sometimes self-made, evaluations of their health status [127]. Further, screening of athletes is performed regularly but not too frequently, typically once a year.

Technological improvements currently offer the possibility to record HR and ECG signal through wearable sensors. These technologies could provide useful information for non-invasive self-evaluation of SrSCD risk, as well as provide data for exercise dose optimization and continuous monitoring of athletes [129]. Wearable physical-activity monitoring sensors are able to record reliably ECG and could provide useful clinical information on the athlete's health status at each training session, especially if combined with software applications for automatic ECG interpretation [127]. Making ECG analysis available everyday out of hospital. Typically, wearable sensors provide a reduced number of ECG leads which not necessarily match a subset of the standard ECG leads. As in the case of chest strap BioHarness 3.0 by Zephyr ([www.zephyranywhere.com](http://www.zephyranywhere.com)). It is a reliable wearable sensor widely used by athletes all over the world which, however, does not replicate any of the standard 12 leads. In signals from wearable

sensors, the typical ECG waves, which are the P wave, the QRS complex and the T waves, are recognizable; however, ECG morphology and amplitude is different.

As known, ECGs belonging to athletes result deviated with respect to normal because of sport-related cardiovascular adaptations characteristic of athletic population. These changes, which are deeply treated in Section I, depend on age, gender, ethnicity, type of sport (*i.e.* dynamic vs static), intensity of training, amount of training (training sessions duration times weekly training rate) and number of practised sports. Sometimes, these physiological deviations may be confounded with a cardiovascular pathology leading to wrong diagnosis or unreasonable disqualification after pre-participation screening. Thus, specific athlete's ECG interpretation guidelines are fundamental when screening athletes. So far, international recommendations for athlete's ECG interpretation have been developed only for resting standard 12-lead ECG for which normal reference values and pathological thresholds, often lead dependent, have been indicated. Consequently, being lead dependent, the normal reference values relative to the standard 12-lead ECG cannot be used to interpret the ECG acquired by wearable sensors. Thus, for a clinical use of the ECG acquired through wearable sensors, reference values specifically obtained for the possibly non-standard ECG leads are needed. As far as we know, no normative reference values have been proposed for ECG obtained with the popular BioHarness 3.0 Zephyr [127][129][130][131]. Thus, the aim of the present work was to provide an initial set of electrocardiographic reference values for resting ECGs of athletes acquired through the BioHarness 3.0 with the scope to support large-scale prevention programs and the continuous monitoring during training session fighting SrSCD.

## **3.2 Materials and Methods**

### **3.2.1 Study population**

Experimental data for this study were taken from the Sport Database [130] and from the Cycling Database at the Cardiovascular Bioengineering Lab of the Università Politecnica of Marche. The two databases contain cardiorespiratory signals acquired in 126 and 12 athletes respectively, recorded through the wearable chest strap BioHarness 3.0 by Zephyr ([www.zephyranywhere.com](http://www.zephyranywhere.com)) during a training session. The ECG signal are one lead sampling at 250 Hz. All athletes gave their informed consent prior to data acquisitions and all acquisition undertaken in compliance with the ethical principles of Helsinki Declaration and approved by the institutional expert committee. According to the acquisition protocol, not always respected by the athletes, each acquisition included a 5-min long resting phase prior to training, an exercise phase and a recovery phase [130]. Only athletes with no previous or current history of cardiorespiratory diseases and not taking any drug, for whom ECG was acquired, were enrolled in the study. Sports practiced by athletes were classified according to the Mitchell's criterion [21]. According to endurance component they were all included in the class C with higher dynamic level. Regarding the static component the seven selected sport disciplines have increasing maximal static component identified with I (low static component), II (medium static component) and III (high static component).

### **3.2.2 Experimental methods**

Resting pre-exercise phases were visually inspected to select a low noise portion of ECG 10-s long. In case of erroneous activation or positioning of the wearable sensor, the extremely corrupted recordings were excluded.

MATLAB R2018b was used for signals processing. Each 10-s ECG was bandpass filtered (cut-off frequencies: 0.5 Hz and 50 Hz; bidirectional 6<sup>th</sup>-order Butterworth) in order to remove baseline wanders and high frequency noise. R-peak positions were automatically identified with Pan-Tompkins algorithm [132]. R peaks were used to compute median RR interval (mRR) and HR. Successively, each cardiac beat was extracted selecting 250 ms before each R peak and a variable time interval after the same R peak. The variable time interval depends on HR. Considering a fixed

time interval of 450 ms it was variably adjusted for HR by using Bazett's equation. The correlation between the extracted beats was computed and the 5 beats which correlate most were used to compute the representative median of the ECG portion. The median beat was then submitted to an automatic procedure [133] for the identification of the following landmarks: peak of the P wave (P peak), peak of the R wave (R peak), onset of the QRS complex (QRS onset), offset of the QRS complex (QRS offset), peak of the T wave (T peak) and offset of the T wave (T offset). Correct location of the automatically identified landmarks was confirmed by visual inspection of an expert cardiologist.

The landmarks were used to evaluate the ECG features typically used in clinics to assess cardiovascular risk in addition to HR: QRS duration (ms), QT interval (ms), QTc computed using Bazett's formula [134] and ST level (mm). For ECG features computation the following formula were used:

$$QRS\ duration = QRSoffset - QRSONSET \quad (5)$$

$$QT\ interval = Toffset - QRSONSET \quad (6)$$

$$QTc = \frac{QT\ interval}{\sqrt{RR}} \quad (7)$$

$$ST\ elevation = \frac{[MedianBeat(QRSoffset) - MedianBeat(QRSONSET)]}{0.1} \quad (8)$$

where the factor 0.1 in ST elevation computation, formula 4, is used to pass from mV to mm.

### 3.2.3 Statistics

Population was stratified in classes considering their age, gender and sport discipline. Normality of ECG parameters of the entire population and of the considered classes were evaluated through the Lilliefors' test; non-normal distributions were reported in terms of median values, first and third percentiles. Wilcoxon ranksum test was performed to assess statistical differences in ECG parameters between the classes. Statistical significance level was set at 0.05.

### 3.3 Results

Table 7 contains the population study information. After the inclusion process, the final amount of selected pre-exercise ECG portions were 51. On average, the athletes were  $29 \pm 11$  years old and exercising  $3.6 \pm 1$  times a week. Among 51 athletes, 38 males and 13 females were found to be eligible for the study.

The selected signal portions belong to subjects practicing the following sport disciplines: Basket, Cycling, Fitness, Jogging, Middle distance running, Tennis and Crossfit. Specifically, 8 athletes were practicing sports in class CI (Jogging and Tennis), 15 in class CII (Basket and Middle-distance running) and 28 in class CIII (Fitness, Cycling and Crossfit). Table 8 contains the classifier and classes of athletic population and their numerosity. Table 9 contains the percentage of identified landmarks on the median beat. An example of median beat with identified landmarks and ECG signal from BioHarness 3.0 by Zephyr is reported in Figure 17. Table 10 contains the median, first and third percentiles of the total population and subclasses.

*Table 7 Population information. Amount of missing data is reported in brackets. Overall value are computed excluding the missing data. Note that for Jogging, even if only two subjects released weight and height the mean  $\pm$ SD of weight and height was computed anyway. Gender was expressed as ratio male/female. Age, weight, height and weekly training rate are expressed as mean  $\pm$  SD.*

<b>Sport</b>	<b>N</b>	<b>Gender M/F</b>	<b>Age (years)</b>	<b>Weight (kg)</b>	<b>Height (cm)</b>	<b>Sport Class</b>	<b>Weekly training rate</b>
Basket	6	7/0 (0)	$22 \pm 4$ (0)	$73 \pm 9$ (0)	$181 \pm 5$ (0)	II	$3.8 \pm 0.4$ (0)
Cycling	9	7/2 (0)	$35 \pm 17$ (0)	$64 \pm 8$ (0)	$172 \pm 6$ (0)	III	$3.3-1.4$ (0)
Fitness	8	6/2 (0)	$25 \pm 5$ (0)	$71 \pm 14$ (0)	$173 \pm 7$ (0)	III	$3.5 \pm 0.5$ (0)
Jogging	4	2/2 (0)	$24 \pm 1$ (0)	$63 \pm 14$ (2)	$172 \pm 8$ (2)	I	- (4)
Middle distance running	9	9/0 (0)	$35 \pm 15$ (0)	$70 \pm 8$ (0)	$177 \pm 3$ (0)	II	$3.9 \pm 1$ (0)
Tennis	4	0/4 (0)	$24 \pm 3$ (0)	$58 \pm 4$ (0)	$168 \pm 7$ (0)	I	$2.5 \pm 0.5$ (0)
Crossfit	11	8/3 (0)	$31 \pm 7$ (0)	$70 \pm 12$ (0)	$176 \pm 7$ (0)	III	$4 \pm 1$ (0)
Overall	51	38/13 (0)	$29 \pm 11$ (0)	$68 \pm 10$ (2)	$175 \pm 6$ (2)	-	$3.6 \pm 1$ (4)

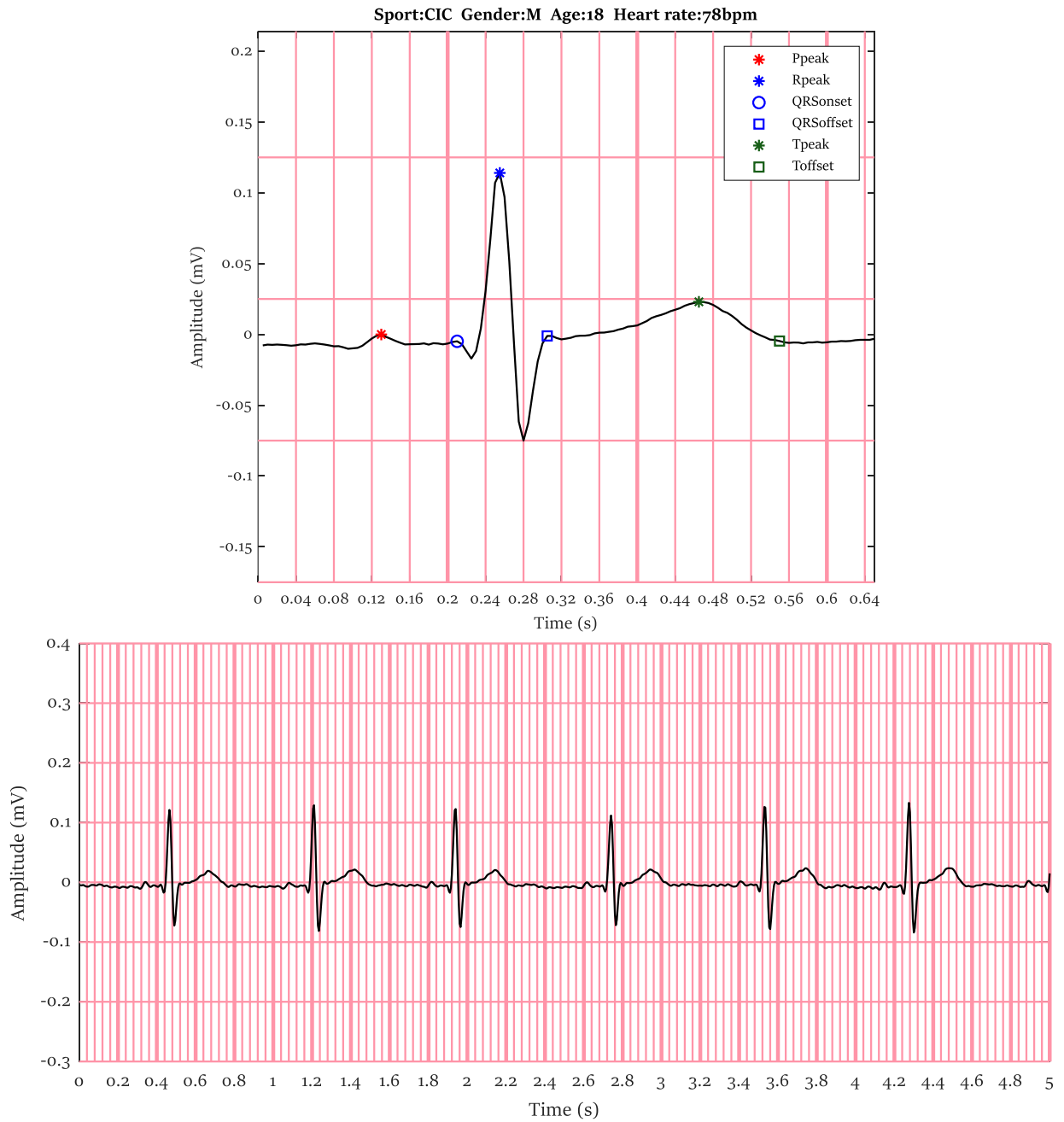


Figure 17 The signal in the image belong to a male cyclist 18 years old, with an HR of 78 bpm. The upper panel shows the median beat with identified landmarks: P peak, R peak, T peak, QRS onset, QRS offset and T offset. The lower panel shows the first 5 s of the 10 s ECG portion from which the median beat was computed.

Table 8 Classes for athletic population stratification and their numerosity.

Classifier	Classes	Number
Gender	Male	38
	Female	13
Age	≤35 year	39
	>35 year	12
Sport	CI	8
	CII	15
	CIII	28

Table 9 Percentage of landmarks identification.

Landmark	Percentage of identification
P peak	68%
QRS onset	100%
R peak	100%
QRS offset	100%
T peak	100%
T offset	100%

Table 10 shows the median, first and third percentiles of the total population and subclasses and the comparison among subclasses.

Stratification	Group	N	HR (bpm)	QRS- duration (ms)	ST- level (mm)	QT- interval (ms)	QTc- interval (ms)
None	All	51	83 [72; 93]	95 [85; 100]	0.00 [-0.09; 0.07]	345 [330; 365]	400 [380; 419]
Gender	Male	38	83 [72; 93]	<b>95 [90; 105]</b>	-0.01 [-0.09; 0.08]	340 [325; 360]	397 [380; 414]
	Female	13	86 [73; 94]	<b>85 [85; 90]</b>	0.01 [-0.07; 0.05]	350 [334; 366]	405 [398; 426]
Male vs Female			0.97	<b>0.005</b>	0.97	0.28	0.19
Age	≤35 years	39	83 [73; 91]	95 [85; 104]	0 [-0.08; 0.08]	345 [326; 364]	399 [377; 422]
	>35	12	79 [71; 94]	93 [85; 100]	-0.04 [-0.11; 0.07]	340 [330; 368]	412 [394; 413]
Under vs Over			0.94	0.79	0.57	0.90	0.37
Class	I	8	77 [66; 91]	90 [88; 100]	0.04 [-0.04; 0.11]	358 [343; 378]	400 [385; 425]
	II	15	88 [73; 102]	90 [86; 100]	-0.03 [-0.07; 0.00]	340 [323; 358]	412 [384; 424]
	III	28	82 [75; 89]	95 [85; 105]	0.01 [-0.12; 0.07]	340 [328; 363]	396 [378; 413]
I vs II			0.19	0.87	0.21	0.19	0.65
I vs III			0.62	0.86	0.51	0.15	0.58
II vs III			0.24	0.91	0.75	0.81	0.16



### 3.4 Discussion and Conclusion

The aim of this work was to provide an initial set of targeted ECG reference value for athlete's ECG recorded in pre-exercise phase by a reliable and most diffused wearable sensor, the chest strap BioHarness 3.0 by Zephyr ([www.zephyranywhere.com](http://www.zephyranywhere.com)) with the scope of increasing wearable device sports applications finalized to large-scale prevention programs.

The Sport Database acquired with chest strap BioHarness 3.0 by Zephyr ([www.zephyranywhere.com](http://www.zephyranywhere.com)) was used for this study [130]. From it, 42 portions (10 s long) of rest ECG acquired in pre-exercise from healthy subjects without previous history of cardiorespiratory diseases and not taking any drug were selected. In addition, 9 rest ECG of cyclists were added, acquired with the same wearable device and by the same Cardiovascular Bioengineering Lab of Università Politecnica of Marche, Italy. The signals were acquired in the environment of training and not in laboratory. The fact that the recordings were not done in a controlled laboratory environment is reflected in higher quantity of noise and interference and thus the worse quality of rest ECG portion that were excluded during the selection phase. Further, sometimes the athletes do not strictly respected the acquisition protocol. These considerations highlighted the importance of following a protocol while acquiring ECG signal with wearable sensors in not controlled environment. Especially an initial phase of resting acquisition is important to enable comparison of resting and stress ECG features, and education of patient is fundamental to correctly place chest strap sensors and avoid noise sources.

The selected 51 ECG portion were processed and a median beat representative of the rest portion computed. Landmarks indicating wave peaks, onset and offset were automatically computed on median beat [133], then corrected by clinician visual inspection. The numerosity of identified landmarks is reported in Table 9, landmarks present a percentage of identification of 100% except for P peak 68%. P wave acquired by chest strap BioHarness 3.0 by Zephyr ([www.zephyranywhere.com](http://www.zephyranywhere.com)) is seldom visible and often covered by the baseline wandering and motion sensors artefact. Given the low reliability in P-wave acquisition and identification, PR interval computation was excluded from the analysis.

The results for the unclassified athletic cohort and for subclasses are reported in Table 10.

Pre-exercise ECG values (both interval and wave durations and ST segment level) over the entire selected population of healthy athletes fall into the normal ranges for ECG features computed from

12-lead ECG [8]. Regarding HR, only one subject showed an HR lower 60 bpm indicating the characteristic adaptive bradycardia in athletes. Some subjects had an HR slightly greater than 100 bpm but never  $> 110$  bpm. This can be justified by the fact that signals were acquired directly on the training court in the 5 minutes immediately before the training, thus sometimes the ideal resting condition of medical clinic were not reached.

Regarding age, the population is  $\geq 18$  years old and adult population should be divided in  $\leq 35$  years old and  $>35$  years old since the causes of SrSCD change between young and middle-age and older athletes, with a greater prevalence of cardiomyopathy and congenital coronary artery anomalies in the first group and coronary atherosclerosis in the second one. The different pathological incidence reflects also in the different pre-participation screening [25][26][27]. Of note, these age limits are not sharp threshold and may be not strictly respected when selecting population for studies, although cardiac changes and different incidence of pathology with aging should be always central. Under and over 35 years old athletic subjects do not show significant differences. The main different value is the HR, which is lower in median in older athletes. Being the older population composed by veterans athletes it could be explained by the greater bradycardia adaptation, which is a landmark of long training. The lower resting HR reflects in the longer QTc interval of  $>35$  years old athletes. Thus, QTc duration difference seems to be dependent on HR rather than repolarization differences.

Gender differences reflects in lower cardiac remodeling and electrical adaptations in female with respect to male, as well as lower incidence of SrSCD. It may be explained by hormonal differences and the lower amount of physical exertion reached by female. In gender stratification, QRS duration is significantly different with female QRS shorter than male one. It can be explained by the greater cardiac remodeling in male athletes and the prolonged conduction time resulting from increased RV size secondary to regular training [64][69]. The differences in QT and QTc duration reflects the results found in literature [127]. QT and QTc median value are greater for female than male athletes (QT 340 vs 350 ms; QTc 397 vs 405 ms) with a similar median HR. This fact indicates that the differences mainly derived from repolarization time differences. The result confirm the need for a greater normality threshold for female (480 ms female vs 470 ms male [73]) in defining LQTS also in wearable sensor ECG interpretation.

Finally, subjects were divided based on sport disciplines according to Mitchell criteria. All sports present in the database belong to the classes with higher dynamic component expressed as maximal oxygen uptake ( $\text{MaxO}_2 >70\%$ ) and identified with letter C, and increasing static component

expressed as maximal voluntary contraction (MVC). Jogging and Tennis belong to the class with low static component (<20% MVC), Basket and Middle distance running belong to the class with medium static component (20% - 50% MVC), Fitness, Crossfit and Cycling belong to the class with high static component (>50% MVC). The division did not report statistically significant differences among sport groups. This indicates that dynamic components of sport seem to be more responsible for sport-related physiological adaptation and the increasing static component has a less relevant influence. It could be interest to study sport with high static components and increasing dynamic one or the sport division by amount of training (duration of training times time weekly training rate). The latter option was not assessed because of lacking date about weekly training rates, which were not released by all subjects.

The main limit of the work is the small study population given by the lack of public database acquired by chest strap BioHarness 3.0 by Zephyr ([www.zephyranywhere.com](http://www.zephyranywhere.com)) and respecting the same protocol of acquisition. Next steps could be to enlarge the study population by acquiring signals from athletes belonging to other sport disciplines and to study the influence of quantity of training.

The study proposed an initial set of normal reference value for the interpretation of athlete's ECG acquired by chest strap BioHarness 3.0 by Zephyr ([www.zephyranywhere.com](http://www.zephyranywhere.com)) in healthy adult athletes. The range of computed duration and ST segment level coincide with normal reference ranges acquired by 12-lead ECG, except for few limit values of heart rate. Resting bradycardia is characteristic feature of highly trained athletes while rest HR slightly greater than 100 bpm may be justified by less relaxed condition of acquisition during pre-training with respected to the monitored environment of medical clinic. Thus, acquisition condition in pre-exercise phase should be always taken into account when performing continuous monitoring in training court. Population specific ECG reference value should be adopted to enable a targeted and personalized screening, most precisely gender division plays a central role and female /male normal reference ranges should be defined. This can promote the development of algorithm of cardiac risk identification from wearable sensors ECG, and increase the sport applications of wearable device for large-scale prevention programs of all level athletes from competitive to amateur and continuous monitoring.

### **III Section: Preliminary biofluid dynamic numerical models of coronary artery in athletes**

#### **4.1 Background**

ECG increases the ability to detect underlying cardiovascular conditions associated with SrSCD. However, this diagnostic tool has low sensitivity and specificity specifically in detecting anomalous coronary arteries, premature coronary atherosclerosis, and aortopathies. Although, CAA and CAD are the major causes of SrSCD along with cardiomyopathies. Thus, an ECG will not detect all conditions predisposing to SrSCD and imaging is essential for the detection of underlying pathologies of coronary vessels in pre-participation screening [73]. Imaging analysis enable the study of mechanic and biofluid dynamic contribution to SrSCD. The gold standard in the assessment of morphology of coronary vessels and diagnosis of CAD is invasive coronary angiography (ICA). The invasive procedure is highly accurate but it has high risks due to the catheter and the radiation dose. In suspected mild and moderate coronary diseases, a non-invasive analysis should be preferred such as computed tomography coronary angiography (CTCA) which is correlated to lower risk for the patient. CMR is also a useful and non-invasive tool to define morphology of coronary origin and course. The computation of diagnostic parameters usually computed invasively, e.g. fractional flow reserve (FFR), can be performed from non-invasive morphologic measurement and computational fluid dynamic tools (CFD). The combination of non-invasive imaging and CFD modelling shows high accuracy, sensitivity and specificity. Biofluid dynamic models enable a non-invasive and low risk evaluation of athletes with suspected CAD and CAA as well as the qualitative modelling of the athlete's heart facilitating the study of cardiovascular system in athletic population. Further CFD simulation can be a potential tool to simulate blood flow under physical exercise condition in a specific coronary geometry given the difficulty of performing accurate and low noise stress imaging while doing physical exercise.

When creating a qualitative model, a reliable geometry is essential to model the physiological adaptation of athletes and wave dynamics in a realistic way. Thus, the aim of this work is to collect geometric data of coronary arteries, then to apply a numerical model (and evaluate the goodness) of the main conduit epicardial coronary arteries representative of the healthy athletic population

cardiac vascular system. Thus to exploit such a tool for the biofluid dynamic study of coronary artery training-related remodeling and the possible causes of impaired blood flow leading SrSCD.

To formulate efficient models of large epicardial coronary arteries, including mechanical characteristics and deformation process a knowledge of structure and properties of coronary arteries is required. The main aspects of anatomy and physiology were provided in the introductory section ‘Anatomy and physiology of the cardiovascular system’. Before the experimental chapters on CFD simulation, the geometric data collection is described. In addition two introductory chapters regarding CFD and blood flux in coronary artery are presented to complete the background behind coronary arteries modelling.

#### **4.1.1 Normal geometry of coronary arteries**

Lumen and external diameter, vessel length and level of tortuosity are necessary for a quantitative description of the normal geometry of coronary arteries [135]. In any normal condition, coronary ostia are typically equal to or greater than the proximal segment of the related coronary artery. Then coronary arteries gradually decrease in size along with the increase of ramifications. Although LAD and LCX generally taper in diameter as each extends from the left main bifurcation, RCA maintains a fairly constant diameter until just before the origin of its posterior descending branch [136].

Many articles have measured the coronary artery sizes of various populations [135][137][138][139][140]. Researchers mainly focused on South Asians (Indians, Nepalese) given the prevalence of coronary disease in this population with corresponding higher mortality and morbidity [30]. Other data were recorded among Caucasians of European origin, North Americans, Koreans and Iranians; while there is a lack of data on coronary artery size of South Americans, Chinese, African and other racial pool of human population [30]. The data of one population are not applicable to another population, indeed some parameters such as diameter are highly variable within different groups, e.g. South Asians seems to have smaller coronary diameter than Caucasians [141]. Several other articles have compared the coronary diameter of one population to the others, concluding that coronary artery diameter varies with population [137][139][30].

Irrespective of the racial and regional origin of the patient, the normal geometry of coronary arteries has a marked individual variability [30].

The lumen diameter of most arterial subsegments is influenced by age, sex, anatomic variation, branch length and myocardial mass and mean diameter can be specified to within  $\pm 0.6$  mm (SD) when accounting for these factors [135].

Regarding age, analysis showed that coronary vessel cross-sectional area and total coronary cross-sectional area, thus diameter, decrease linearly with age [135][63]. Different explanation have been given to decline in coronary dimensions with age: 1) Decline in physical activity diminishes coronary dimensions, since there is no more periodic stimulation by exercise provokes increases in coronary blood flow that, in turn, enhances basal coronary size and/or compliance [63]; 2) intimal thickening and stiffening because of atherosclerotic plaque [135].

Moreover analysis showed that coronary vessel cross-sectional area and total coronary cross-sectional area, thus diameter, have a direct linear relation with increase with regional myocardial mass [63]. This relation can also justify the differences between male and female. Indeed women tended to have narrower coronary arteries than men and in some studies when normalizing for BSA the difference vanished [140]. Other analysis obtained opposite result and difference persisted after adjustment for body size. BSA-normalized coronary area in women is approximately 90% that in men, a finding in agreement with the observation that BSA-normalized LV mass in women is approximately 90% of that in men [135]. Thus, the size of coronary arteries is related with the myocardial mass and normal coronary artery size is usually normalized for BSA.

Normally coronary arteries are not tortuous, sometimes the branches of LCA and RCA show tortuosity that have a major impact on the supply of blood to the heart during exercise and at rest [142]. Generally, the tortuosity is observed in LAD branch and the degree of tortuosity varies from mild to severe depending on the curves of the blood vessel [142]. Tortuosity leads to a variation of blood flow causing a reduction in blood pressure distal to the tortuous segment leading to myocardial ischemia [142]. Tortuosity of coronary artery tree has a significant positive relation with age but no significant relation with lumen diameter was found [135].

Lumen diameter of branches is strongly affected by vessel length [135]. The principal determinant of branch diameter was the extent of its epicardial distribution, as characterized by its length relative to the distance from its origin to the LV apex [135]. Concerning specifically vessel length, it varies based on the dominance; left dominance implies longer LCA branches and right

dominance the reverse. The following lengths regard right dominance case, found in 80 – 90 % of subjects: LM length ranges from 1-25 mm before bifurcating; LAD measures from 10-13 cm in length, whereas non-dominant LCX measures about 6-8 cm; RCA (supplying posterior descending and/or atrioventricular nodal artery) is about 12-14 cm in length before giving rise to the posterior descending artery [136].

It is clear that the most measured morphometric data is lumen diameter. Table 11 contains the coronary diameters of Caucasians and Indians. The data are taken from two of the studies cited above in which researchers measured coronary diameters in the higher number of point along the coronary tree [135][137]. The articles regard only in vivo quantitative measurement through imaging techniques such as coronary angiography. The cited measurements are taken from database of general population who underwent coronary angiography and then result normal to the examination. Instead, studies done on dissected and postmortem specimens were excluded since weight of the heart and diameter of the vessel lumen being determined from them, seems to be affected by an error due to factors such as fixation, preservation, and analysis of dissected specimens [30]. In Table 11, a few measurements are reported as example (diameter of LM, proximal LAD-LCX-RCA, mid LAD-RCA and distal LAD-LCX-RCA), for the complete set of measurements refer to the cited studies, which contains more coronary size value measured in different points along the coronary tree [135][137].

*Table 11 Coronary diameters in different point of coronary tree. The abbreviation refer to the acronym of coronary arteries, and 'p'=proximal, 'm'=mid distance, 'd'=distal .*

Reference Article	Methods and Data	Population	Female	Male
Dodge Jr et al. [135]	Coronary angiography Lumen diameters at 96 specified points in the coronary anatomy (mm)	North Americans 83 patients (73 men and 10 women) who have no evidence of atherosclerotic disease and a mean age 45±13 years.	LM 4.0 ± 0.5 pLAD 3.3 ± 0.4 mLAD 3.2 ± 0.5 dLAD 3.1 ± 0.5 pLCX 2.9 ± 0.5 dLCX 2.9 ± 0.6 pRCA 3.4 ± 0.7 mRCA 3.3 ± 0.6 dRCA 3.2 ± 0.6	LM 4.5 ± 0.6 pLAD 3.7 ± 0.5 mLAD 3.6 ± 0.5 dLAD 3.5 ± 0.6 pLCX 3.4 ± 0.5 dLCX 3.3 ± 0.5 pRCA 4.0 ± 0.6 mRCA 3.9 ± 0.6 dRCA 3.8 ± 0.5
Shaikrishna et al. [137]	Coronary angiography Female and male coronary artery diameter (mm)	Indians 94 patients Sex(M/F) 63:31 Age 49.23±9.43 years (range 32-66 years) BSA 1.68±0.17m <sup>2</sup> (range 1.25-2.00m <sup>2</sup> )	LM 3.40 ± 0.58 pLAD 2.72 ± 0.48 mLAD 2.17 ± 0.5 dLAD 1.51 ± 0.31 pLCX 2.68 ± 0.59 dLCX 1.77 ± 0.60 pRCA 2.55 ± 0.57 mRCA 2.31 ± 0.13 dRCA 2.01 ± 0.40	LM 3.72 ± 0.65 pLAD 2.85 ± 0.59 mLAD 2.24 ± 0.49 dLAD 1.63 ± 0.38 pLCX 2.82 ± 0.63 dLCX 2.10 ± 0.68 pRCA 2.75 ± 0.60 mRCA 2.47 ± 0.46 dRCA 2.14 ± 0.61

#### **4.1.1.1 Normal geometry of coronary arteries in athletic population**

Changes in hemodynamic forces, including shear stress and Transmural pressure, can lead to remodeling arteries and arterioles. Shear stress is a central signal for vascular remodeling at all levels of the arteriolar tree.

Shear stress is the frictional force on the endothelium applied by the blood as it flows through the vessel and it is elevated when blood flow increases without a compensating change in vessel diameter. Thus, it is an important hemodynamic variable for the increase in luminal diameter of arteries, in particular in smaller resistance vessels where it induces formation of vasodilators leading to increased arteriolar diameter neutralizing the shear stress. Shear stress effect is mediated by an increased formation of NO, which in turn interact with vascular endothelial growth factor (VEGF), important in arteriogenesis. A vast number of compounds are affected by shear stress and several of these may influence arterial growth. Arterial wall thickness is more dependent on transmural pressure, which is the difference between the pressure inside and outside of the vessel, is elevated with increased blood pressure. High load resistance exercise leads to pronounced blood pressure changes, in particular resistance exercise with large muscle groups during which systolic blood pressure can exceed 300 mmHg. Severe resistance training may also lead to permanent elevations in resting blood pressure which could contribute to increased vascular wall thickness. It has been proposed that a more chronic increase in blood pressure may have a greater impact on arterial wall thickness compared to the transient increases that occur during exercise. Although systolic arterial blood pressure is increased during endurance exercise, the increase is limited and the effect on diastolic and mean arterial blood pressure is small. In endurance trained individuals, the arteries undergo structural adaptations leading to an increased diameter and reduced wall thickness and the volume of the arteriolar net is increased. The functional consequence of an increase in arterial diameter is reduced resistance during high levels of perfusion, whereas changes in wall thickness and wall composition (vascular smooth muscle, endothelium and extracellular matrix constituents) have implications for vascular compliance. Endurance training increases arterial compliance whereas strength training can reduce arterial compliance [23] [60].

Concerning coronary circulation, some studies have shown that the resting diameter of endurance trained individuals is similar to that of sedentary individuals. However, other studies proved the adaptive growth of the coronary circulation in response to exercise in the healthy heart of top level athletes subjected to chronic exercise [60]. Coronary artery diameter is related to the level of



fitness measured by metabolic equivalent test (MET). It was shown that each MET increase in fitness was associated with a mean  $0.03 \pm 0.01$  mm larger diameter of the left main, a  $0.04 \pm 0.01$  mm larger diameter of the left anterior descending, a  $0.05 \pm 0.01$  mm larger diameter of the left circumflex, and a  $0.07 \pm 0.01$  mm larger diameter of the right coronary artery ( $p = 0.002$ ). This correlation between fitness and coronary artery diameters was most prominent for high fitness levels above 10 METs [143]. Exercise training induces increases in coronary transport capacity through adaptations in the coronary microcirculation including increased arteriolar diameters and/or densities and changes in the vasomotor reactivity of coronary resistance arteries. Periodic stimulation by exercise provokes increases in coronary blood flow that, in turn, enhances basal coronary size and/or compliance in main coronary arteries [63]. At the capillary level, angiogenesis is present, it is the growth of new capillary vessels from existing capillaries, a process involving only endothelial cells and restricted to the level of the terminal microcirculation [60]. As these exchange vessels increase in number, some may be enlarged and transformed at their proximal ends into supplying arterioles or small arteries by a process described as 'arteriolarization' [60]. The increase of capillary density is a consequent of the heart remodeling and increased myocardium mass with training. Indeed, energy production in the normal healthy heart depends principally on oxidative phosphorylation, as glycolytic metabolism is capable of generating no more than 5% of the adenosine triphosphate (ATP) that is required for normal contractile performance. As result of this strong dependence on oxidative metabolism, increases in cardiac myocardium and activity require an almost instantaneous parallel augmentation of  $O_2$  supply also at rest. In contrast to skeletal muscle tissue, which has very low metabolic requirements during quiescent resting conditions, the heart continuously pumps blood in resting human subjects. Consequently, under resting conditions the  $O_2$  consumption normalized per gram of myocardium is 20-fold higher than  $O_2$  consumption of resting skeletal muscle tissue. This high  $O_2$  extraction is facilitated by a high capillary density of 3000-4000 per  $mm^2$ . Because of the high resting levels of myocardial  $O_2$  extraction, increases in  $O_2$  demand produced by exercise are principally mediated by an increase in coronary flow [14]. Capillaries and resistance vessel adaptation seems to precede conduit vessels structural remodeling. Indeed, the coronary flow reserve (indicative of resistance vessel adaptation) increases in response to short-term training, in the absence of changes in epicardial dilator responses to nitroglycerine or adenosine, suggesting that adaptation of resistance arteries may precede that associated with conduit vessels [62]. This indicates the importance of study time course, with studies involving longer interventions being more likely to demonstrate structural remodeling [62]. An example is the invasive follow up study performed by Windecker

et al. [144]. They analyzed the effect of endurance training program 5 month long on coronary artery size and function in healthy volunteers (gender: male; age:  $36 \pm 5$  years). Quantitative coronary angiography with intracoronary Doppler measurements were performed before and after completion of a physical endurance exercise program of 5 months duration. The right, left main, and left anterior descending coronary artery cross-sectional area increased significantly in response to exercise. The results are reported in Table 12. It is evident that regular physical endurance exercise in young men without cardiovascular disease or risk factors results in an adaptive increase of epicardial coronary artery calibers [144]. It is difficult to collect a vast number of accurate epicardial coronary sizes of healthy athletic population, since they do not need to undergo invasive and dangerous imaging such as quantitative coronary angiography in healthy condition.

*Table 12 Coronary diameters in different point of coronary tree of Caucasians men before and after exercise program, measured with coronary angiography. The abbreviation refer to the acronym of coronary arteries, and 'p'=proximal, 'm'=mid distance, 'd'=distal.*

Diameter (mm)	Before exercise program	After exercise program
LM+RCA	$5.7 \pm 2.6$	$6.4 \pm 3.1$
LM	$4.5 \pm 2.1$	$4.6 \pm 2.1$
pRCA	$3.58 \pm 2.0$	$4.38 \pm 2.4$
mRCA	$3.2 \pm 1.9$	$3.4 \pm 1.9$
dRCA	$2.6 \pm 1.5$	$2.7 \pm 1.7$
pLAD	$3.4 \pm 1.9$	$3.6 \pm 2.0$
mLAD	$2.5 \pm 1.4$	$2.6 \pm 1.4$
pLCX	$2.5 \pm 1.8$	$2.6 \pm 1.8$

#### **4.1.1.2 Aorta and physiological remodeling with exercise**

Coronary arteries arise from the aortic root, more precisely from the sinuses of Valsalva. Given the importance of artery characteristic for wall waves dynamic and coronary blood flow, it is necessary to understand aorta behavior with exercise training. A pair of studies show that sport related adaptation are not present. The association of exercise and aortic root dilation is inconsistent. Dilated aortic root is uncommon among competitive athletes:  $\geq 40$  mm in 1.3% of males and  $\geq 34$  mm in 0.9% of females (99th percentiles). Dilatation of the aortic root is unlikely to represent a physiological adaptation, and is most likely an expression of pathology. The observation of a 2.5- fold increase in the aortic root over eight years of follow-up in male athletes with enlarged aortic root at initial assessment supports this fact. Other small studies report greater

diameters in strength-trained compared to endurance-trained athletes, but also with a low prevalence of dilated aortic root [37][59].

#### **4.1.2 Pulsatile coronary blood flow and Wave Dynamics**

As elsewhere in the arterial circulation, it is pressure gradient between the aorta (aortic pressure = entrance pressure) and the peripheral capillaries that provides the driving force for coronary blood flow [145]. However, the effective coronary back pressure that impedes coronary flow is generated by extravascular compressive forces of surrounding ventricular myocardium and it cannot be equated to right atrial blood pressure. Thus, ventricular contraction results in high intramyocardial pressures that compress the intramural coronary blood vessels, thereby opposing coronary arterial inflow further pumping back the blood from intramural vessels [14]. Unlike most other systemic vascular beds, blood flow in coronary arteries peaks in diastolic phase rather than systolic phase, so when blood pressure in the aorta is substantially lower than the peak systolic pressure [145]. The blood flow in the coronary arteries is very pulsatile with zero or even reversing flow in systole [146]. The two major determinants of coronary flow are the pulsatile aortic pressure and the myocardial contraction/relaxation and its interaction with vascular system in systole [146]. During systolic phase the epicardial vessel perfuse more, while the endocardial (deeper) vessel perfuse later because during systole are blocked by the contracted cardiac muscle [14]. Moreover, the coronary flux in LV has a diastolic dependent perfusion and significantly decreased during systole given the high pressure, while the flux in RV is present during the entire cardiac cycle because it operates at lower pressure range [147].

The relative importance of aortic and microcirculatory contributions to phasic coronary blood flow was explained in terms of a series of wavefronts that underlie the changes in pressure and flow in arteries [145]. The systolic phase extremely affect the wave propagation given the influence of contraction of myocardial muscle on wave dynamics [16]. Indeed systolic-diastolic variations in coronary blood flow is attributed to an active myocardial pump [145].

Justin E Davies et al. [145] believe that pressure and velocity waves are responsible for directing the flow of blood in the coronary artery circulation. These waves can originate from both the upstream aortic (proximal origin) and downstream microcirculatory (distal origin) ends of the artery and can either accelerate or decelerate the flow of blood. To identify the origin and nature

of these waves, it is necessary to have simultaneous recordings of pressure and velocity. Increases in pressure can result in either acceleration or deceleration of blood, depending on the origin of the pressure wave. An increase in pressure originating from the aortic end (proximal origin) of the vessel will accelerate blood velocity. In contrast, if the increase in pressure originates from the downstream microcirculatory end (distal origin), blood velocity will decelerate. In both cases, the rise in pressure is considered by wave intensity theory to be as result of a compression wave, which has a “pushing” effect. The opposite pattern is found with decreasing pressure. A decrease in pressure originating from the proximal end will decelerate blood flow, and a decrease originating from the distal end will accelerate flow. Any decrease in pressure is considered by wave intensity theory to be a result of expansion waves, which have a “suction” effect. Justin E Davies et al. [145] identified 6 predominating waves in the cardiac cycle. These waves occur in the same sequence during each cardiac cycle. The sequence was the same in each subject, although the intensity and timing of the individual waves differed between subjects. The wave profile was very similar in each of the left coronary arteries. Three characteristic waves were identified during ventricular contraction, and 3 were associated with ventricular relaxation. Although cumulative wave intensity values varied between subjects, the proportions of individual waves were comparable between subjects. Waves were characterized by their origin and direction of travel (forward-traveling waves originating proximally and backward-traveling waves originating distally), character (pushing or suction), and effect on coronary blood flow velocity (acceleration or deceleration wave). This theory of wave dynamics is shown in Figure 18 from the study of Justin E Davies et al. [145]; that figure concentrate on left circumflex coronary artery but the same analysis can be performed on the other segment of the left coronary and also on the right coronary. Figure 19, taken from the same study represent the sequence of energy waves in the human coronary artery during the cardiac cycle [145]. From figure 19 it is also remarkable that diastolic perfusion of coronary artery (when aortic valve is closed and ventricle is relaxed) is restricted to phase 6 thus to the late forward travelling pushing wave, hence the modelling of coronary flow during systolic phase is extremely important.

In left ventricle, peak coronary blood flow occurs in diastole because of the dominance of a “suction” wave, the dominant backward-traveling suction wave, generated by myocardial microcirculatory decompression. Coronary in right ventricle presents a different blood flow given the different contraction dynamic, delayed with respect to the left ventricle (Figure 20). Given the previous result about wave dynamics in left branch we can infer that blood flow in RCA may be firstly accelerated by a contraction wave at the aortic end, then attenuated by the contraction of the

myocardium and myocardial compression wave, and a second peak in coronary blood flow occurs in diastole because of the dominance of a “suction” wave (Figure 20, right graph).

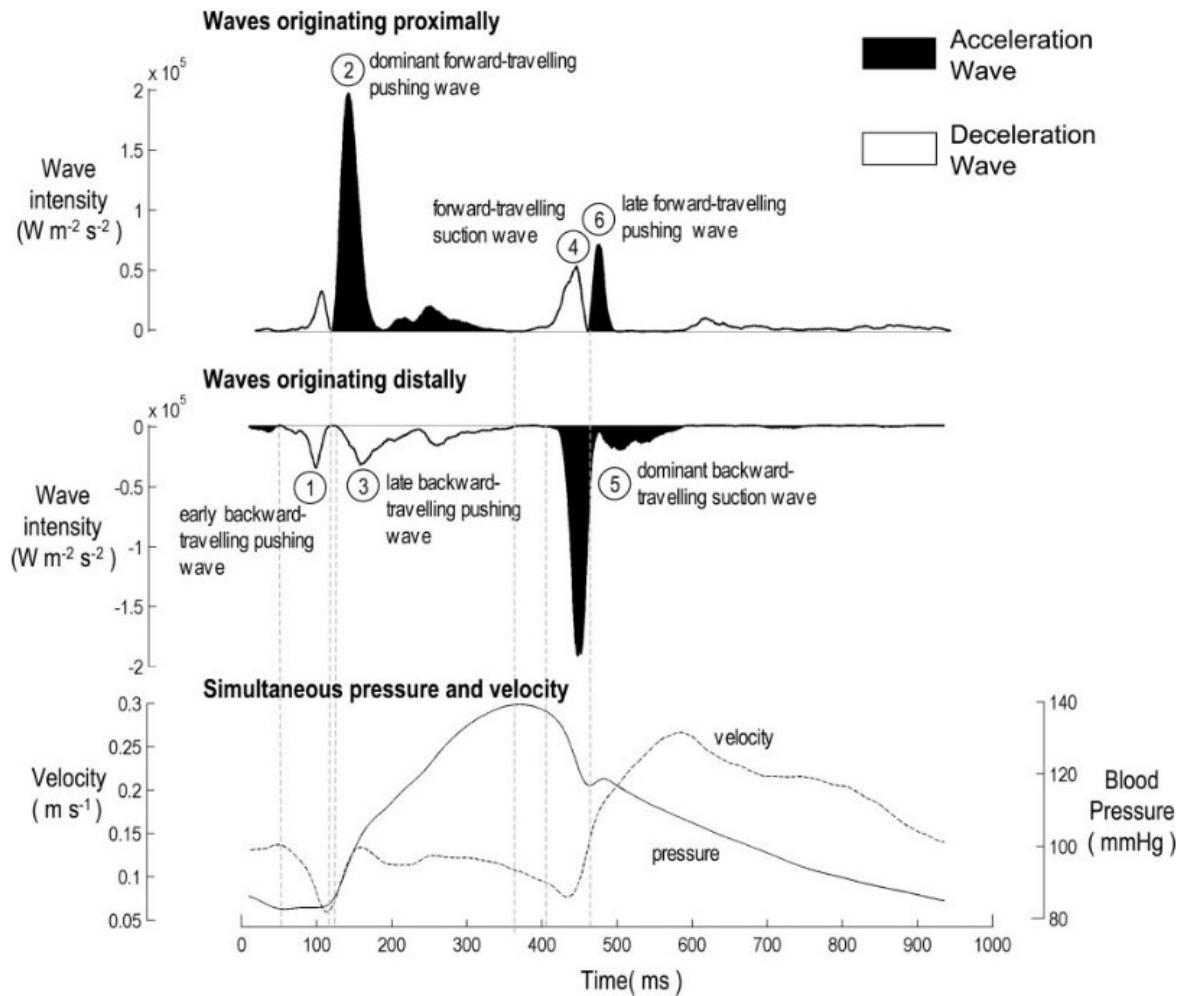


Figure 18 Wave dynamic and their influence on coronary flux characteristics (pressure and velocity) in the human circumflex artery. The upper portion of the figure represent waves originating proximally ( $WI \leq$ , upper panel), wave originating distally ( $WI \geq$ , middle panel). Coronary artery flow velocity and pressure are shown in the lower panel. Dashed line shows the onset of each wave. Figure taken from Justin E Davies et al. [145].

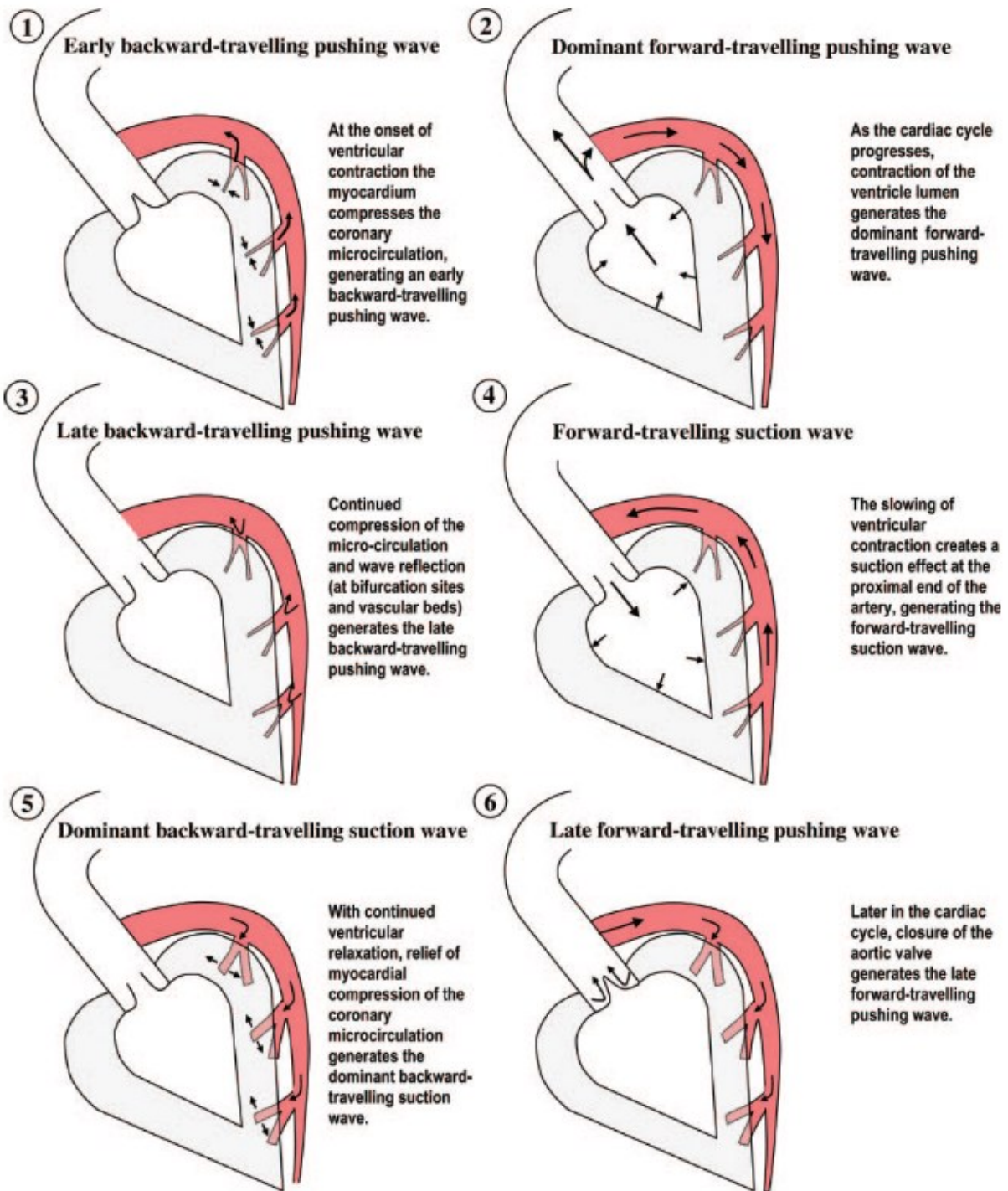


Figure 19 Sequence of energy waves in the human coronary artery during the cardiac cycle. Arrows represent direction of wave motion rather than direction of blood flow. Figure taken from Justin E Davies et al. [145].

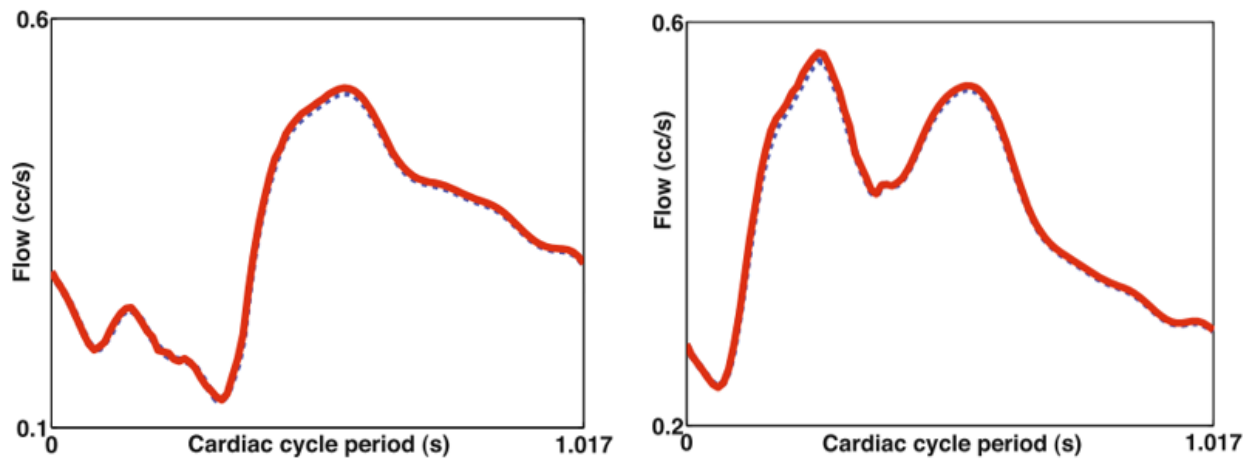


Figure 20 The red line curves are a representative shape of coronary blood flux in LAD (left side panel) and RCA (right side panel) during cardiac cycle. Figure taken from Dibyendu Sengupta et al. [148].

Pahlevan et al. [124] described, through a mono-dimensional model, the coronary wave dynamics which determine the coronary blood flow (myocardial perfusion) as a combination of aortic waves (affecting the workload of the heart) and waves generated at the myocardial end of coronary vasculature [124]:

- At the aortic side, compression waves and suction waves are created during the cardiac cycle and are determined by the dynamic into the aorta.
- At the myocardial end, compression waves and suction waves are created by contraction and relaxation of cardiac muscle.

Regarding the first point, the dynamic into the aorta, pressure and flow waves, is determined by the pulsatile flow generated by the heart [149]. Pressure and flow waves propagate and reflect throughout arterial vasculature, thus playing a dominant role in the hemodynamics of the arterial system and the hemodynamic load on the heart, which has two parts: steady and pulsatile [149]. The steady load depends on the resistance from the arterial network to the mean part of the flow [149]. The pulsatile load depends on the interaction between the heart's pumping characteristics (stroke volume, heart rate, and ejection fraction) and arterial wave dynamics [149]. Four important factors seem to control the level of the pulsatile load applied to the heart [149]:

- rigidity of the aorta and other large vessels,
- interaction between the left ventricular and the terminal of the vasculature in the upper and lower parts of the body,
- wave reflection,
- balance between the heart rate and the body length

As said all this dynamics affect the blood flow into the coronary artery, which has two components: a blood flow from the aortic side toward the coronary microcirculation, and a blood flow in the reverse direction from coronary microcirculation toward the aorta [124]. Since the favored direction of the coronary blood flow is from aorta to myocardium, aortic compression and myocardial suction waves are assisting while aortic suction and myocardial compression waves are impeding the blood flow toward the myocardium [124]. These waves can act constructively or destructively. Under normal conditions, these waves act constructively where they minimize the heart workload and maximize coronary perfusion. Under abnormal conditions, the waves act destructively which results in the elevation of the heart workload (increase in myocardial oxygen demand) and/or reduction of the coronary blood flow (decrease in myocardial oxygen delivery) [124].

Cardiovascular system is designed to work in optimized condition, so minimizing the pulsatile workload of the heart by optimizing the four factor affecting it [124]. For example using a computational model of the aorta, it was shown that there is an optimum heart rate at each level of aortic rigidity that minimizes the pulsatile workload of the heart [124][149]. Although an optimal condition at rest dictates a suboptimal state during extreme conditions, e.g. exercise. In fact physical exercises increase heart rate, ejection fraction, heart contractility, stroke volume, blood pressure, and aortic rigidity (as a consequence of pressure elevation and diameter extension) affecting significantly the coronary blood flow and increasing the pulsatile workload by resonance behavior of waves [124]. Under healthy (optimized) conditions, the heart beats at its shifted optimum HR during exercise, minimizing pulsatile workload [124].

Remembering that coronary blood flow is the result of the complex interactions of four different waves, interaction that become crucial for myocardial perfusion when, during the exercise, the cardiovascular system operates close to its limit [145][124]. Any cardiovascular abnormality can enhance the opposing coronary waves or weaken the assisting coronary waves resulting in coronary blood flow reduction (pathological coronary waves) [124].As an example some pathological condition and the relation with wave dynamics are reported. In hypertrophic heart diseases, the coronary blood flow is impaired due to abnormalities of both waves generated at the myocardial end of the coronary arteries. In hypertrophic condition, because of abnormality of the left ventricular flow wave, there is a possible formation of pathological aortic waves, which can enhance LV workload [124]. Instead, the aortic compression waves get impaired in coronary arterial origin anomaly diseases leading to a reduction of coronary blood flow [124]. Similarly,



abnormal coronary wave interaction caused by atherosclerotic coronary artery diseases decreases coronary blood flow promoting acute ischemia during exercise [124]. As last example, aortic stenosis leads to a combination of the elevated reduced coronary blood flow and myocardial workload because of pathological aortic waves [124].

Increased workload and reduced coronary blood flow are not the only mechanisms through which pathological waves can trigger SCD. Indeed, pathological waves can cause aneurysm rupture or aortic rupture by creating resonance in radial wall dilation waves that propagate on the vessel wall [124]. Therefore, anomalies in wave dynamics in aorta and coronary arteries can be a potential cause of sport related sudden cardiac death (SrSCD) [124]. Thus, pathological waves can act as a trigger toward cardiac death when a structural abnormality is present or geometrical anomalies of coronary arteries can induce an abnormal propagation of pulsatile flux in the coronary themselves [124]. Moreover, pathological waves can be a potential reasons for SrSCD when there are no apparent cardiovascular structural abnormalities [124].

#### **4.1.2.1 Pulsatile coronary blood flow and wave dynamics during exercise**

During heavy exercise, coronary blood flow is different from the resting condition. The increase in ventricular contraction and HR increase leads to a higher coronary back pressure during systole. The increase in back pressure is overcome by the increase in mean arterial pressure but mostly the large reduction in coronary resistance. Coronary vasodilation (mainly stimulated by NO during exercise) is responsible for the 4- to 6-fold increase in coronary blood flow. Maximal exercise is accompanied by reductions in coronary vascular resistance to levels as low as 20% - 30% of basal resting values in humans [14]. Coronary resistance arteries (coronary small arteries and coronary arterioles) determines the vascular resistance. Their length, cross-sectional area, density and number of parallel vessels (reduction in total resistance with parallel arrangement) further determines blood flow to various myocardial regions. In order to accomplish the increase of blood flow and diffusion capacity, coronary resistance arteries and capillaries increase in numerical densities and diameters thanks to exercise related structural adaptation of coronary resistance arteries increases arteriolar densities In healthy coronary circulation the coronary vasodilator reserve capacity outweighs the higher extravascular compressive forces [14]. However, in presence of reduced distal perfusion pressure (e.g. due to a coronary stenosis) the exercise-induced increase in extravascular compressive forces can result in impaired myocardial perfusion [14].

Regarding the relation blood flow and cardiac cycle, the high HR produced by exercise result in progressive expansion of systole onto diastolic phase, with a related increase (40% - 50% of total coronary blood flow) in left ventricular coronary inflow during systolic interval [14]. LV requires an increase in myocardial blood flow even at relatively low levels of exercise to meet the high myocardial O<sub>2</sub> extraction level. Instead, in RV, the metabolic need is met by increasing O<sub>2</sub> extraction at mild exercise and by a greater increase in blood flow during heavy exercise (3- to 6-fold), most likely reflecting the larger increase in right ventricular work (O<sub>2</sub> consumption) due to pronounced elevations in pulmonary pressure during exercise [14].

To conclude coronary circulation is not functionally and structurally static. Vascular adaptation in athlete's heart enables higher performance to meet the increased metabolic demand of myocardium. To have a deep knowledge of the several exercise related adaptations mechanisms it is suggested the reading of Dirk J. et al. work [14], from which the following Figure 21 was taken. The image shows all the mechanisms contributing to exercise changes in coronary blood flow, mechanisms that should be considered when modelling the flow of the athletic population.

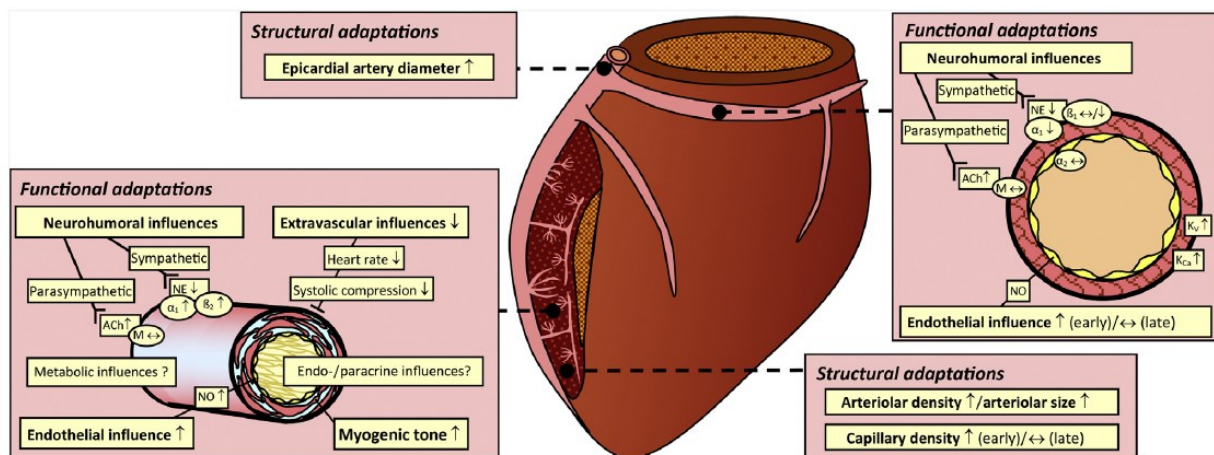


Figure 21 Graph summarizing the structural and functional coronary adaptations to chronic exercise training in normal subjects. ACh, Acetylcholine; M, muscarinic receptor; NE, norepinephrine;  $\alpha_1$ ,  $\alpha_1$ -adrenergic receptor;  $\beta_1$ ,  $\beta_1$ -adrenergic receptor;  $\beta_2$ ,  $\beta_2$ -adrenergic receptor; Kv, voltage-dependent K channel; KCa, Ca<sup>2+</sup>-dependent K channel. [14].

### **4.1.3 Computational fluid dynamics and three-dimensional model of pulsatile coronary blood flow**

Computational fluid dynamics (CFD) is a powerful engineering tool that uses computer-based simulation to simulate different fluid flows. CFD has been recently applied in biomedical field thanks to high performance hardware and software, which can cope with the modelling of the high complexity of human anatomy and physiology that govern body fluid behavior. Fluid flow can usually be described through fundamental mathematical equations, the governing equations of the process. These mathematical equations are solved through numerical simulation by means of commercial CFD programs [150]. CFD analysis can be divided into three steps: pre-processing, solving and post-processing [150]. Preprocessing starts with the modelling of geometry of the region of interest. Then the geometry is divided into a finite number of elements (cells), composing a mesh. Usually, the larger is the number of cells the better is the solution accuracy, but also the longer is the computational time. The third step is the selection of the analytic model, able to describe the phenomena, and the definition of fluid and conduit properties. Blood is usually modelled as a non-Newtonian fluid because it has varying viscosities according to its shear rate, and coronary geometry varies according to cardiac cycle phases. Algebraic form of the governing equation are solved, including the boundary conditions. In our case, inlet and outlet boundary conditions should be specified. In coronary artery modelling, boundary conditions are blood pressure and blood flow velocity and they can be measured from patients either invasively or non-invasively. These boundary conditions vary according to the cardiac cycle and the unique conditions of coronary circulation [150]. In transient problems, CFD methods solve iteratively the algebraic problem for different time intervals, named time steps. The solving step consists in the numerical solution of the problem through finite difference, finite element, finite volume, and spectral methods. Usually, the finite volume method is adopted for cardio-vascular systems [150]. The post-processing consists in analyze the computational results (changes in blood flow profiles, pressure distribution, wall shear stress (WSS), oscillating shear index (OSI), and shear rate). Results can be visualized in several ways: domain geometry and grid display, vector plots, line and shaded contour plots, two-dimensional and three-dimensional surface plots, particle tracking, and color postscript outputs, cyclic motion view during cardiac cycles [150].

#### 4.1.3.1 Numerical model of the coronary arteries

Three-dimensional model with CFD have been used to study pulsatile coronary flux. They can be powerful tools to study the relation between geometrical anomalies of coronary arteries, abnormal wave dynamics and impaired pulsatile flux in the coronaries. Pulsatility of coronary circulation can be accurately simulated on the basis of the measured branching pattern, vascular geometry, and material properties of the coronary vasculature [146]. Coronary geometry for the construction of the 3D model can be constructed from medical images data acquired by Intravascular Ultrasound (IVUS) with angiographies, Magnetic Resonance Imaging (MRI) and Computed Tomography images (CT) [151]. There are three main approaches to simulate the pulsatile blood flow and pressure waves in the vascular system [146]:

- Womersley's solution of pulsatile blood flow
- One dimensional wave propagation solution
- Three dimensional solution of pulsatile blood flow

Initially, pulsatile flux simulations were carried out assuming that the arterial wall is rigid [152]. Therefore, the interaction between the arterial wall and the blood domain is not taken into account. Recent studies combined the arterial wall domain with the blood domain, taking into account the interaction between the blood and the arterial wall. Fluid Structure Interaction (FSI) models can incorporate the deformation that blood causes to the arterial wall and vice versa.

The propagation of pulsatile flux was studied with 3D model in different works: Torii et al. [153] studied the effect of deformability of coronary wall on the hemodynamic; Buradi et al. [142] studied the effect of tortuosity of coronaries; Coogan et al. [154] reproduced the propagation of pulsatile flux in the system aorta, coronaries, thoracic and cerebral arteries; Bahrami et al. [155] reproduced the pulsatile flux in the coronary bifurcation. These 3D models are characterized by a fluid and structure interaction (FSI) with (1) deformable structure and (2) pulsatile flux.

(1) Regarding the structure deformability, the deformation of the system is probably determined by the propagation of the flux but primary by the condition of solicitation imposed by the cardiac muscle and the aortic root, which determine the characteristic of the pulsatile flux itself. Comparison analysis of FSI and flux induced deformation in rigid and deformable models of coronaries gave comparable and not significantly differences [151][153]. Of note, these studies, Torii et al. [153] and Siogkas et al. [151], modelled the coronary system without considering the

myocardium motion which instead is fundamental for wave dynamics. Thus, the above mentioned result could no longer hold when the further factors affecting wall deformability more than flux (myocardium motion and aortic root condition) are considered especially in condition with altered boundary condition of myocardium and aortic root motion as in pathology or increased solicitation of hemodynamic system as in sport or stressful situation [124]. Moreover, the two studies approximately modelled the deformable wall as a Mooney-Rivlin hyperplastic material with homogeneous and isotropic characteristics [151][153]. Although arterial wall is known to have heterogeneous and anisotropic structure owing to multiple compositions including collagen fibres and to fibre direction [13]. For sure, the deformation of the artery wall, which is severely underestimated by assuming the wall is rigid and it is best evaluated using physiologically accurate model [156].

Moreover, wall deformability is important also when studying the boundary condition in the aortic root and in the sinus of Valsalva since a rigid model of the aortic root can simulate a stiffness characteristic of pathological condition that gives an abnormal propagation of flux in coronary arteries [157][158].

Rigid wall model has the advantage that only the arterial lumen needs to be reconstructed and discretized [151]. Consequently, blood flow simulations are carried out on the lumen, resulting thus to quick, yet relatively accurate results. A rigid wall geometry is usually chosen for simplified simulations. On the contrary, FSI methods requires more time for the simulations than the simulations with rigid walls since the lumen and the arterial wall need to be reconstructed and discretized [151]. However, the simulations are more realistic and approach the human circulatory system more accurate [151]. Although a deformable geometry needs the evaluation and definition of deformable characteristics of real tissues, with risk of not accurate simulations if erroneous parameters of deformability are imposed. The choice of wall vessel model is fundamental. From the above consideration, we can infer that in first instance a rigid wall model can be chosen to construct a qualitative model of coronary arteries for pulsatile flow but in the future the wall deformability should be included to obtain more accurate and realistic results. Indeed FSI model can take into account the primary influence of myocardium and aortic root on the coronary wave dynamics.

(2) Regarding the pulsatile flux, it is imposed by inlet and outlet boundary condition of pressure and/or velocity waves. Reproducing rigid coronary model, the accurate determination of boundary condition at inflow in terms of velocity is necessary for the simulation of pulsatile flux. In this

setting, it must be noted that the pulsatile flux in coronary is different from the one in the aortic root but influenced by it [154]. In physiological terms, the more realistic boundary conditions are the ones directly measured on the patient, e.g. Torii et al. used impulses of pressure and velocity measured invasively by a pressure probe and intravascular US Doppler ECG gated [153]. Although the procedures are invasive, this is the only way to obtain accurately these informations, which are the key pieces in these type of models [153]. The invasiveness of the measurement makes the viability of velocity and especially pressure information very sparse [153]. For this reason the next section discusses the modelling of inlet and outlet conditions in order to derive boundary conditions for qualitative case models from non-invasive measurements.

#### **4.1.3.2 Boundary conditions for the pulsatile flux**

The inlet boundary condition is usually a flow rate or flow velocity. For the pulsatile flow simulation, the patient-specific flow waveform is usually used directly as an inflow condition [159]. While Duanmu et al. [160], in a 1D model, estimated the inlet flow rates to the left and right coronary branches from a lumped parameter model, considering an HR of  $t_c = 0.9s$  and a coronary blood flow equal to 4–5% of CO [161].

When not modelled from imaging data the vascular bed downstream the conduit vessel is usually mimicked with a structured-tree model [162][163]. Windkessel model applied as outflow boundary condition often represents the impedance and the capacitance of this vascular bed. There have been many Windkessel models developed, two-element, three-element, four-element modified Windkessel and others, higher the number of elements the more complex model and higher the number of parameters to be estimated [159]. In Windkessel model the vascular resistance and vessel compliance are represented analogous to electrical resistance and capacitance and pressure difference and mass flow are represented analogous to a potential difference and electrical current [159]. Vascular downstream resistance and capacitance have to be estimated when applying a Windkessel model as boundary condition to simulate the presence of vascular network downstream to conduit artery [159]. The downstream boundary condition after the RC component is essentially the venous bed approximated to have zero pressure [159]. When vasodilation has to be simulated in the resistance vessels the resistance element in Windkessel model is reduced to 30% of resistance at rest [159]. This is the case when simulating Adenosine administration and induced hyperaemia for the computation of coronary flow reserve (CFR) [159]. To be noted that

for completely mimic the Adenosine administration the HR increases by 40–50% of baseline as well as SV by ~10% , ultimately increasing the average cardiac output [159]. Resistance decrement can also simulate physical exercise induced vasodilation. The resistance of coronary vascular network is lowered accordingly to the level of exercise. Further CO, HR and coronary flow should be increase to simulate the effect of the increased metabolic demand [147]. Parameters used in these simulations, as CO, HR and SV, can be measure directly from the patient or statistical population average haemodynamic parameters for qualitative models can be adopted [147] [159]. Obviously if patient specific data are far from the population average the simulation will be less accurate thus statistical average values should be preferred in case of qualitative model rather than patient specific quantitative assessment.

The influence of intramyocardial pressure on pressure and flow waveforms in coronary arteries can be mimic in the boundary condition [159]. In Ernest W. C. Lo et al. [159], intramyocardial pressure is assumed to be purely dependent on and linearly proportional to left ventricular pressure and its waveform can be taken from the literature and then scaled for patient-specific systolic pressure. The diastolic pressure can be approximated to zero. They applied an intramyocardial pressure on the surrounding pressure across the capacitive component of the Windkessel model boundary condition in the main branches of left coronary artery. Instead Duanmu et al. [160] added a time dependent feedback pressure to the distal boundary condition (structured-tree model) in order to account for the intramyocardial pressure. The time-dependent feedback pressure was computed with the following formula:

$$p_f(x, t) = \varphi p_v(t) + p_s \quad (9)$$

where  $p_s = 20\text{mmHg}$ . The time-dependent feedback pressure  $p_f$  is proportional to the ventricular pressure plus the coronary bed pressure  $p_s$ . The ventricular-pressure feedback ratio  $\varphi$  depends on the location of the vascular bed supplied by the terminal vessel because the left and right ventricle peak-systolic pressures are different:  $\varphi=33\%$  for LV,  $\varphi=25\%$  for RV and  $\varphi=22\%$  for septum [160]. Also Kim et al. varies the intramyocardial pressure condition depending on the location of the terminal vessel. They used the left ventricular pressure to represent the intramyocardial pressure of the left coronary arteries and the right ventricular pressure to represent the intramyocardial pressure of the right coronary arteries [147].

## 4.2 Materials and methods

### 4.2.1 Reconstruction of coronary artery geometry

Geometrical data were taken from two correlated studies about the lumen diameter in normal coronary arteries and the intrathoracic spatial location of coronary segments [135][164]. Data derived from angiographic imaging on male right dominant subjects were considered. Geometric data includes radius of coronary section and polar coordinates of centre of coronary section for their intrathoracic localization. The coordinates are referred to a frame located into the ostium of the considered vessel as shown in Figure 22. Polar coordinates were transformed in Cartesian ones to facilitate the geometry implementation into AutoCAD software. Cartesian coordinates are derived from polar coordinates based on the following relation (10):

$$\vec{R} = (R\cos\phi\sin\theta \ i, R\sin\phi \ j, R\cos\phi\cos\theta \ k) \quad (10)$$

with  $R$ ,  $\phi$  and  $\theta$  polar coordinates.

Coronary arteries were divided in numbered segments and data for proximal, middle and distal sections on each segment were provided. The nomenclature to identify segments and corresponding measurements is reported in Table 13 for RCA and Table 14 for LCA.

Based on literature results on sport related adaptation of vessels, to model the vasodilated vessels of generic athletic population an increment value was added to the coronary artery diameter on each section. Left main diameter was increased of 0.03 mm, left anterior descending diameter was enlarged of 0.04 mm, the diameter of the left circumflex was increased of a 0.05 mm, and diameter of the right coronary artery was increased of a 0.07 mm [143][144]. Only the coronary diameter was modified to simulate vasodilation, the intrathoracic position of vessels and their length remain unchanged. The vessel without vasodilation are called RCA and LCA (composed of LM, LAD, LCX) the name of vessels with vasodilation are the same plus the suffix 'vd'.

The two geometry, general population and athletes, were implemented using a CAD software and then transferred in Ansys software for the CFD analysis



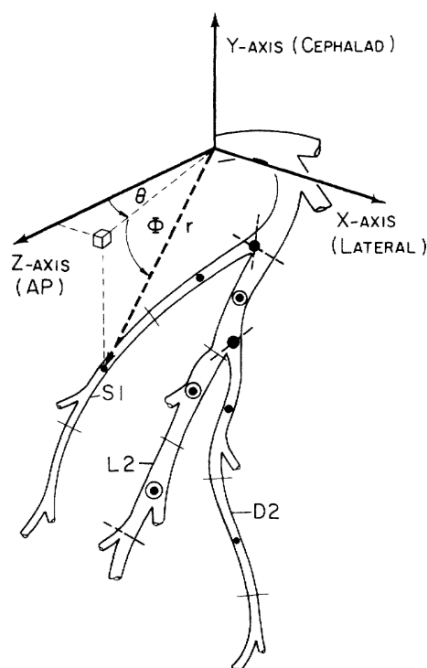


Figure 22 Drawing of trigonometric relation of angles and axes used in defining the thoracic location of artery segments. The x (lateral), y (cephalad), and z (anterior) axes are fixed in the patient with the origin at the left coronary ostium. The dots along the vessels represent where the section were measured [135][164].

Table 13 Nomenclature of right coronary artery segments. The number increase starting from ostium towards the end of the vessel. The letter 'p' means proximal, 'm' means middle, 'd' means distal. The abbreviation RCA means right coronary artery

Nomenclature	RCA segment Description
R1p	RCA first segment proximal
R1m	RCA first segment middle
R1d	RCA first segment distal
R2p	RCA second segment proximal
R2m	RCA second segment middle
R2d	RCA second segment distal
R3p	RCA third segment proximal
R3m	RCA third segment middle
R3d	RCA third segment distal

Table 14 Nomenclature of left coronary artery segments. The number increase starting from ostium towards the end of the vessel. The letter 'p' means proximal, 'm' means middle, 'd' means distal. The abbreviation LAD means left anterior descending coronary artery

Nomenclature	LCA segment Description
LMp	Left main proximal
LMm	Left main middle
LMd	Left main distal
L1p	LAD first segment proximal
L1m	LAD first segment middle
L1d	LAD first segment distal
L2p	LAD second segment proximal
L2m	LAD second segment middle
L2d	LAD second segment distal
L3p	LAD third segment proximal
L3m	LAD third segment middle
L3d	LAD third segment distal
C1p	Circumflex first segment proximal
C1m	Circumflex first segment middle
C1d	Circumflex first segment distal
C2p	Circumflex second segment proximal
C2m	Circumflex second segment middle
C2d	Circumflex second segment distal

## 4.2.2 Numerical simulation

The numerical simulation was performed in Ansys software, specifically using the packages Ansys Transient Structural and Ansys Fluent.

### 4.2.2.1 Mesh creation

The flux happens in the geometric domains defined before and the variables governing the flux are velocity and pressure. Fluid flow is described by mass and momentum conservation equations. Given the complexity of solving in analytic way these equations, the fluid domain is divided in finite volume elements. Each element has a simplified geometry into which mass and momentum are balanced and equations are solved with numeric methods in each volume obtaining a set of algebraic equations. To accomplish this task a mesh of tetrahedral cells was applied to the geometry. The default dimensions were leaved for meshing.

#### 4.2.2.2 Setup

In the setup settings, it is possible to define boundary conditions, materials and physical model. The same settings were used for both the base geometry and the dilated ones.

Blood was modelled with constant density ( $1060 \text{ kg/m}^3$ ) and constant viscosity ( $3.5 \times 10^{-3} \text{ Pa}\cdot\text{s}$ ). The order of magnitude of Re number was estimated and it resulted lower than 1000 thus a laminar flow was hypothesized and the *laminar model* was selected to solve NS equation.

The wall of domain was considered stationary and rigid. No-slip boundary condition with the wall was applied.

At the inlet and outlet surface the velocity and pressure boundary condition were applied respectively. Standard curves were taken from literature, namely physiology book. The time duration of the waves in a pseudo-periodic event is dependent on the period thus on HR, which was supposed to be 66 bpm

The inlet condition was a flux velocity (m/s), Figure 23 (RCA) and Figure 24 (LCA).

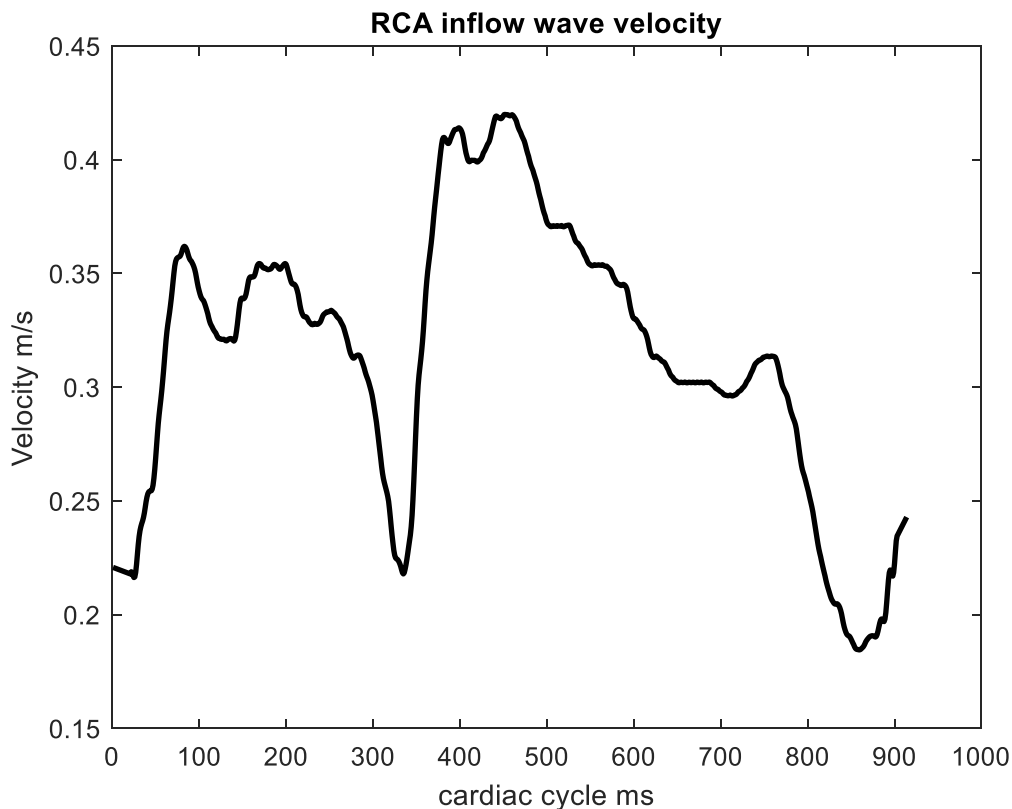


Figure 23 Inflow velocity boundary condition for right coronary artery

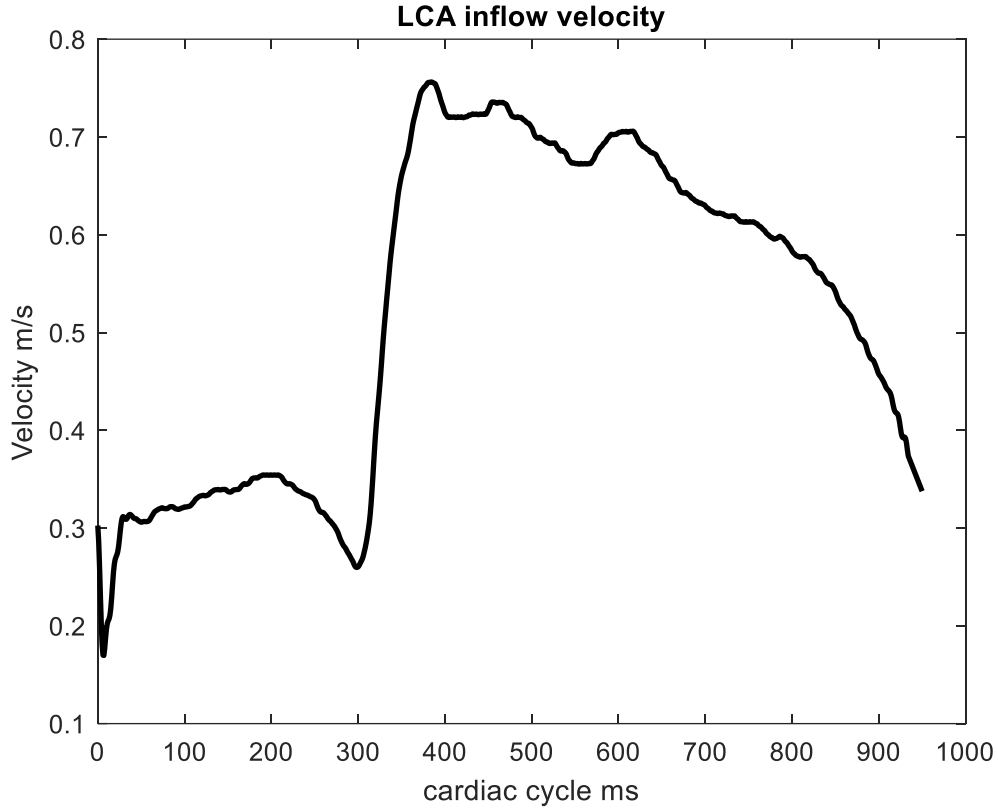


Figure 24 Inflow velocity boundary condition for left coronary artery

Outflow boundary condition was implemented to model the pressure exercised by ventricular myocardium contraction that oppose resistance to the flow. The pressure at outflow was modelled as a time dependent feedback pressure. The following formula was used to estimate the pressure wave at outflow boundary condition [160]:

$$p_f(x, t) = \varphi p_v(t) + p_s \quad (11)$$

where  $p_s = 20\text{mmHg}$  and it is the coronary bed pressure. The ventricular-pressure  $p_v$  curve were taken from physiology book both for right and left ventricles [10]. This pressure is multiplied by feedback ratio  $\varphi$  depends on the location of the vascular bed supplied by the terminal vessel:  $\varphi=33\%$  for LV (LAD and LADvd),  $\varphi=25\%$  for RV (RCA and RCAvd) and  $\varphi=22\%$  for LCX and LCXvd [160]. The waveform of  $p_f$  applied is reported in Figure 25 (LCA) and Figure 26 (RCA). The pressure curves, as in the rest of the discussion, are reported both in Pa because is the units of the simulator, and in mmHg because is the clinical unit to treat blood pressure.

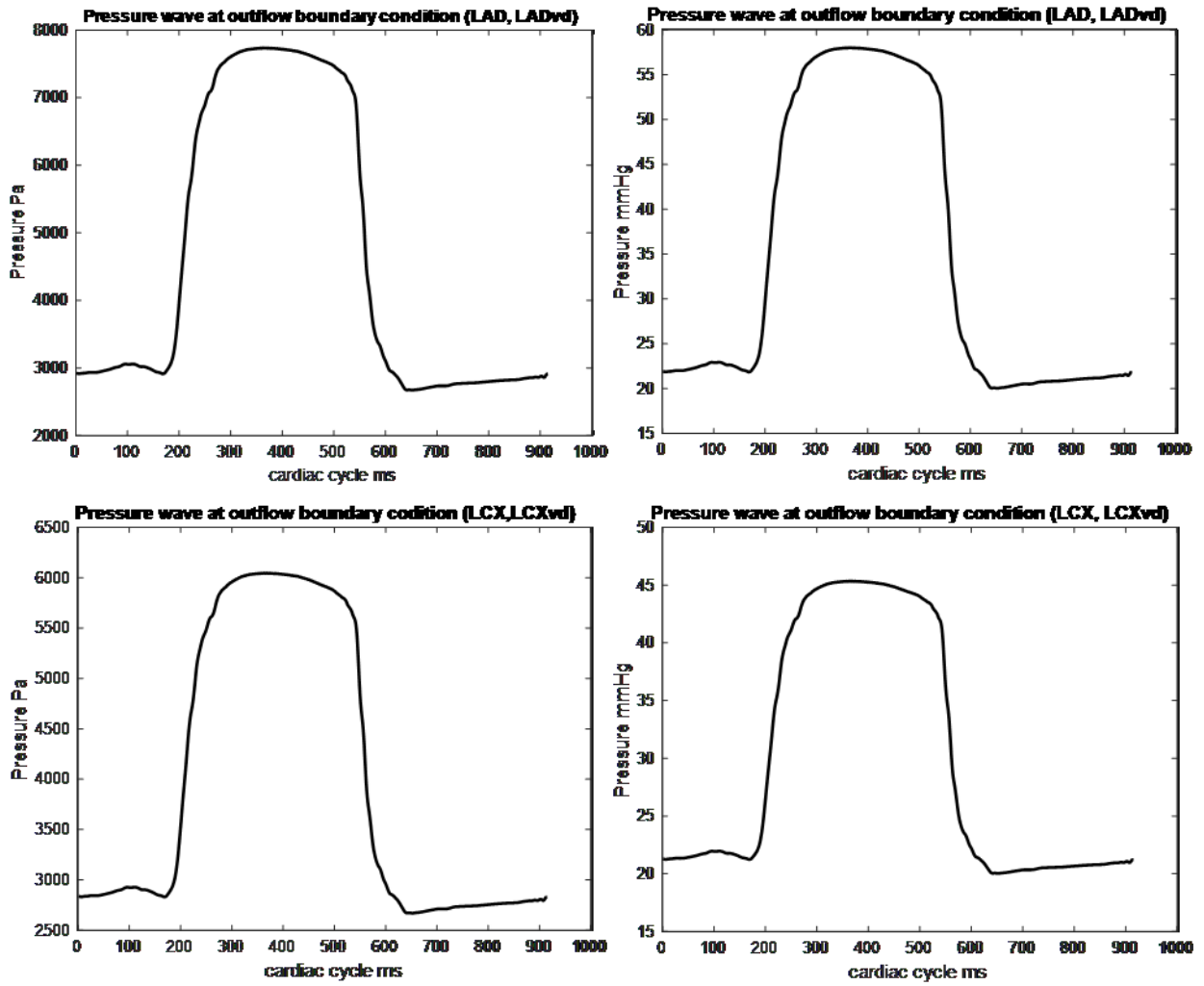


Figure 25 Outflow pressure boundary condition on LCA and LCAvd. The upper panels show the pressure boundary condition applied to LAD and LADvd. The lower panels show the pressure boundary condition applied to LCX and LCXvd. The left side panels show the pressure in Pa as received in input in the simulator, while the right side panels show the pressure condition in mmHg, which is the unit used in medical settings for blood pressure.

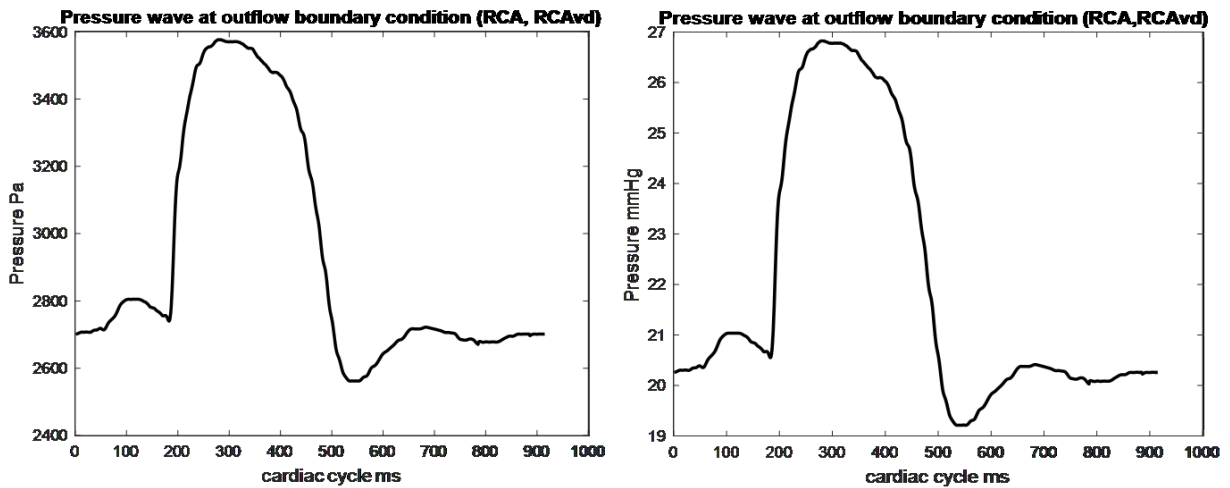


Figure 26 Outflow pressure boundary condition on RCA and RCAvd. The left side panels show the pressure in Pa as received in input in the simulator, while the right side panels show the pressure condition in mmHg, which is the unit used in medical settings for blood pressure.

## 4.3 Results

### 4.3.1 Reconstruction of coronary artery geometry

The coordinates and dimensions for coronary artery reconstruction are presented in Table 15 (RCA) and Table 16 (LCA). Figure 27 represents the central axes of segments and the central point of each section at which level measurements were taken from RCA. Figure 28 shows the reconstructed geometry of RCA displayed in Ansys. Figure 29 represents the central axes of segments and the central point of each section at which level measurements were taken from LCA. Figure 30 shows the reconstructed geometry of LCA displayed in Ansys.

*Table 15 Coordinates and dimension of RCA and RCAvd: polar coordinates ( $R, \phi, \vartheta$ ), Cartesian coordinates ( $x, y, z$ ) and diameter of coronary section are reported.*

coronary segment	R	$\theta$	$\phi$	x	y	z	coronary diameter (cm)	Vasodilated coronary diameter (cm)
R1p	0,5	289	338	-0,43833	-0,1873	0,150931	0.400	0.407
R1m	1,7	292	336	-1,43994	-0,69145	0,581774	0.390	0.397
R1d	2,6	294	330	-2,057	-1,3	0,915835	0.380	0.387
R2p	3,4	291	321	-2,4668	-2,13969	0,946914	0.350	0.357
R2m	4,6	288	312	-2,92735	-3,41847	0,951155	0.340	0.347
R2d	5,6	283	305	-3,1297	-4,58725	0,722549	0.320	0.327
R3p	6,2	276	298	-2,89478	-5,47428	0,304253	0.320	0.327
R3m	6,4	269	291	-2,29321	-5,97491	-0,04003	0.310	0.317
R3d	6,7	15	287	0,506998	-6,40724	1,892143	0.310	0.317

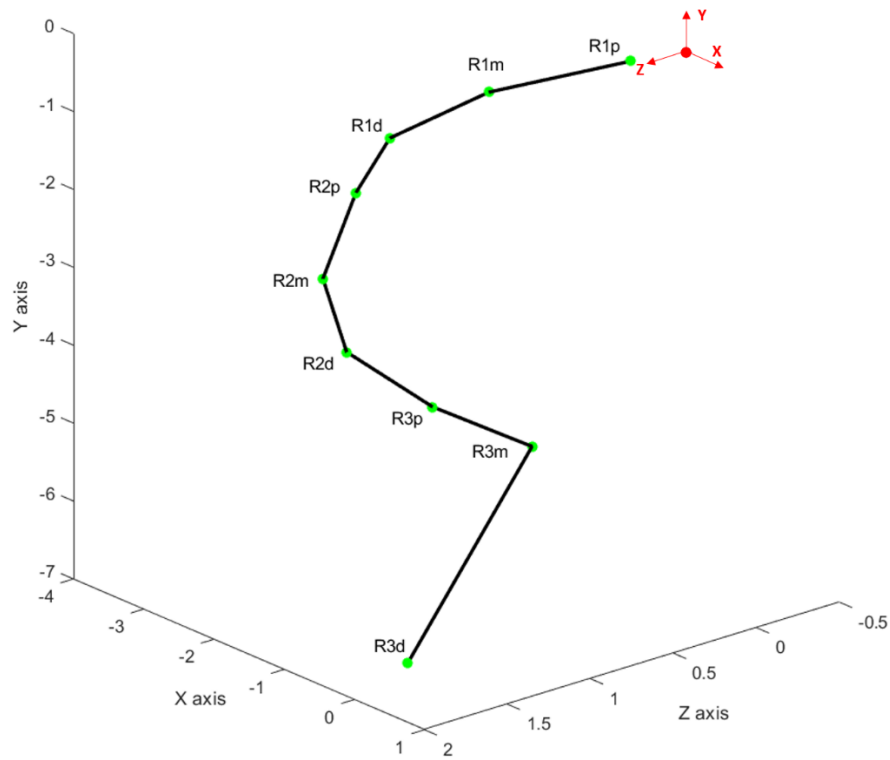


Figure 27 Central axes of RCA segments. The axes connect the central point (green dot) of each section at which level measurements were taken. The red frame is the frame centered in the ostium respect to which measurements were performed.

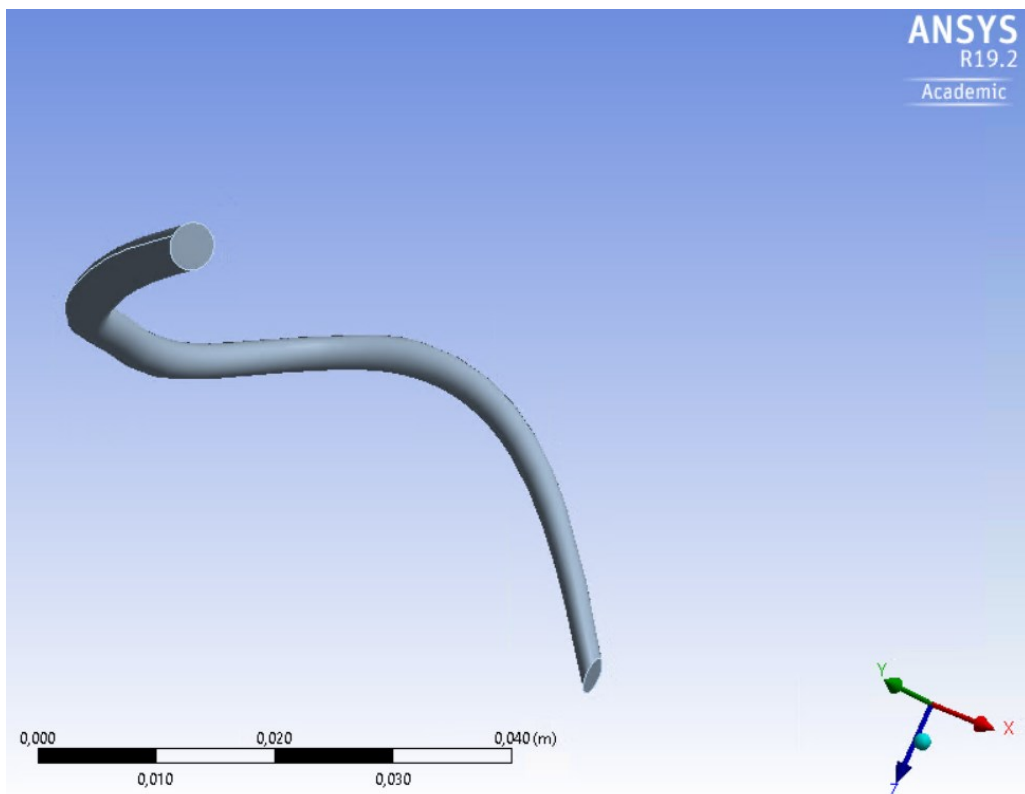


Figure 28 Geometry of RCAvd displayed in Ansys. The reconstructed geometry for RCA is the same but with lower section diameter.

Table 16 Coordinates and dimension of LCA and LCAvd: polar coordinates ( $R$ ,  $\phi$ ,  $\vartheta$ ), Cartesian coordinates ( $x$ ,  $y$ ,  $z$ ) and diameter of coronary section are reported.

Coronary segment	R	$\theta$	$\phi$	x	y	z	Coronary diameter (cm)	Vasodilated coronary diameter (cm)
LMp	0,3	83	7	0,295544	0,036561	0,036288	0.450	0.453
LMm	0,7	80	4	0,687686	0,04883	0,121258	0.450	0.453
LMd	1,1	79	0	1,07979	-2,7E-16	0,20989	0.450	0.453
L1p	1,6	70	-3	1,501448	-0,08374	0,546482	0.370	0.374
L1m	2,3	63	-5	2,041517	-0,20046	1,040205	0.360	0.364
L1d	3	59	-8	2,546476	-0,41752	1,530077	0.350	0.354
L2p	4	51	-9	3,070312	-0,62574	2,48629	0.290	0.294
L2m	5,3	44	-12	3,601236	-1,10193	3,729189	0.250	0.254
L2d	6,5	39	-17	3,911844	-1,90042	4,830724	0.230	0.234
L3p	8	33	-23	4,010743	-3,12585	6,176003	0.200	0.24
L3m	10,1	30	-32	4,282643	-5,35218	7,417755	0.170	0.174
L3d	11,8	31	-40	4,655596	-7,58489	7,748213	0.140	0.144
C1p	1,4	86	-12	1,366071	-0,29108	0,095525	0.340	0.345
C1m	1,8	94	-24	1,640376	-0,73213	-0,11471	0.340	0.345
C1d	2,2	102	-31	1,84456	-1,13308	-0,39207	0.330	0.335
C2p	2,6	107	-33	2,085264	-1,41606	-0,63753	0.280	0.285
C2m	3,1	116	-37	2,225207	-1,86563	-1,08531	0.280	0.285
C2d	3,6	120	-41	0,506998	-6,40724	1,892143	0.310	0.315



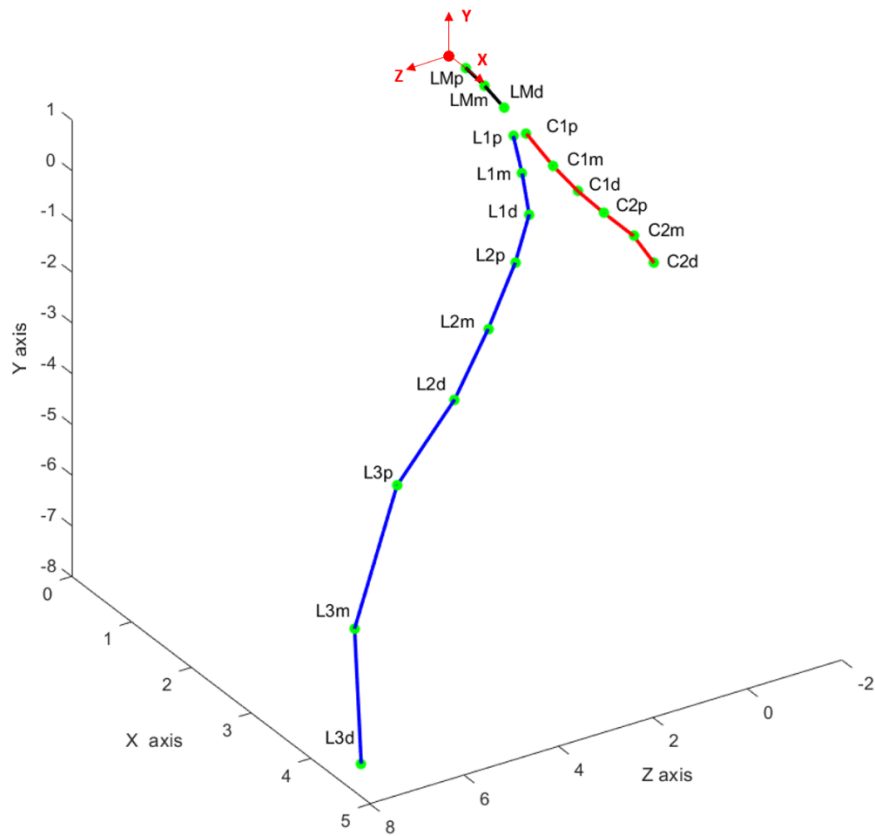


Figure 29 Central axes of LCA segments. The axes connect the central point (green dot) of each section at which level measurements were taken. The red frame is the frame centered in the ostium respect to which measurements were performed. The black axes are relative to the left main, the blue ones to the left anterior descending artery and the red ones to the circumflex branch.

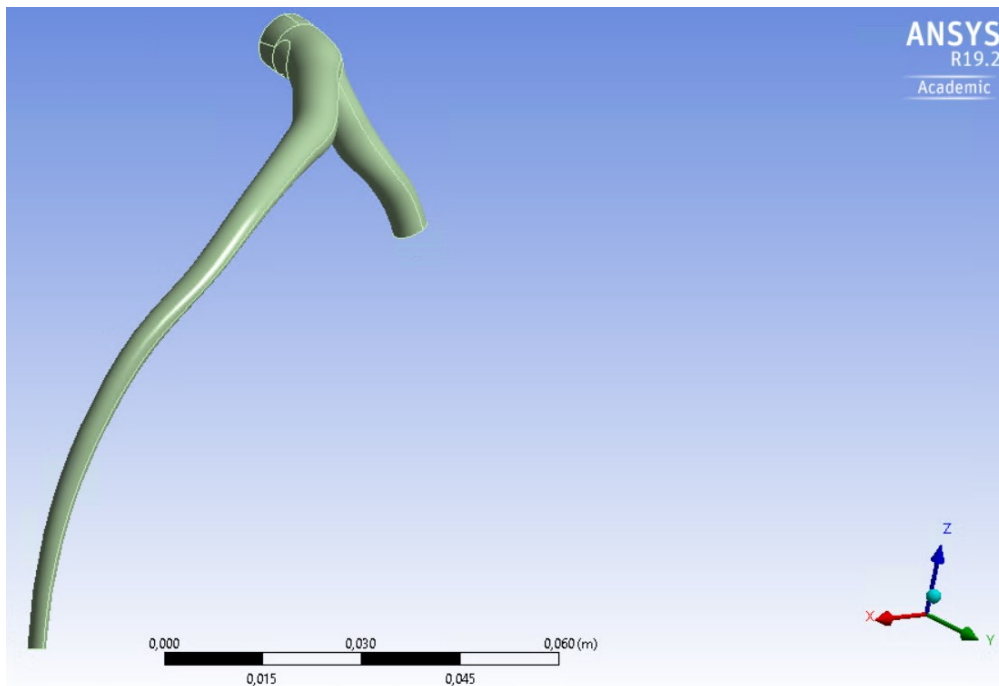


Figure 30 Geometry of LCA displayed in Ansys. The reconstructed geometry for LCAvd is the same but with increased section diameter.

### 4.3.2 Meshing

The RCA vessel has a mesh of 13267 nodes and 61229 elements. The RCAvd vessel has a mesh of 12962 nodes and 59608 elements. The LCA vessel has a mesh of 23008 nodes and 109763 elements. The LCAvd vessel has a mesh of 20576 nodes and 97273 elements.

An example of the meshing process for RCA and LCA is presented in Figure 31 and Figure 32 respectively.

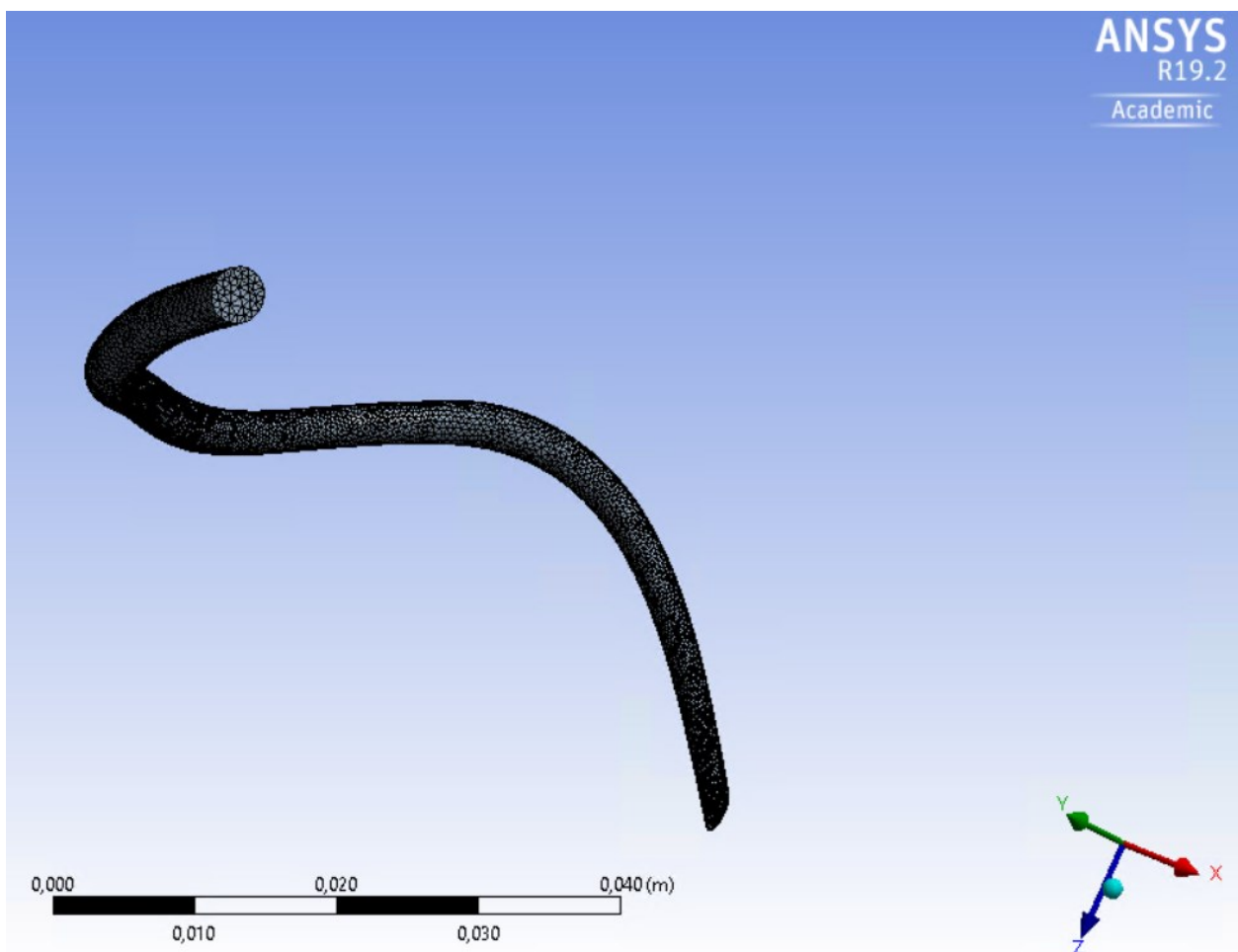


Figure 31 Mesh on RCAvd. The mesh has 12962 nodes and 59608 elements.

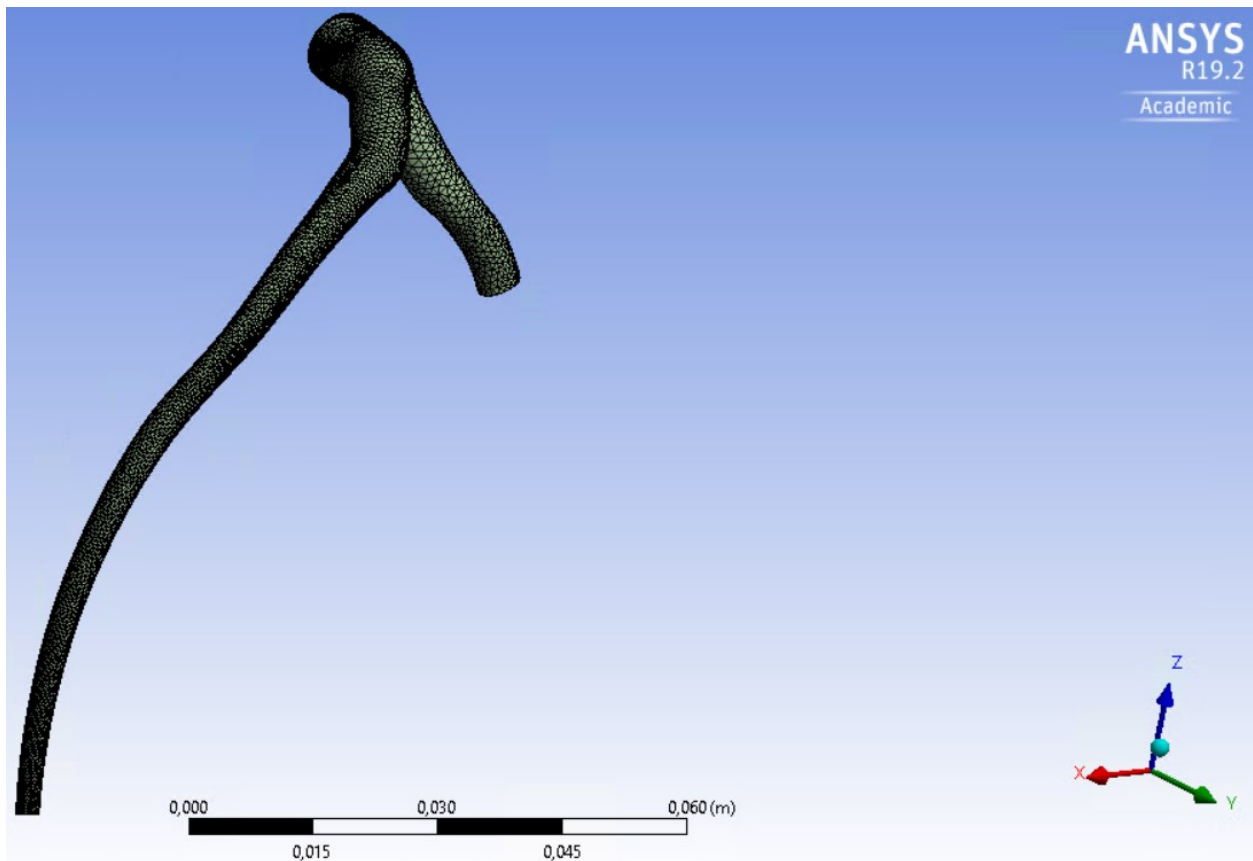


Figure 32 Mesh on LCA. The mesh has 23008 nodes and 109763 elements.

### 4.3.3 Numerical simulation results

The following figures present the global results of the simulation: inflow pressure waves and outflow velocity waves. Figure 33 shows the inflow pressure waves over the cardiac cycle obtained for RCA and RCAvd. Figure 34 shows the outflow velocity waves over the cardiac cycle obtained for RCA and RCAvd. The same waves were computed for LCA and LCAvd, but the simulation produced a non-physiologic flux inversion, thus the result of that simulation are not reported neither analysed below (Figure 35).

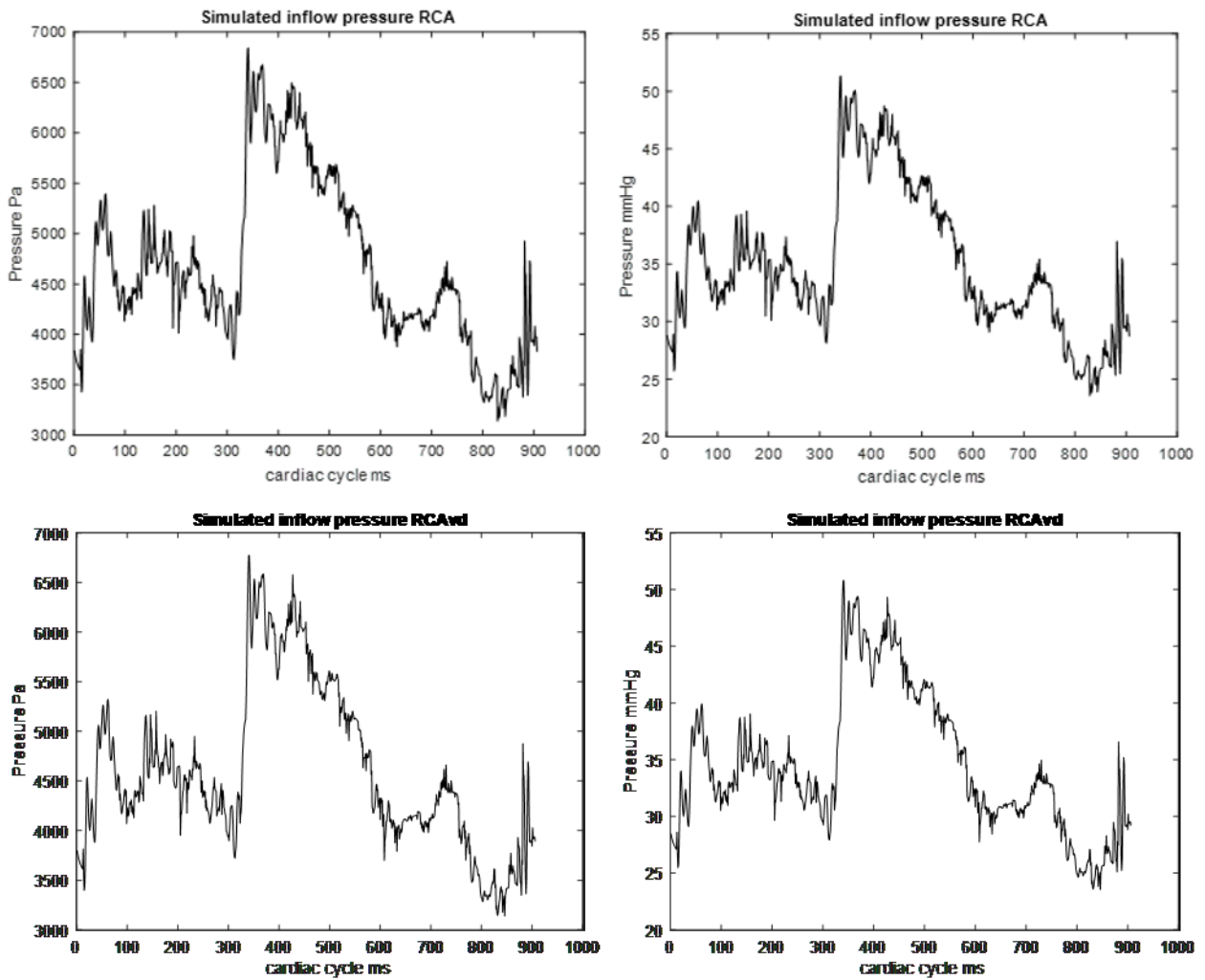


Figure 33 Simulated inflow pressure wave over cardiac cycle in RCA (upper panels) and RCAvd (lower panels). The left side panels show the pressure in Pa as given in output by the simulator, while the right side panels show the pressure wave in mmHg, which is the unit used in medical settings for blood pressure.

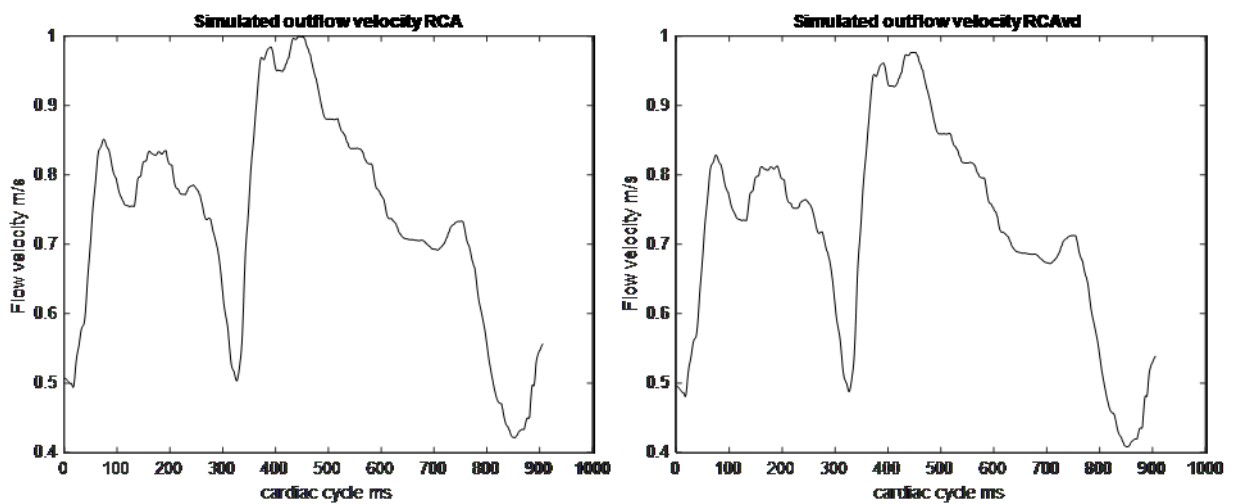


Figure 34 Simulated outflow velocity wave over cardiac cycle in RCA (left panel) and RCAvd (right panel).

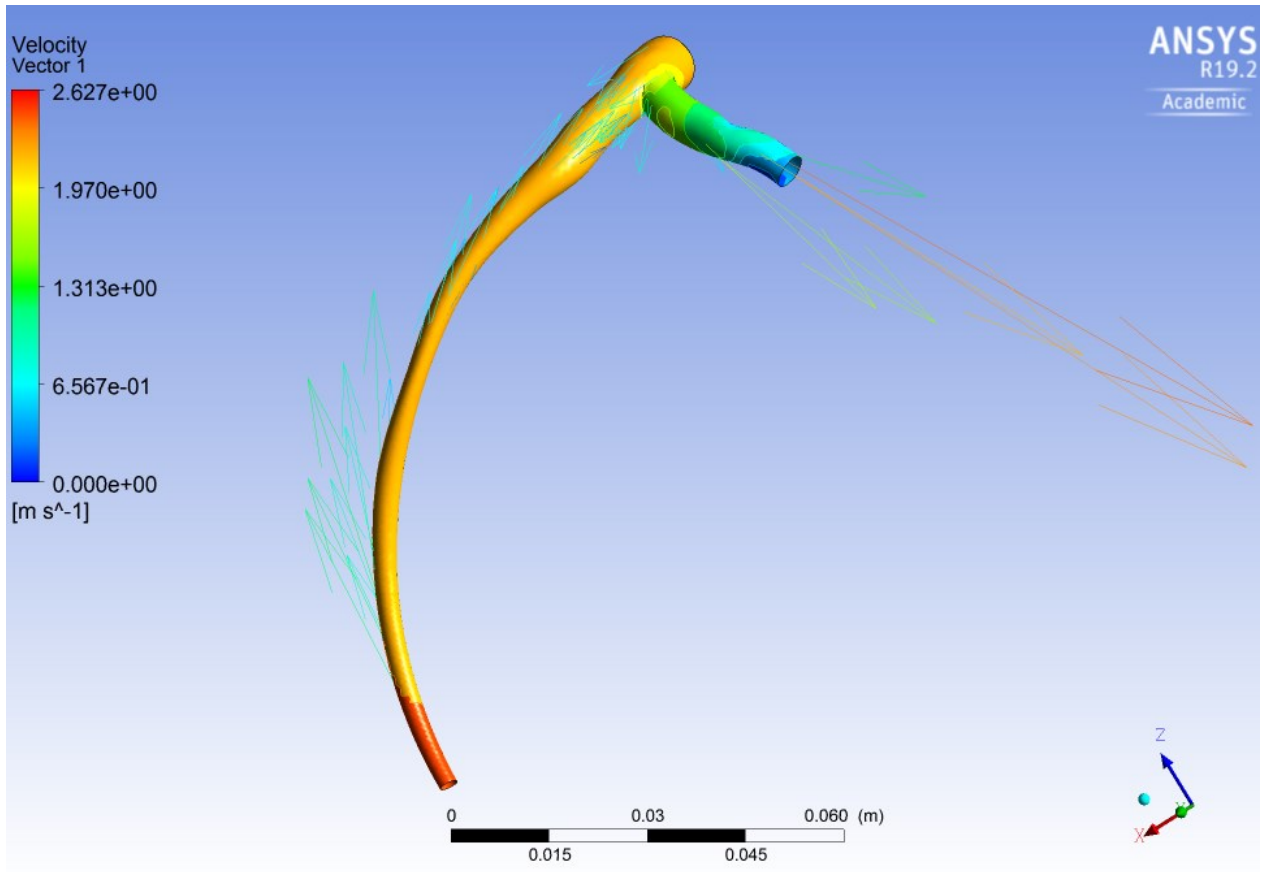


Figure 35 LCA simulation, not normal inverted flux indicated by velocity arrows and by the inverted pressure gradient.

Results at specific time instants were computed for maximal pressure and velocity conditions. They were reported in Table 17. Figure 36 is the wall shear stress map at maximum outflow velocity condition for RCA and RCAvd. Figure 37 is the pressure distribution at maximum inflow pressure condition for RCA and RCAvd.

Table 17 Specific time instant results. Under each measurement the time instant in which they were taken is reported in brackets.

RESULTS				
	Maximum inflow pressure (Pa)	Pressure difference input-output (mmHg)	Maximum outflow velocity (m/s)	Wall shear stress (Pa)
RCA	6842 (340 ms)	22.8319 (339 ms)	0.9996 (455 ms)	29.91 (455 ms)
RCAvd	6774 (340 ms)	22.4419 (339 ms)	0.9764 (462 ms)	30.02 (462 ms)

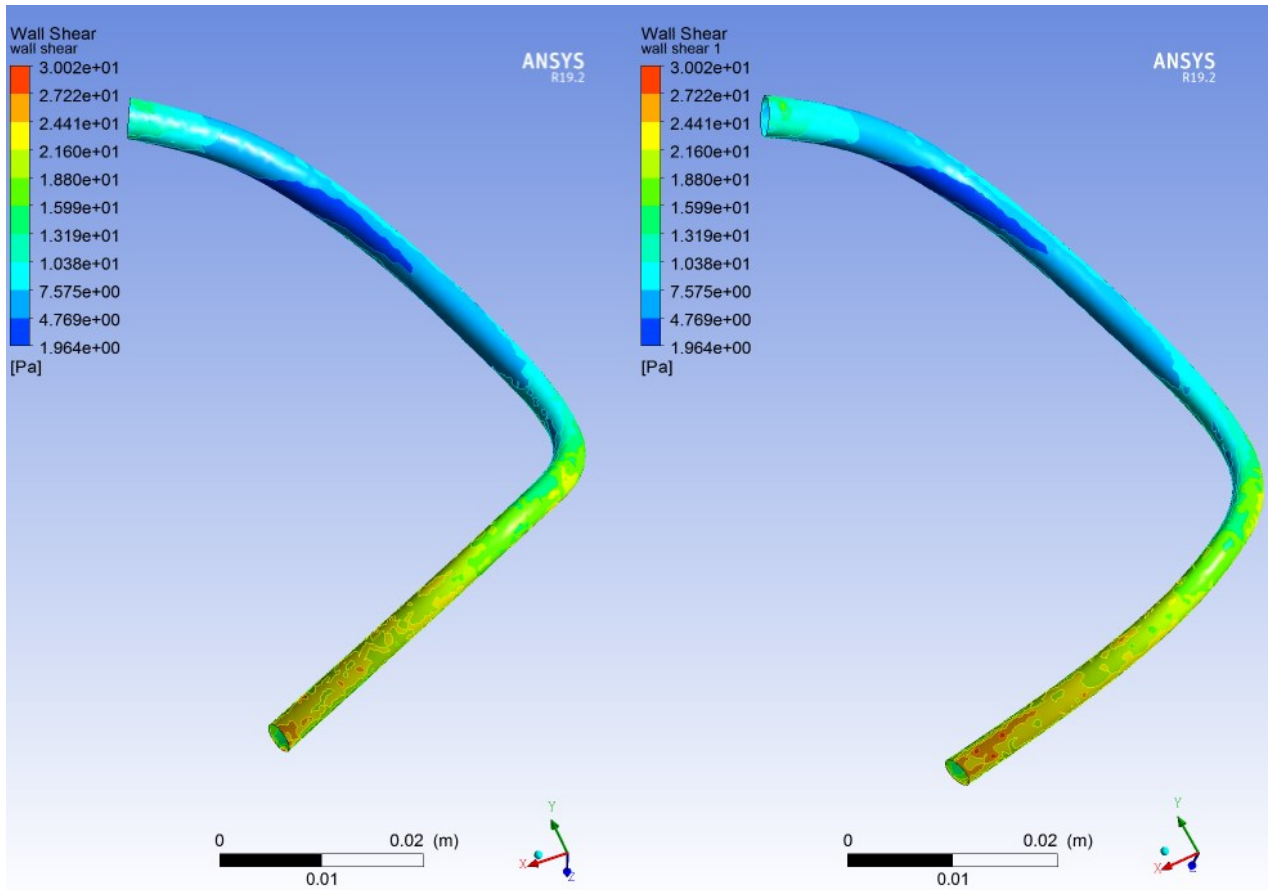


Figure 36 Wall shear at maximum outflow velocity. RCA is the right side, RCAvd is the left side.

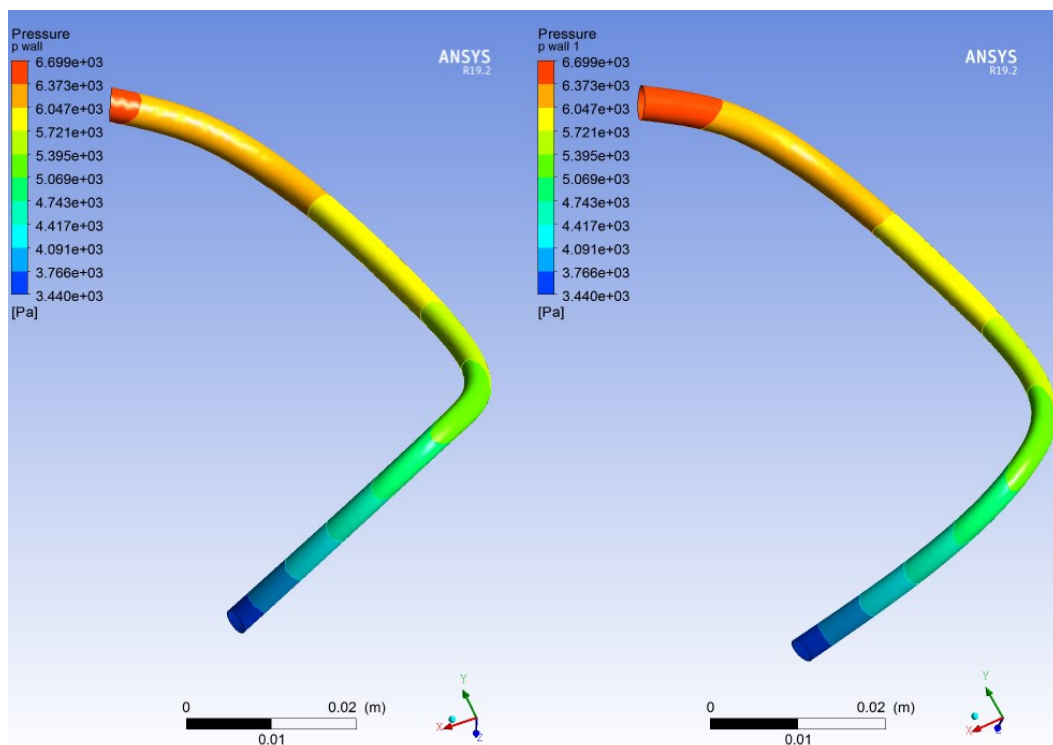


Figure 37 Pressure distribution at maximum inflow pressure. RCA is the right side, RCAvd is the left side.

## 4.4 Discussion and Conclusion

In pre-participation screening, ECG has not the sensitivity to detect all the possible causes of SrSCD, especially in case of CAA and CAD, they may remain undiagnosed if there is no presence of severe ischemic pattern in ECG signal [73]. Imaging analysis has a pivotal role, namely non-invasive technique such as CTCA and CMR. Non-invasive imaging has lower risk with respect to ICA and it can be performed successfully on young athletes with suspected mild coronary pathology. The sensitivity and specificity of this analysis further increase in diagnosis or exclusion of CAA and CAD when combining non-invasive imaging methods and CFD. CFD simulation can be used to implement qualitative models of athlete's vascular system to study sport-related adaptation and anomalies in wave dynamics that can possible lead to SrSCD. Given that background, the aim of this work was to collect geometric data of coronary arteries and to produce from them a qualitative model. Further, the study evaluates the goodness of the produced qualitative model of the main conduit epicardial coronary arteries representative of the healthy athletic population cardiac vascular system.

Geometric data obtained from coronary angiography in healthy subjects were collected mainly from 4 papers [135][143][144][164]. From data collection, it emerged that Asian population (concerning ethnicity) and females (concerning gender) have the smallest coronary dimension. Further Asian subjects showed higher prevalence of coronary disease with corresponding higher mortality and morbidity. Coronary diameter is the geometric parameter affected by training-related remodeling, which induce vasodilation of conduit arteries in the long term.

The data from [135] and [164] were used to create the model since researchers measured coronary diameter and relative intrathoracic location in a higher number of vessel sections with respect to other works. Specifically the data belonging to male subjects and coronary right dominance (the most frequent) was used to model the conduit epicardial arteries. To model the long term training-induced vasodilation, a physiologic estimation of diameter increment was added [143][144]. We implemented a normal geometry representative of generic population and a vasodilated geometry to assess the influence of training-induced vasodilation of conduit coronary arteries.

The two geometries have stationary not deformable walls. Although deformability is essential to use the model when studying the transient flow in pathologic condition, *e.g.* coronary bridge. Indeed wall deformability enable to create a model with myocardium contribution to wall motion. In this case, the myocardium contribution to coronary flow was considered in the outflow

boundary conditions by applying a pressure proportional to the ventricular pressure mimic the pressure exercised by myocardium on coronary ending.

Inflow velocity and outflow pressure were applied as boundary conditions, while inflow pressure and outflow velocity waves were obtained from simulation. For LCA and LCAvd, the simulation produced a non-physiologic flux inversion showed in Figure 35, in which is visible the inversion in pressure gradient and the flux directed from LCA end to LCX end. Thus, the result of that simulation are not analysed.

Analyzing visually the inflow pressure waves for RCA and RCAvd, it is notable a shift in amplitude towards lower pressure range with respect to normal simulation and in vivo data from literature. We inferred that it depends on the rigidity of wall. Indeed part of energy and pressure is given by wall deformability, but the vessel walls were stationary and rigid, thus the model may lack a pressure contribution given by the deformability and motion of walls. Another cause might be the goodness of boundary condition, thus patient specific wave, mass flow or pressure at inflow boundary, or Windkessel models, which includes also the resistance of downstream capillary bed, should be implemented in future studies. Although, taking into account the low goodness of pressure results, we could observe that the pressure difference between input and output area has no significant difference between the RCA and RCAvd, with a slightly decrement in the vasodilated case. This small decrement can be justified by the small increase in coronary diameter through Poiseuille formula.

The outflow velocity waves demonstrated to have a more reliable trend for RCA and RCAvd, with a lower velocity in systolic phase and a greater flow velocity in diastolic phase. As expected the maximum flow velocity is lower in vasodilated vessel. However, maximum value of the shear stress is higher in the RCAvd than in RCA. This fact is not physiologically reasonable and it may derive from approximation made by the model. Although from the shear stress mapping (Figure 36) the max shear stress seems to be located on the outlet edge rather than on the wall for RCAvd.

The proposed preliminary model offers a qualitative geometry structure of healthy conduit coronary arteries. On the other hand, the model should be improved by introducing wall deformability, which may have a fundamental role in reproducing pressure wave dynamics and myocardium/vessel interaction, and by providing more detailed boundary conditions. In addition, future study should introduce the training-related increase in blood volume as well as a more accurate model of blood.



## Discussion and Conclusion

SrSCD is the leading medical cause of death across all sports. Increased cardiovascular load during exercise in people with an underlying cardiovascular abnormality can trigger SCD [1][2][3]. SrSCD could occur not only during sport activity but also after exercise at rest or during sleep [1]. Given the growing sport participation among general population, SrSCD is recognized as a public health concern [4]. Prevention and screening of athletic population can contrast sudden cardiac arrest. Pre-participation screening represents the first-line test for the diagnosis of cardiovascular pathology in sport participants. Although, its cost-effectiveness is widely debated with the main goal to balance among saved lives, economic costs and legal, ethical and psychological issues [127][128]. Currently, pre-participation screening include clinical and family history, physical examination and rest 12-lead ECG [15]. Unfortunately, most screenings are usually recommended for competitive athletes, while amateur athletes and people occasionally practicing sport are typically left to optional, sometimes self-made, evaluations of their health status [127]. Further, screening of athletes is performed regularly but not too frequently, typically once a year. Thus, the main objective of sport medicine specialists is to develop individualized pre-participation screening and effective risk stratification algorithms for the early identification of sport participants with underlying cardiovascular disease at risk of SrSCD [15]. When developing screening protocol for athletes, clinicians must focus on the electrical and structural changes, which contribute to physiological and functional adaptations to make the heart more efficient. Indeed sport-related adaptation may manifest with abnormal ECG pattern or cardiac dimension, which must not be interpreted as sign of cardiovascular pathologies. Further, expected physiologic changes and incidence/manifestation of pathology have variability by age, sport, gender, and ethnicity [4]. Testing of screening protocols are mainly based on result from Caucasian young adult athletes participating in competitive sports, thus excluding the magnitude and complexity of athletic population. To account for this aspect, all the factors contributing to the variability of sport-related physiologic adaptation and diseases had a central role in the literature review on mechanoelectric contributions to sport-related sudden cardiac death. Age was mainly related with diseases incidence: cardiomyopathies and CAA were the cause behind SrSCD in young athletes, while CAD is the most frequent cause of SrSCD in older athletes. Gender, intensity and quantity of training contributes more to the different sport-related physiological adaptation, with male and higher trained athletes presenting the greater remodelling of cardiovascular system. From the

review two main problems emerged in sport cardiology field: (1) the lack of normative and guidelines for continuous monitoring of athletes during training; (2) low sensitivity and specificity of ECG in detecting mechanical causes of SrSCD (CAA and CAD, which may remain undiagnosed if there is no presence of severe ischemic pattern in ECG signal).

Addressing the first problem, wearable sensor technologies recording cardiac signals enable the continuous monitoring of athlete's cardiac status before and during training or competition. Moreover, they may be applied in the wide screening of amateur athletic population. However, at our knowledge, there are no interpretation guidelines for ECG acquired by wearable sensors. Both European and American cardiology associations have proposed several interpretation guidelines for standard 12 lead ECG acquired at rest, but they cannot be applied to wearable sensors ECG. In fact, wearable sensors usually acquire a single lead which has not precise correspondence with one of the 12 leads. Thus, we derived normal reference values from ECG acquired through chest strap BioHarness 3.0 by Zephyr ([www.zephyranywhere.com](http://www.zephyranywhere.com)) from healthy athletes. ST level, interval and wave durations coincided with the normal values from 12 lead ECG. Further, we found a significant difference between male and female values (QRS duration and QTc), suggesting that gender stratification is central to produce more accurate personalized pre-participation screening.

Concerning the second issue, non-invasive imaging combined with CFD have a pivotal role in evaluating suspected mild coronary pathologies in young athletes given the lower risks. Further CFD can be used to implement qualitative model of athlete's cardiovascular system and study the mechanical and fluid dynamic contribution to SrSCD. In this setting, a reliable model with realistic geometry is essential. Thus, we collected geometrical data and intrathoracic coordinates of healthy conduit coronary arteries to develop a reliable geometry of a preliminary model of RCA and LCA. During the collection of data, we found out that conduit epicardial arteries are subjected to vasodilation as sport-related remodelling, so a uniform increase in diameter was added to mimic vasodilation in athletic qualitative model. The numerical analysis, conducted with a rigid boundary model, suggests that implementation of wall deformability has a central role. Therefore, future studies are planned to implement a more realistic model of materials and fluid structure interaction.

## Reference

- [1] K. G. Harmon, J. A. Drezner, M. G. Wilson, and S. Sharma, “Incidence of sudden cardiac death in athletes: A state-of-the-art review,” *Br. J. Sports Med.*, vol. 48, no. 15, pp. 1185–1192, 2014.
- [2] M. Borjesson and A. Pelliccia, “Incidence and aetiology of sudden cardiac death in young athletes : an international perspective,” *Br J Sport. Med*, pp. 644–648, 2009.
- [3] S. F. Defroda, C. Mcdonald, C. Myers, A. I. Cruz, B. D. Owens, and A. H. Daniels, “Sudden Cardiac Death in the Adolescent Athlete : History , Diagnosis , and Prevention,” *Br. J. Sports Med.*
- [4] M. R. Caruso, L. Garg, and M. W. Martinez, “Cardiac Imaging in the Athlete : Shrinking the ‘ Gray Zone ,’” *Curr Treat Options Cardiovasc Med*, vol. 8, 2020.
- [5] C. L. Stanfield, *Principles of Human Physiology*, 5th ed. .
- [6] R. E. Klabunde, *Cardiovascular Physiology Concepts*, 2nd ed. .
- [7] F. H. Netter, *Atlas of Human Anatomy*, 7th ed. .
- [8] T. B. Garcia and N. E. Holtz, *12-Lead ECG: The art of interpretation. .*
- [9] G. Rozinaj, “High Resolution of the ECG Signal by Polynomial Approximation,” *Radioengineering*, no. April, 2006.
- [10] W. Boron and E. Boulpaep, *Medical Physiology*, 3rd ed. .
- [11] M. Loukas, A. Sharma, and C. Blaak, “The Clinical Anatomy of the Coronary Arteries,” *J. Cardiovasc. Trans. Res.*, pp. 197–207, 2013.
- [12] H. Chen and G. S. Kassab, “Microstructure-Based Biomechanics of Coronary Arteries in Health and Disease,” *J Biomech.*, vol. 49, no. 12, pp. 2548–2559, 2016.
- [13] G. Holzapfel, “Constitutive modelling of arteries,” *Proc. R. Soc. A Math. Phys. Eng. Sci.*, pp. 1551–1597, 2010.
- [14] D. J. Duncker, R. J. Bache, D. Merkus, and M. H. Laughlin, “Exercise and the Coronary Circulation,” in *Muscle and Exercise Physiology*, Elsevier Inc., 2004, pp. 467–504.

- [15] C. De Innocentiis, F. Ricci, N. Aung, Q. Mary, and C. Tana, “Athlete ’ s Heart : Diagnostic Challenges and Future Perspectives Athlete ’ s Heart : Diagnostic Challenges and Future Perspectives,” *Sport Med.*, no. September, 2018.
- [16] R. Kovacs and A. L. Baggish, “Cardiovascular adaptation in athletes,” *Trends Cardiovasc. Med.*, vol. 26, no. 1, pp. 46–52, 2016.
- [17] N. Sheikh *et al.*, “Comparison of Electrocardiographic Criteria for the Detection of Cardiac Abnormalities in Elite Black and White Athletes,” *Circulation*, pp. 1637–1649, 2014.
- [18] R. Beaudry and M. J. Haykowsky, “A Modern Definition of the Athlete ’ s Heart — for Research and the Clinic,” *Cardiol. Clin.*, vol. 34, no. 4, pp. 507–514, 2016.
- [19] D. Oxborough, D. Augustine, S. Gati, K. George, and A. Harkness, “A guideline update for the practice of echocardiography in the cardiac screening of sports participants : a joint policy statement from the British Society of Echocardiography and Cardiac Risk in the Young,” *Echo Reasearch Pract.*, pp. 1–10, 2018.
- [20] C. C. Erickson, “Discrimination of the “ Athlete ’ s Heart ” from real disease by electrocardiogram and echocardiogram,” *Cardiol. Young*, vol. 27, pp. 80–88, 2017.
- [21] J. H. Mitchell, W. Haskell, P. Snell, and S. P. Van Camp, “Task Force 8 : Classification of Sports,” *JACC*, vol. 45, no. 8, pp. 1364–1367, 2005.
- [22] G. Finocchiaro *et al.*, “Effect of Sex and Sporting Discipline on LV Adaptation to Exercise,” *JACC Cardiovasc. Imaging*, vol. 10, no. 9, pp. 5–12, 2017.
- [23] Y. Hellsten and M. Nyberg, “Cardiovascular Adaptations to Exercise Training,” *Compr. Physiol.*, vol. 6, no. January, pp. 1–32, 2016.
- [24] M. Galderisi *et al.*, “The multi-modality cardiac imaging approach to the Athlete ’ s heart : an expert consensus of the European Association of Cardiovascular Imaging,” *Eur. Hear. J. – Cardiovasc. Imaging*, 2015.
- [25] D. Corrado *et al.*, “Cardiovascular pre-participation screening of young competitive athletes for prevention of sudden death : proposal for a common European protocol Consensus Statement of the Study Group of Sport Cardiology of the Working Group of Cardiac Rehabilitation and,” *Eur. Heart J.*, no. June 2004, pp. 516–524, 2005.

- [26] D. Corrado, C. Basso, and G. Thiene, “Sudden cardiac death in athletes : what is the role of screening ?,” *Curr Opin Cardiol*, pp. 41–48, 2012.
- [27] M. Borjesson *et al.*, “Cardiovascular evaluation of middle-aged / senior individuals engaged in leisure-time sport activities : position stand from the sections of exercise physiology and sports cardiology of the European Association of Cardiovascular Prevention and Rehabilitat,” *Eur. J. Cardiovasc. Prev. Rehabil.*
- [28] L. Le, “The Impending Dilemma of Electrocardiogram Screening in Athletic Children,” *Pediatr Cardiol*, pp. 1–13, 2016.
- [29] K. Narayanan and W. Bougouin, “Sudden Cardiac Death During Sports Activities in the General Population,” *Card. Electrophysiol. Clin.*, vol. 9, no. 4, pp. 559–567.
- [30] A. Dhakal, S. Pandey, A. Maskey, and S. Yadav, “Does populational difference influence the size of adult human coronary,” pp. 36–40, 2017.
- [31] E. Marijon, M. Tafflet, D. S. Celermajer, and F. Dumas, “Sports-Related Sudden Death in the General Population,” *Circulation*, pp. 672–681, 2011.
- [32] E. D. Paratz *et al.*, “Cardiac arrest and sudden cardiac death registries : a systematic review of global coverage,” *Open Hear.*, pp. 1–10, 2020.
- [33] J. Scharhag, P. Bohm, J. Dvorak, and T. Meyer, “F-MARC : the FIFA Sudden Death Registry ( FIFA-SDR ),” *Br. J. Sports Med.*, no. May, 2015.
- [34] T. Meyer, “Data from a nationwide registry on sports-related sudden cardiac deaths in Germany,” *Eur. J. Prev. Cardiol.*, 2016.
- [35] I. M. Asif, K. G. Harmon, and A. Americans, “Incidence and Etiology of Sudden Cardiac Death : New Updates for,” *Sports Health*, 2017.
- [36] J. H. Kim and A. L. Baggish, “Differentiating Exercise-Induced Cardiac Adaptations From Cardiac Pathology : The ‘ Grey Zone ’ of Clinical Uncertainty,” *Can. J. Cardiol.*, vol. 32, no. 4, pp. 429–437, 2016.
- [37] H. Dores, A. Freitas, A. Malhotra, M. Mendes, and S. Sharma, “The hearts of competitive athletes: An up-to-date overview of exercise-induced cardiac adaptations Hélder,” *Rev. Port. Cardiol.*, vol. 34, no. 1, pp. 51–64, 2015.
- [38] J. Morganroth, B. J. Maron, and W. L. Henry, “Comparative Left Ventricular Dimensions

- in Trained Athletes,” *Ann. Intern. Med.*, pp. 521–524, 1975.
- [39] B. M. Pluim, A. H. Zwinderman, A. Van Der Laarse, and E. E. Van Der Wall, “The Athlete ’ s Heart A Meta-Analysis of Cardiac Structure and Function,” *Circulation*, pp. 336–344, 2000.
- [40] M. Scharf, M. H. Brem, M. Wilhelm, U. J. Schoepf, M. Uder, and M. M. Lell, “Atrial and Ventricular Functional and Structural Adaptations of the Heart in Elite Triathletes Assessed with Cardiac Methods : Results :,” *Radiology*, vol. 257, no. 1, pp. 71–79, 2010.
- [41] S. E. E. Page, “Left Atrium Size in Elite Athletes,” *JACC Cardiovasc. Imaging*, vol. 8, no. 7, pp. 753–762, 2015.
- [42] V. Utomi *et al.*, “Predominance of normal left ventricular geometry in the male ‘ athlete ’ s heart ’ Study population,” *Heart*, no. May, 2014.
- [43] G. Mcclean *et al.*, “Electrical and structural adaptations of the paediatric athlete ’ s heart : a systematic review with meta- analysis,” *Br J Sport. Med*, no. March, 2017.
- [44] A. Pelliccia, F. Culasso, F. M. Di Paolo, and B. J. Maron, “Physiologic Left Ventricular Cavity Dilatation in Elite Athletes,” *Ann Intern Med*, pp. 23–31, 1999.
- [45] P. Demola *et al.*, “Hemodynamic and ECG responses to stress test in early adolescent athletes explain ethnicity-related cardiac differences,” *Int. J. Cardiol.*, vol. 289, pp. 125–130, 2019.
- [46] J. Rawlins *et al.*, “Ethnic Differences in Physiological Cardiac Adaptation to Intense Physical Exercise in Highly Trained Female Athletes,” *Circulation*, pp. 1078–1085, 2010.
- [47] M. Sandeep Basavarajaiah, MBBS *et al.*, “Ethnic Differences in Left Ventricular Remodeling in Highly-Trained Athletes Relevance to Differentiating Physiologic Left Ventricular Hypertrophy From Hypertrophic Cardiomyopathy,” *J. Am. Coll. Cardiol.*, vol. 51, no. 23, 2008.
- [48] H. Heidbuchel, “The athlete ’ s heart is a proarrhythmic heart , and what that means for clinical decision making,” *Europace*, pp. 1401–1411, 2018.
- [49] T. J. W. Dawes *et al.*, “Ventricular Structure and Function Moderate Physical Activity in Healthy Adults Is Associated With Cardiac Remodeling,” *Circ Cardiovasc Imaging*, pp. 1–8, 2016.

- [50] C. Luigi *et al.*, “Range of right heart measurements in top-level athletes : The training impact Range of right heart measurements in top-level athletes : The training impact,” *Int. J. Cardiol.* , no. February 2018, 2011.
- [51] A. Zaidi *et al.*, “Physiological Right Ventricular Adaptation in Elite Athletes of African and Afro-Caribbean Origin,” *Circulation*, pp. 1783–1792, 2013.
- [52] H. Mosén and K. Steding-Ehrenborg, “Atrial remodelling is less pronounced in female endurance-trained athletes compared with that in male athletes,” *Scand. Cardiovasc. J.*, pp. 20–26, 2014.
- [53] A. Pelliccia *et al.*, “Prevalence and Clinical Significance of Left Atrial Remodeling in Competitive Athletes,” *J. Am. Coll. Cardiol.*, vol. 46, no. 4, pp. 690–696, 2005.
- [54] A. D. Andrea, L. Riegler, R. Cocchia, R. Scarafilo, D. Salvo, and P. Caso, “Left atrial volume index in highly trained athletes,” *Am. Heart J.*, vol. i, no. June 2008, 2010.
- [55] S. Kou *et al.*, “Echocardiographic reference ranges for normal cardiac chamber size : results from the NORRE study,” *Eur. Hear. J. – Cardiovasc. Imaging*, pp. 680–690, 2014.
- [56] S. Nistri *et al.*, “Determinants of echocardiographic left atrial volume : implications for normalcy,” *Eur. J. Echocardiogr.*, no. August, 2011.
- [57] R. Lampert, “Evaluation and Management of Arrhythmia in the Athletic Patient,” *Prog. Cardiovasc. Dis.*, vol. 54, no. 5, pp. 423–431, 2012.
- [58] G. F. Gjerdalen, J. Hisdal, E. E. Solberg, T. E. Andersen, Z. Radunovic, and K. Steine, “Atrial Size and Function in Athletes,” *Int J Sport. Med*, pp. 1170–1176, 2015.
- [59] J. M. Black, E. J. Stöhr, R. Shave, and J. I. Esformes, “Influence of exercise training mode on arterial diameter : A systematic review and meta-analysis,” *J. Sci. Med. Sport*, vol. 19, no. 1, pp. 74–80, 2016.
- [60] M. D. Brown, “The Athlete ’ s Heart Exercise and coronary vascular remodelling in the healthy heart Experimental Physiology : In this review the evidence for structural adaptations of the coronary circulation in the healthy adult heart in,” *Exp. Physiol.*, 2003.
- [61] P. Sotiriou, E. Kouidi, A. Karagiannis, N. Koutlianos, and P. Geleris, “Arterial adaptations in athletes of dynamic and static sports disciplines – a pilot study,” *Clin Physiol Funct Imaging*, pp. 183–191, 2019.

- [62] D. J. Green, A. Spence, N. Rowley, D. H. J. Thijssen, and L. H. Naylor, “Vascular adaptation in athletes : is there an ‘ athlete ’ s artery ’?”, *Exp Physiol*, vol. 3, pp. 295–304, 2012.
- [63] W. Leung, M. L. Stadius, and E. L. Alderman, “Determinants of Normal Coronary Artery Dimensions in Humans,” *Circulation*, pp. 2294–2306.
- [64] M. G. Wilson *et al.*, “Prevalence of electrocardiographic abnormalities in West-Asian and African male athletes,” *Br J Sport. Med*, pp. 341–347, 2012.
- [65] A. Pelliccia *et al.*, “Prevalence of abnormal electrocardiograms in a large , unselected population undergoing pre-participation cardiovascular screening,” *Eur. Heart J.*, pp. 2006–2010, 2007.
- [66] J. A. Drezner *et al.*, “Normal electrocardiographic fi ndings : recognising physiological adaptations in athletes,” *Br J Sport. Med*, pp. 125–136, 2013.
- [67] R. Stein, C. M. Medeiros, G. A. Rosito, L. I. Zimmerman, J. P. Ribeiro, and P. Alegre, “Intrinsic Sinus and Atrioventricular Node Electrophysiologic Adaptations in Endurance Athletes,” *J. Am. Coll. Cardiol.*, vol. 39, no. 6, pp. 1033–1038, 2002.
- [68] S. M. Leite, J. Freitas, M. Campelo, and M. J. Maciel, “Electrocardiographic evaluation in athletes: ‘Normal’ changes in the athlete’s heart and benefits and disadvantages of screening,” *Rev. Port. Cardiol.*, vol. 35, no. 3, pp. 169–177, 2016.
- [69] F. M. Di Paolo *et al.*, “The Athlete ’ s Heart in Adolescent Africans,” *JAC*, vol. 59, no. 11, pp. 1029–1036, 2012.
- [70] M. Brosnan *et al.*, “Comparison of Frequency of Signi fi cant Electrocardiographic Abnormalities in Endurance Versus Nonendurance Athletes,” *Am. J. Cardiol.*, vol. 113, no. 9, pp. 1567–1573, 2014.
- [71] C. S. S. S. Colombo and G. Finocchiaro, “The Female Athlete ’ s Heart : Facts and Fallacies,” *Curr Treat Options Cardio Med*, 2018.
- [72] A. Pelliccia *et al.*, “Clinical Investigation and Reports Clinical Significance of Abnormal Electrocardiographic Patterns in Trained Athletes,” *Circulation*, pp. 278–284, 2000.
- [73] S. Sharma *et al.*, “International Recommendations for Electrocardiographic Interpretation in Athletes,” *J. Am. Coll. Cardiol.*, vol. 69, no. 8, 2017.



- [74] M. J. Brosnan, “Athlete ’ s ECG – Simple Tips for Navigation,” *Hear. Lung Circ.*, vol. 27, no. 9, pp. 1042–1051, 2018.
- [75] C. Calore *et al.*, “Prevalence and clinical meaning of isolated increase of QRS voltages in hypertrophic cardiomyopathy versus athlete ’ s heart : Relevance to athletic screening,” *Int. J. Cardiol.*, vol. 168, no. 4, pp. 4494–4497, 2013.
- [76] A. Zaidi *et al.*, “Clinical significance of electrocardiographic right ventricular hypertrophy in athletes : comparison with arrhythmogenic right ventricular cardiomyopathy and pulmonary hypertension,” *Eur. Heart J.*, vol. 34, pp. 3649–3656, 2013.
- [77] A. Zorzi, M. Elmaghawry, and D. Corrado, “Evolving interpretation of the athlete ’ s electrocardiogram : From European Society of Cardiology and Stanford criteria , to Seattle criteria and beyond .,” *J. Electrocardiol.*, vol. 48, pp. 283–291, 2015.
- [78] P. A. Noseworthy *et al.*, “Correlates and the Effects of Exercise Training,” *Circ Arrhythm Electrophysiol*, vol. 4, no. 4, pp. 432–440, 2013.
- [79] M. Potse, R. Rosso, F. Sacher, J. T. Tikkanen, H. Wellens, and G. Yan, “The Early Repolarization Pattern,” *J. Am. Coll. Cardiol.*, vol. 66, no. 4, pp. 0–7, 2015.
- [80] A. Zorzi *et al.*, “Differential Diagnosis Between Early Repolarization of Athlete ’ s Heart and Coved-Type Brugada Electrocardiogram,” *Am. J. Cardiol.*, vol. 115, no. 4, pp. 529–532.
- [81] D. Corrado *et al.*, “Recommendations for interpretation of 12-lead electrocardiogram in the athlete,” *Eur. Heart J.*, pp. 243–259, 2010.
- [82] M. Papadakis *et al.*, “The prevalence , distribution , and clinical outcomes of electrocardiographic repolarization patterns in male athletes of African / Afro-Caribbean origin,” *Eur. Heart J.*, pp. 2304–2313, 2011.
- [83] M. Papadakis *et al.*, “Prevalence and significance of T-wave inversions in predominantly Caucasian adolescent athletes,” pp. 1728–1735, 2009.
- [84] C. Calore *et al.*, “Sports cardiology Electrocardiographic anterior T-wave inversion in athletes of different ethnicities : differential diagnosis between athlete ’ s heart and cardiomyopathy,” pp. 2515–2527, 2016.
- [85] F. Migliore *et al.*, “Prevalence of Cardiomyopathy in Italian Asymptomatic Children With

- Electrocardiographic T-Wave Inversion at Preparticipation Screening,” *Circulation*, 2011.
- [86] A. Malhotra *et al.*, “Anterior T-Wave Inversion in Young White Athletes and Nonathletes,” *J. Am. Coll. Cardiol.*, vol. 69, no. 1, pp. 1–9, 2017.
- [87] D. Corrado, C. Basso, G. Rizzoli, M. Schiavon, and G. Thiene, “Does Sports Activity Enhance the Risk of Sudden Death in Adolescents and Young Adults ?,” *J. Am. Coll. Cardiol.*, vol. 42, no. 11, pp. 1959–1963, 2003.
- [88] N. Sheikh and S. Sharma, “Impact of ethnicity on cardiac adaptation to exercise,” *Nat. Rev. Cardiol.*, 2014.
- [89] A. Malhotra and S. Sharma, “Cardiomyopathy Hypertrophic Cardiomyopathy in Athletes,” *Eur. Cardiol. Rev.*, pp. 80–82, 2017.
- [90] B. Keeton and D. Holmgren, “Age- and gender-specific mortality rates in childhood hypertrophic cardiomyopathy,” *Eur. Heart J.*, pp. 1160–1167, 2008.
- [91] L. A. Dejgaard *et al.*, “Vigorous exercise in patients with hypertrophic cardiomyopathy,” *Int. J. Cardiol.*, vol. 250, pp. 157–163, 2018.
- [92] B. J. Gersh *et al.*, “2011 ACCF / AHA Guideline for the Diagnosis and Treatment of Hypertrophic Cardiomyopathy : Executive Summary,” *JAC*, vol. 58, no. 25, pp. 2703–2738, 2011.
- [93] N. Sheikh, M. Papadakis, F. Schnell, V. Panoulas, A. Malhotra, and M. Wilson, “Cardiomyopathies Clinical Profile of Athletes With Hypertrophic Cardiomyopathy,” *Circ Cardiovasc Imaging*, pp. 1–9, 2015.
- [94] P. M. Elliott *et al.*, “2014 ESC Guidelines on diagnosis and management of hypertrophic cardiomyopathy The Task Force for the Diagnosis and Management of Hypertrophic Cardiomyopathy of the European Society of Cardiology ( ESC ),” *Eur. Heart J.*, pp. 2733–2779, 2014.
- [95] S. A. Casey, T. E. Gohman, A. K. Almquist, and D. M. Aeppli, “Clinical Course of Hypertrophic Cardiomyopathy in a Regional United States Cohort,” *JAMA*, 1999.
- [96] S. Sharma, B. J. Maron, G. Whyte, S. Firoozi, P. M. Elliott, and W. J. McKenna, “Left Ventricular Hypertrophy in Athletes Physiologic Limits of Left Ventricular Hypertrophy in Elite Junior Athletes : Relevance to Differential Diagnosis of Athlete ’ s Heart and

- Hypertrophic Cardiomyopathy,” *J. Am. Coll. Cardiol.*, vol. 40, no. 8, pp. 1431–1436, 2002.
- [97] Md. Sabiha Gati, PHD, a Sanjay Sharma, MD, b Dudley Pennell, “The Role of Cardiovascular Magnetic Resonance Imaging in the Assessment of Highly Trained Athletes,” *JACC Cardiovasc. Imaging*, vol. 11, no. 2, 2018.
- [98] A. Pelliccia, B. J. Maron, R. De Luca, F. M. Di Paolo, A. Spataro, and F. Culasso, “Remodeling of Left Ventricular Hypertrophy in Elite Athletes After Long-Term Deconditioning,” *Circulation*, pp. 944–949, 2002.
- [99] S. S. S Basavarajaiah, M Wilson, S Junagde, G Jackson, G Whyte, “Physiological left ventricular hypertrophy or hypertrophic cardiomyopathy in an elite adolescent athlete: role of detraining in resolving the clinical dilemma,” *Br J Sport. Med*, pp. 727–729, 2006.
- [100] S. Caselli, M. S. Maron, J. A. Urbano-moral, N. G. Pandian, B. J. Maron, and A. Pelliccia, “Differentiating Left Ventricular Hypertrophy in Athletes from That in Patients With Hypertrophic Cardiomyopathy,” *Am. J. Cardiol.*, vol. 114, no. 9, pp. 1383–1389, 2014.
- [101] M. S. Maron *et al.*, “Hypertrophic Cardiomyopathy Is Predominantly a Disease of Left Ventricular Outflow Tract Obstruction,” *Circulation*, pp. 2232–2239, 2006.
- [102] L. Faber, “Two-dimensional strain analysis of the global and regional myocardial function for the differentiation of pathologic and physiologic left ventricular hypertrophy : a study in athletes and in patients with hypertrophic cardiomyopathy,” *Int J Cardiovasc Imaging*, pp. 91–100, 2011.
- [103] G. D. Aquaro *et al.*, “Reference Values of Cardiac Volumes , Dimensions , and New Functional Parameters by MR : A Multicenter , Multivendor Study,” *J. MAGN. Reson. IMAGING*, pp. 1055–1067, 2016.
- [104] S. E. Petersen *et al.*, “Differentiation of athlete ’ s heart from pathological forms of cardiac hypertrophy by means of geometric indices derived from cardiovascular magnetic resonance,” *J. Cardiovasc. Magn. Reson.*, pp. 551–558, 2005.
- [105] M. D. Domenico Corrado, M.D., Ph.D., Mark S. Link, M.D., and Hugh Calkins, “Arrhythmogenic Right Ventricular Cardiomyopathy,” *N Engl J Med*, pp. 61–72, 2017.
- [106] A. Zaidi *et al.*, “Clinical Differentiation Between Physiological Remodeling and

- Arrhythmogenic Right Ventricular Cardiomyopathy in Athletes With Marked Electrocardiographic Repolarization Anomalies,” *J. Am. Coll. Cardiol.*, vol. 65, no. 25, 2015.
- [107] B. J. Maron and A. Pelliccia, “The Heart of Trained Athletes Cardiac Remodeling and the Risks of Sports , Including Sudden Death,” *Circulation*, pp. 1633–1644, 2006.
- [108] W. B. Abernethy, J. K. Choo, and A. M. Hutter, “Echocardiographic Characteristics of Professional Football Players,” *J. Am. Coll. Cardiol.*, vol. 41, no. 2, pp. 280–284, 2003.
- [109] G. Claessen *et al.*, “Exercise cardiac magnetic resonance to differentiate athlete ’ s heart from structural heart disease,” *Eur. Hear. J. - Cardiovasc. Imaging*, vol. 32, pp. 1062–1070, 2018.
- [110] B. J. Maron *et al.*, “AHA / ACC Scientific Statement Eligibility and Disqualification Recommendations for Competitive Athletes With Cardiovascular Abnormalities : and Other Cardiomyopathies , and Myocarditis and American College of Cardiology,” *Circulation*, pp. 273–280, 2015.
- [111] P. Angelini, “Imaging Approaches for Coronary Artery Anomalies : Purpose and Techniques,” *Curr. Cardiol. Rep.*, pp. 1–6, 2019.
- [112] A. L. Rao, J. C. Salerno, and I. M. Asif, “Evaluation and Management of Wolff-Parkinson-White in Athletes,” *Sports Health*, pp. 326–332, 2014.
- [113] S. Marrakchi, I. Kammoun, E. Bennour, L. Laroussi, M. BenMiled, and S. Kachboura, “Inherited primary arrhythmia disorders : cardiac channelopathies and sports activity,” *Herz*, no. January, 2018.
- [114] I. Goldenberg *et al.*, “Risk Factors for Aborted Cardiac Arrest and Sudden Cardiac Death in Children With the Congenital Long-QT Syndrome,” *Circulation*, pp. 2184–2191, 2008.
- [115] A. Pelliccia *et al.*, “Pre-participation cardiovascular evaluation for athletic participants to prevent sudden death : Position paper from the EHRA and the EACPR , branches of the ESC . Endorsed by APHRS ,” *Europace*, pp. 139–163, 2017.
- [116] A. S. Vink, S. B. Clur, A. A. M. Wilde, and N. A. Blom, “Effect of age and gender on the QTc-interval in healthy individuals and patients with long-QT syndrome,” *Trends Cardiovasc. Med.*, vol. 28, no. 1, pp. 64–75, 2018.

- [117] P. J. Schwartz and L. Crotti, “QTc Behavior During Exercise and Genetic Testing for the Long-QT Syndrome,” *Circulation*, pp. 2181–2184, 1985.
- [118] J. M. Horner, M. M. Horner, and M. J. Ackerman, “The diagnostic utility of recovery phase QTc during treadmill exercise stress testing in the evaluation of long QT syndrome,” *HRTM*, vol. 8, no. 11, pp. 1698–1704, 2011.
- [119] R. W. Sy *et al.*, “Derivation and Validation of a Simple Exercise-Based,” *Circulation*, 2011.
- [120] A. Adler *et al.*, “The phenomenon of ‘QT stunning’: The abnormal QT prolongation provoked by standing persists even as the heart rate returns to normal in patients with long QT syndrome,” *Hear. Rhythm*, vol. 9, no. 6, pp. 901–908, 2013.
- [121] S. G. Priori *et al.*, “2015 ESC Guidelines for the management of patients with ventricular arrhythmias and the prevention of sudden cardiac death The Task Force for the Management of Patients with Ventricular Arrhythmias and the Prevention of Sudden Cardiac Death of the Europea,” *Eur. Heart J.*, pp. 2793–2867, 2015.
- [122] E. H. Chung, “Brugada ECG patterns in athletes,” *J. Electrocardiol.*, 2015.
- [123] A. Pelliccia, M. Borjesson, B. Villiger, F. Di Paolo, and C. Schmied, “Incidence and etiology of sudden cardiac death in young athletes,” *Schweizerische Zeitschrift für «Sportmedizin und Sport.*, pp. 74–78.
- [124] N. M. Pahlevan and M. Gharib, “Pathological wave dynamics : A postulate for sudden cardiac death in athletes,” *Med. Hypotheses*, vol. 82, no. 1, pp. 64–70, 2014.
- [125] A. Uberoi *et al.*, “Interpretation of the Electrocardiogram of Young Athletes,” *Circulation*, pp. 746–757, 2011.
- [126] J. A. Drezner *et al.*, “Electrocardiographic interpretation in athletes : the ‘ Seattle Criteria ,’” *Br J Sport. Med*, pp. 122–124, 2013.
- [127] A. Agostinelli *et al.*, “CaRiSMA 1 . 0 : Cardiac Risk Self-Monitoring Assessment,” *Open Sports Sci. J.*, vol. 10, pp. 179–190, 2017.
- [128] S. S. Chugh and J. B. Weiss, “Sudden Cardiac Death in the Older Athlete,” *J. Am. Coll. Cardiol.*, vol. 65, no. 5, pp. 493–502, 2015.
- [129] P. Düking, A. Hotho, H. Holmberg, F. K. Fuss, and B. Sperlich, “Comparison of Non-

- Invasive Individual Monitoring of the Training and Health of Athletes with Commercially Available Wearable Technologies,” *Front. Physiol.*, vol. 7, 2016.
- [130] A. Sbröllini *et al.*, “Data in brief Sport Database : Cardiorespiratory data acquired through wearable sensors while practicing sports,” *Data Br.*, vol. 27, p. 104793, 2019.
- [131] D. Nepi *et al.*, “Validation of the Heart-Rate Signal Provided by the Zephyr BioHarness 3 .0,” *Comput. Cardiol. (2010).*, pp. 361–364, 2016.
- [132] J. Pan and J. Willis, “A Real-Time QRS Detection Algorithm,” vol. 1, no. 3, pp. 230–236, 1985.
- [133] D. Marinucci, A. Sbröllini, I. Marcantoni, M. Morettini, C. A. Swenne, and L. Burattini, “Artificial Neural Network for Atrial Fibrillation Identification in Portable Devices,” *MDPI sensors*, 2020.
- [134] H. C. Bazett, “An analysis of the time-relations of electrocardiograms,” vol. 2, 1997.
- [135] J. T. D. Jr, B. G. Brown, E. L. Bolson, and H. T. Dodge, “Lumen Diameter of Normal Human Coronary Arteries Influence of Age , Sex , Anatomic Variation , and Left,” *Circulation*, pp. 232–246, 1992.
- [136] C. P. Registry, P. Cardiology, and T. I. Heart, “Anatomy , Histology , and Pathology of Coronary Arteries : A Review Relevant to New Interventional and Imaging Techniques- Part I,” *Clin. Cardiol.*, vol. 15, no. 6, 1992.
- [137] C. Saikrishna *et al.*, “Normal coronary artery dimensions in Indians,” pp. 159–164, 2006.
- [138] A. Dhakal, R. Nath, and A. Maskey, “Coronary artery dimensions in the Nepalese population,” *J. Anat. Soc. India*, vol. 64, no. 1, pp. 27–31, 2015.
- [139] S. Ghaffari, N. Sepehrvand, N. Aslanabadi, B. Sohrabi, A. Separham, and P. Jamshidi, “Coronary artery dimensions : Iranian population versus Indo-Asians and Caucasians,” *Asian Cardiovasc. Thorac. Ann.*, 2015.
- [140] B. K. Raut, V. N. Patil, and G. Cherian, “Coronary artery dimensions in normal Indians,” *Indian Heart J.*, vol. 69, no. 4, pp. 512–514, 2017.
- [141] G. Y. H. Lip, V. S. Rathore, R. Katira, R. D. S. Watson, and S. P. Singh, “Do Indo-Asians have smaller coronary arteries ?,” *Postgrad. Med. J.*, vol. 75, no. 886, pp. 463–466, 1999.

- [142] A. Buradi and A. Mahalingam, “Impact of coronary tortuosity on the artery hemodynamics,” *Integr. Med. Res.*, vol. 40, no. 1, pp. 126–147, 2019.
- [143] J. S. Ho *et al.*, “Relation of Coronary Artery Diameters With Cardiorespiratory Fitness,” *Am. J. Cardiol.*, vol. 121, no. 9, pp. 1065–1071, 2018.
- [144] S. Windecker *et al.*, “Effect of endurance training on coronary artery size and function in healthy men : an invasive followup study,” *Am. J. Physiol.*, pp. 2216–2223, 2020.
- [145] J. E. Davies *et al.*, “Evidence of a Dominant Backward-Propagating ‘ Suction ’ Wave Responsible for Diastolic Coronary Filling in Humans , Attenuated in Left Ventricular Hypertrophy,” *Circulation*, pp. 59–61, 2006.
- [146] Y. Huo and G. S. Kassab, “Pulsatile blood flow in the entire coronary arterial tree : theory and experiment,” *J Physiol Hear. Circ Physiol*, pp. 1074–1087, 2006.
- [147] I. E. Vignon-clementel, C. A. Figueroa, and K. E. Jansen, “Patient-Specific Modeling of Blood Flow and Pressure in Human Coronary,” *Ann. Biomed. Eng.*, 2010.
- [148] D. Sengupta, A. M. Kahn, J. C. Burns, S. Sankaran, S. C. Shadden, and A. L. Marsden, “Image-based modeling of hemodynamics in coronary artery aneurysms caused by Kawasaki disease,” *Biomech. Model. Mechanobiol.*, vol. 11, pp. 915–932, 2011.
- [149] N. M. Pahlevan and M. Gharib, “Aortic Wave Dynamics and Its Influence on Left Ventricular Workload,” *PLoS One*, vol. 6, no. 8, 2011.
- [150] B. Lee, “Computational Fluid Dynamics in Cardiovascular Disease,” *Korean Circ. J.*, pp. 423–430, 2011.
- [151] P. Siogkas, A. Sakellarios, and D. I. Fotiadis, “Blood flow in arterial segments : rigid vs . deformable walls simulations,” *J. Serbian Soc. Comput. Mech.*, vol. 5, pp. 69–77, 2011.
- [152] J. G. M. Yers, J. A. M. Oore, M. O. Jha, K. W. J. Ohnston, and C. R. E. Thier, “Factors Influencing Blood Flow Patterns in the Human Right Coronary Artery,” *Ann. Biomed. Eng.*, vol. 29, pp. 109–120, 2001.
- [153] R. Torii *et al.*, “Fluid – structure interaction analysis of a patient-specific right coronary artery with physiological velocity and pressure waveforms,” *Commun. Numer. Methods Eng.*, pp. 565–580, 2009.
- [154] J. S. Coogan, J. D. Humphrey, and C. A. Figueroa, “Computational simulations of

- hemodynamic changes within thoracic , coronary , and cerebral arteries following early wall remodeling in response to distal aortic coarctation,” *Biomech. Model. Mechanobiol.*, 2012.
- [155] S. Bahrami and M. Norouzi, “A numerical study on hemodynamics in the left coronary bifurcation with normal and hypertension conditions A numerical study on hemodynamics in the left coronary bifurcation,” *Biomech. Model. Mechanobiol.*, no. July, 2018.
- [156] L. Kallekar, C. Viswanath, and M. Anand, “Effect of Wall Flexibility on the Deformation during Flow in a Stenosed Coronary Artery,” *MDPI fluids*, 2017.
- [157] G. Pisani *et al.*, “Role of the sinuses of Valsalva on the opening of the aortic valve,” *J. Thorac. Cardiovasc. Surg.*, vol. 145, no. 4, pp. 999–1003, 2013.
- [158] S. Nobari, R. Mongrain, R. Leask, and R. Cartier, “The effect of aortic wall and aortic leaflet stiffening on coronary hemodynamic : a fluid – structure interaction study,” *Med Biol Eng Comput*, pp. 923–936, 2013.
- [159] E. W. C. Lo, L. J. Menezes, and R. Torii, “Impact of Inflow Boundary Conditions on the Calculation of CT-Based FFR,” *MDPI fluids*, 2019.
- [160] Z. Duanmu *et al.*, “A One-Dimensional Hemodynamic Model of the Coronary Arterial Tree,” *Front. Physiol.*, vol. 10, no. July, pp. 1–12, 2019.
- [161] S. Mantero, T. Marottat, and S. D. Milanese, “A lumped parameter model to evaluate the fluid dynamics of different coronary bypasses,” *Med. Eng. Phys.*, vol. 18, no. 6, pp. 477–484, 1996.
- [162] M. Olufsen, C. S. Peskin, E. M. Persen, W. Y. Kim, A. Nadim, and J. Larsen, “Numerical Simulation and Experimental Validation of Blood Flow in Arteries with Structured-Tree Outflow Conditions,” *Ann. Biomed. Eng.*, vol. 28, pp. 1281–1299, 2000.
- [163] M. S. Olufsen, “Structured tree outflow condition for blood flow in larger systemic arteries,” *Am. J. Physiol.*, pp. 257–268.
- [164] J. T. D. Jr, B. G. Brown, E. L. Bolson, and H. T. Dodge, “Intrathoracic Spatial Location of Specified Coronary Segments on the Normal Human Heart,” *Circulation*, vol. 78, pp. 1167–1180, 1988.



## **Acknowledgement**

I thank Prof. Laura Burtini for her valuable and constructive suggestions during the planning and development of this Master Thesis. I further thank her for the massive opportunities offered during the Master course.

I would like to express my deep gratitude to my supervisor Dott. Agnese Sbrillini, for her patient guidance, enthusiastic encouragement and useful critiques.

I would like to thank Dott. Gianluca Zitti for performing the experiments on which part of the research is based and for his essential assistance.

I would also like to thank Prof. Maurizio Brocchini, Dr. Marco Pozzi and Dr. Massimo Colaneri for their contributions.

I extend my thanks to all the members of Cardiovascular Bioengineering Lab for their presence in these two years.